X선 회절과 결맞음성

Hyunjung Kim

Department of Physics
Sogang University

서강대학교
SOGANG UNIVERSITY

Center for Ultrafast Phase Transformation

Why X-ray?

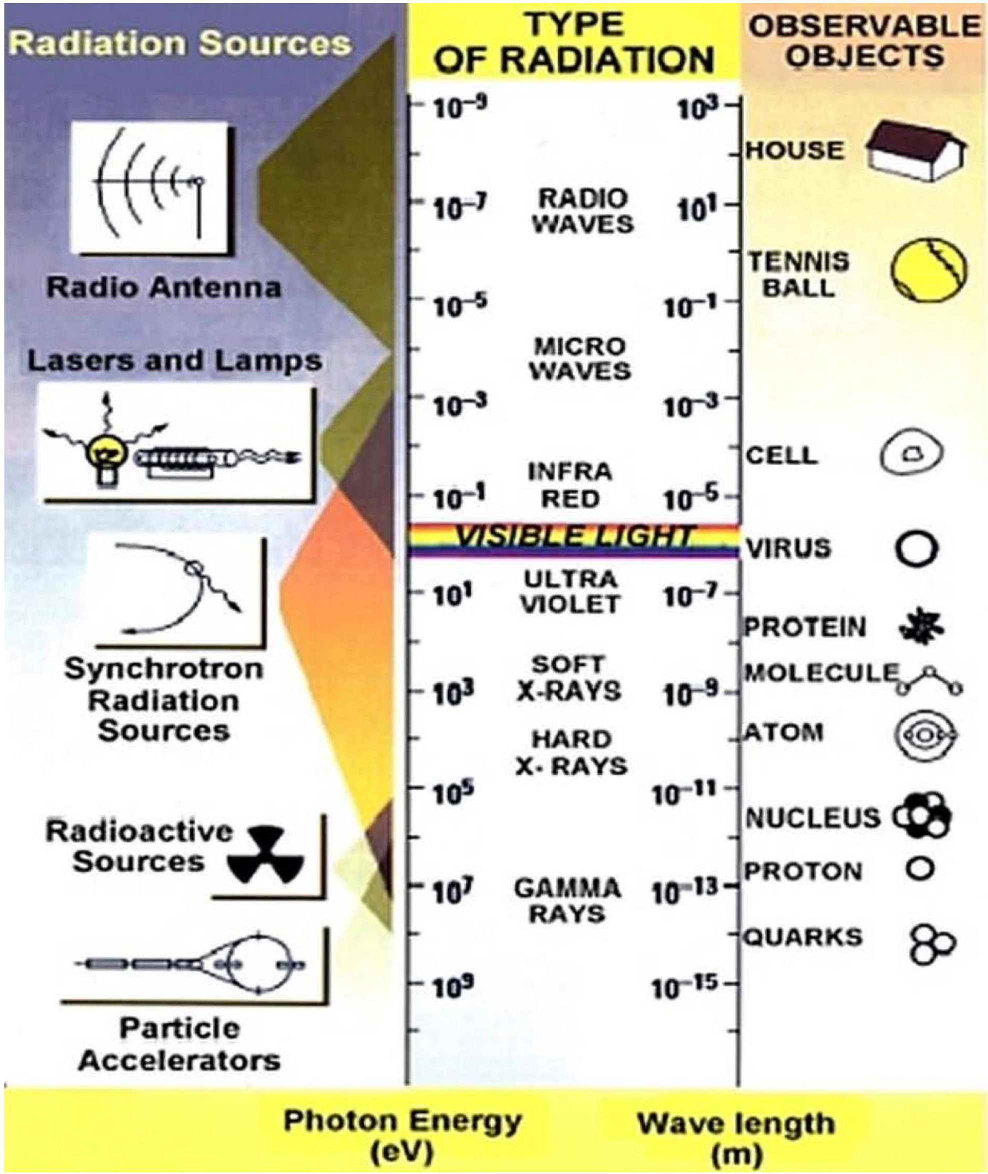

Wavelength
≈
Object size
≈
Angstroms for Condensed Matter Research

$$\lambda[\text{Å}] = \frac{12.398}{E_{ph}[\text{keV}]}$$

E (keV)	λ(Å)
0.8	15.0
8.0	1.5
40.0	0.3
100.0	0.125

Typical interatomic distance in a crystal is 3.5 Å

X-rays

$\lambda = 10$ nm–0.01 nm
E = 0.1keV–100 keV   ($E=h\nu=hc/\lambda=hck$),
Charge=0, Magnetic moment=0, Spin=1

Soft X-rays : $\lambda \geq 1$ nm, $E \leq 1$keV
Hard X-rays: $\lambda \leq 1$ nm, $E \geq 1$keV

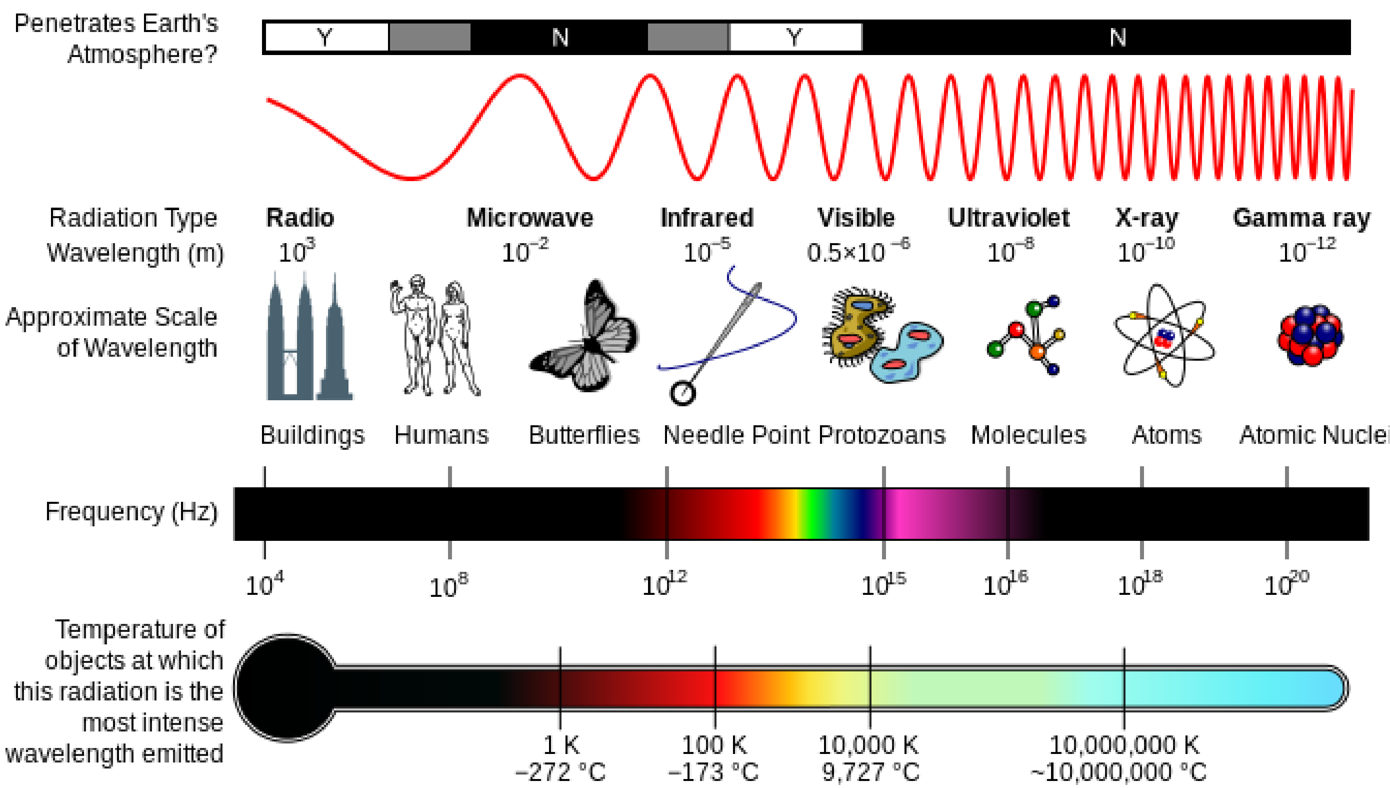

(1) Classical Description

transverse Electro-Magnetic wave : **Light!**

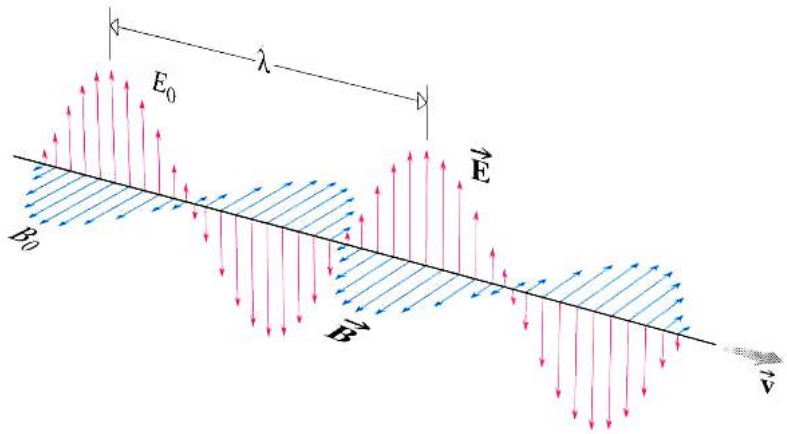

λ(wavelength) : 0.01 nm ~ 10 nm

c(speed of light) : $3\times10^{8}\,\mathrm{m/sec}$

ν(frequency) : $\nu = \dfrac{c}{\lambda}$

ω(angular frequency) : $\omega = 2\pi\nu$

Scatter, Interfere, Diffract → Superpose

(2) Quantum Mechanical Description (particle nature)

$$E = h\nu = \hbar\omega = h\frac{c}{\lambda}$$

h (Planck constant) = $6.63\times10^{-34}\,\mathrm{Joule\cdot sec}$

$$E\cdot\lambda = 12400\ \mathrm{eV}\cdot\mathring{A}$$

(Hard) x-ray Energy : 124 keV ~ 1.24 keV

(3) Maxwell's Equations (wave nature)

$$\nabla \cdot \vec{E} = 4\pi\rho$$ Coulomb's law

$$\nabla \times \vec{E} = -\frac{1}{c}\frac{\partial \vec{B}}{\partial t}$$ Faraday's law

$$\rightarrow \nabla^2 E = \frac{1}{c^2}\frac{\partial^2 \vec{E}}{\partial t^2}$$: wave equation

$$\nabla \cdot \vec{B} = 0$$ Absence of free magnetic poles

$$\nabla \times \vec{B} = \frac{4\pi}{c} J + \frac{1}{c}\frac{\partial \vec{E}}{\partial t}$$ Ampere's law

Solution : $\vec{E}(\vec{r},t) = \vec{E}_o \exp(i(\vec{k}\cdot\vec{r} - \omega t))$

$$\left|\vec{k}\right| = \frac{2\pi}{\lambda}$$: wave vector

Wave equation :

$$\nabla^2 \vec{E} = \frac{1}{c^2}\frac{\partial^2 \vec{E}}{\partial t^2}$$

Spherical coordinate:

$$\left[\frac{1}{r^2}\frac{\partial}{\partial r}\left(r^2\frac{\partial}{\partial r}\right)+\frac{1}{r^2\sin\theta}\frac{\partial}{\partial\theta}\left(\sin\theta\frac{\partial}{\partial\theta}\right)+\frac{1}{r^2\sin^2\theta}\frac{\partial^2}{\partial\varphi^2}\right]\vec{E} = \frac{1}{c^2}\frac{\partial^2 \vec{E}}{\partial t^2}$$

Cartesian coordinate:

$$\left(\frac{\partial^2}{\partial x^2}+\frac{\partial^2}{\partial y^2}+\frac{\partial^2}{\partial z^2}\right)\vec{E} = \frac{1}{c^2}\frac{\partial^2 \vec{E}}{\partial t^2}$$

Plane wave solution :

$$\vec{E}(\vec{r},t) = \vec{E}_o \exp(i(\vec{k}\cdot\vec{r} - \omega t))$$

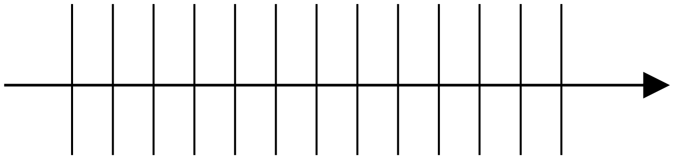

$$\left|\vec{k}\right| = \frac{2\pi}{\lambda}$$: wave vector

Spherical wave solution:

$$\sim \frac{1}{r}\exp\left[i\left(kr-\omega t\right)\right]$$

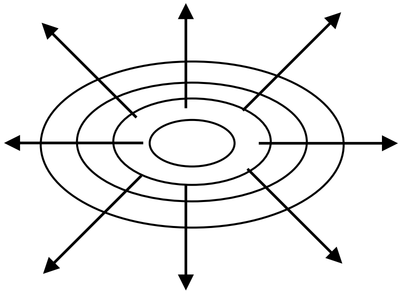

(4) Polarization

$$\mathbf{E}(\mathbf{r},t) \;=\; \mathbf{E}_0 \exp(i(\mathbf{k}\cdot\mathbf{r} - \omega t))$$

$$|\mathbf{k}| = \frac{2\pi}{\lambda}$$: wave vector

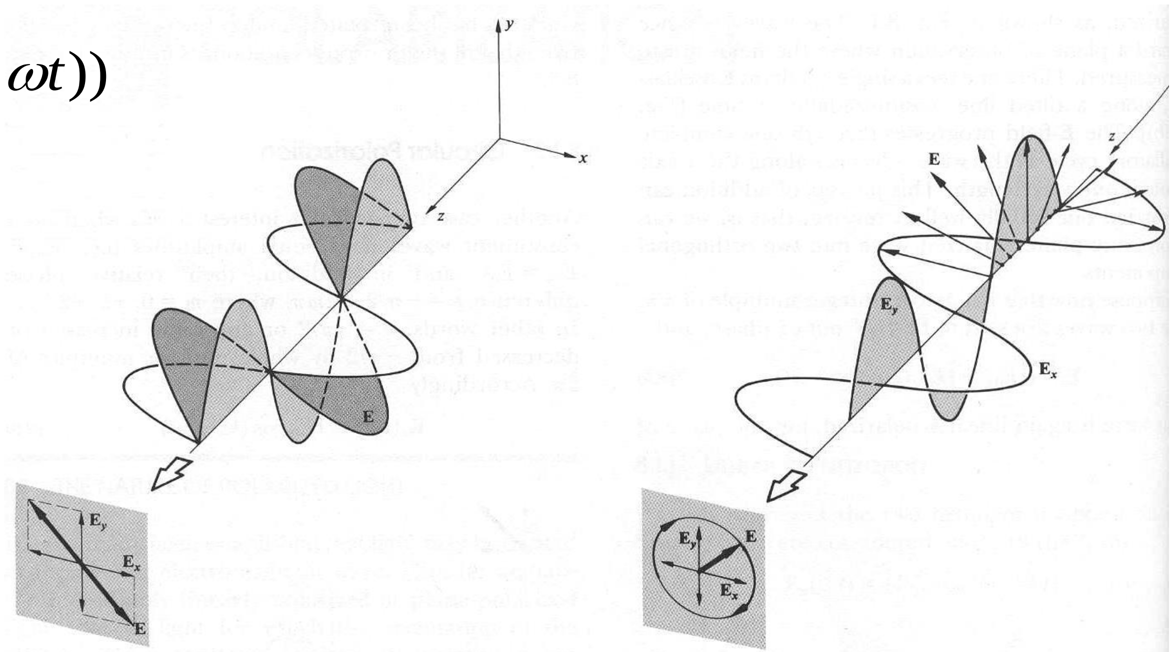

Linear polarization **Circular polarization**

$$\mathbf{E}(\mathbf{r},t) = \hat{x}E_0 \exp(i(\mathbf{k}\cdot\mathbf{r} - \omega t)) + \hat{y}E_0 \exp(i(\mathbf{k}\cdot\mathbf{r} - \omega t + \frac{\pi}{2}))$$

$$= E_o(\hat{x} + i\hat{y}) \exp(i(\mathbf{k}\cdot\mathbf{r} - \omega t))$$

- **Polarization** : the direction of electric field
  always perpendicular to the direction of the propagation.
  parallel to the acceleration of the electric charge
- **Phase** : the argument in the exponential

(5) Coherence

Coherence length : the length scale within which the phase of the electromagnetic field is correlated

(a) Longitudinal coherence length, L_L

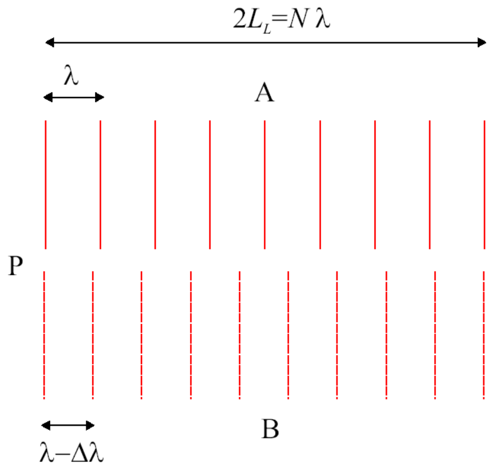

(b) Transverse coherence length, L_T

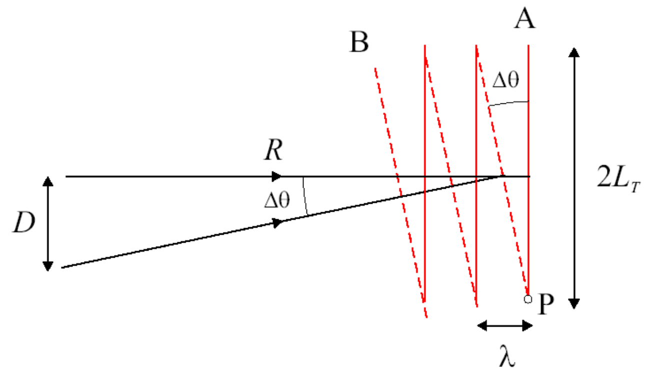

$$2L_L = N\lambda = (N+1)(\lambda - \Delta\lambda)$$

$$N \approx \lambda / \Delta\lambda$$

$$\Rightarrow L_L = \frac{1}{2}\frac{\lambda^2}{\Delta\lambda}$$

$$2L_T \Delta\theta = \lambda$$

$$\Rightarrow L_T = \frac{1}{2}\frac{\lambda}{D/R} = \frac{\lambda}{2}\left(\frac{R}{D}\right)$$

If two waves are in-phase at a point, how far do we have to go away before the waves are out of phase? → coherence length (L_L, L_T)

Use of X-ray

- ✓ Imaging: Real Space Measurement: I(r)

(Medical application)


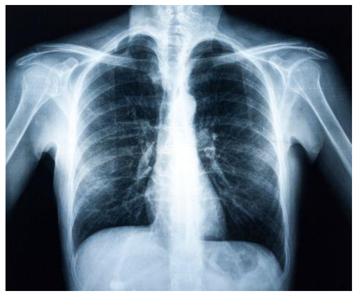

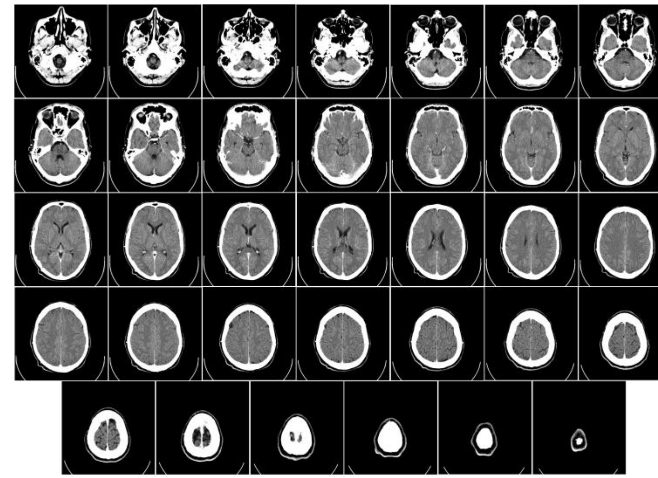

Differences in Absorption

Computed Tomography scan

- ✓ X-ray Scattering or Diffraction: Reciprocal Space Measurement : I(q), I(θ)

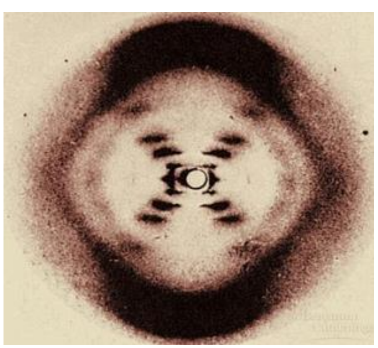
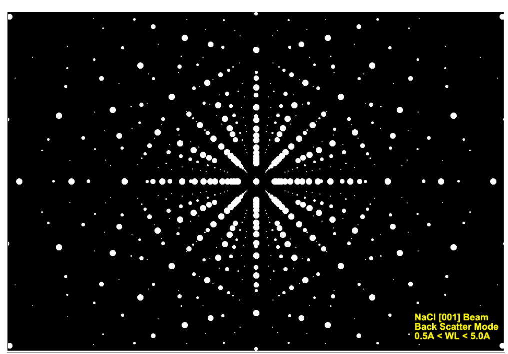

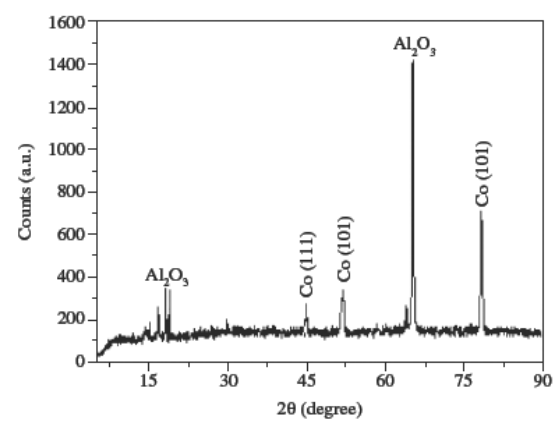

Nobel Prizes for Research with X-Rays

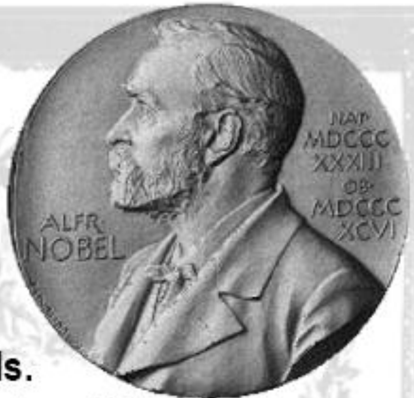

1901 W. C. Röntgen in Physics for the discovery of x-rays.
1914 M. von Laue in Physics for x-ray diffraction from crystals.
1915 W. H. Bragg and W. L. Bragg in Physics for crystal structure determination.
1917 C. G. Barkla in Physics for characteristic radiation of elements.
1924 K. M. G. Siegbahn in Physics for x-ray spectroscopy.
1927 A. H. Compton in Physics for scattering of x-rays by electrons.
1936 P. Debye in Chemistry for diffraction of x-rays and electrons in gases.
1962 M. Perutz and J. Kendrew in Chemistry for the structure of hemoglobin.
1962 J. Watson, M. Wilkins, and F. Crick in Medicine for the structure of DNA.
1979 A. McLeod Cormack and G. Newbold Hounsfield in Medicine for computed axial tomography.
1981 K. M. Siegbahn in Physics for high resolution electron spectroscopy.
1985 H. Hauptman and J. Karle in Chemistry for direct methods to determine x-ray structures.
1988 J. Deisenhofer, R. Huber, and H. Michel in Chemistry for the structures of proteins that are crucial to photosynthesis.

2009 Venkatraman Ramakrishnan, Thomas A. Steitz and Ada E. Yonath
in Chemistry for “studies of the structure and function of the ribosome" X-ray crystallography

Structure-Function Relationships

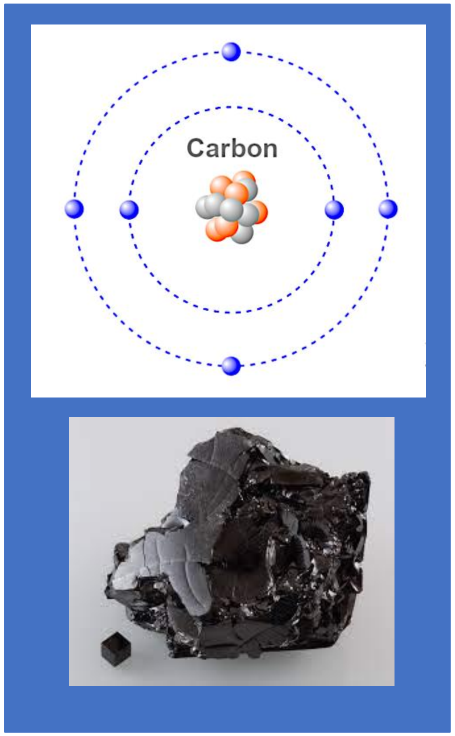

Diamond

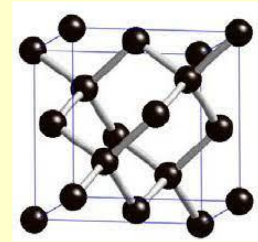

Graphite

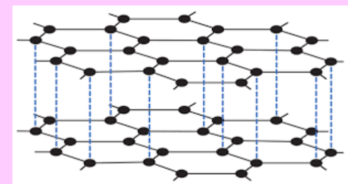

Graphene

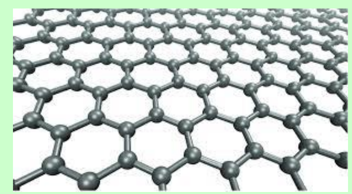

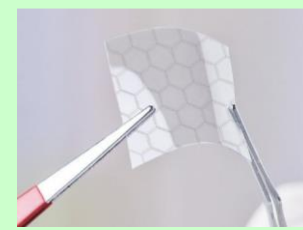

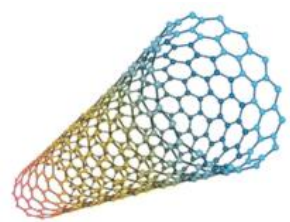

Carbon nanotube

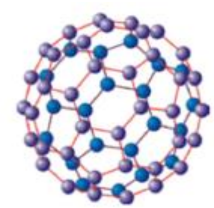

C60-fullerene

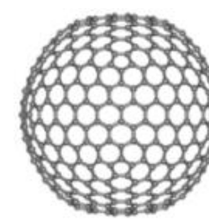

C540-fullerite

→ Materials Control and Engineering

Structure Determination

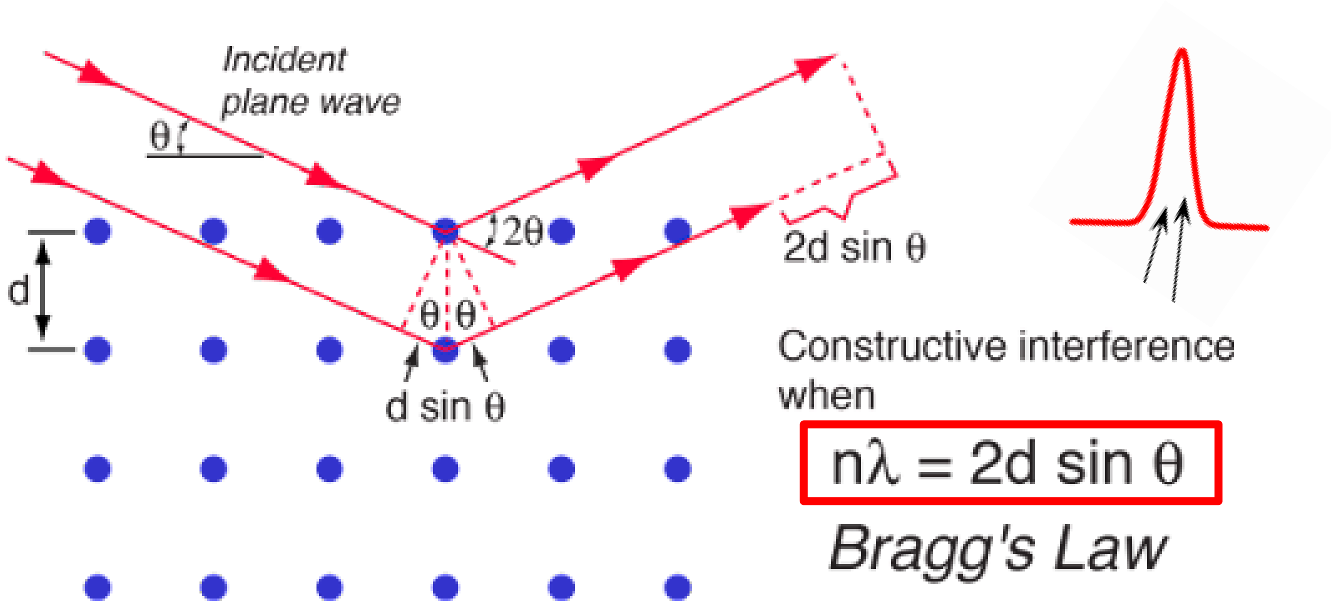

Hard X-rays: λ ≤ 1 nm, E ≥ 1keV
Soft X-rays: λ ≥ 1 nm, E ≤ 1keV

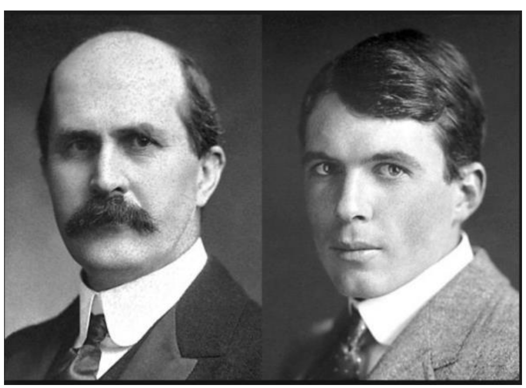

William & Lawrence Bragg
Novel Prize for Physics 1915

Content

- X-ray interaction with matter
- Scattering cross-section
- Diffraction
- Why Synchrotron?
- Coherent X-rays

X-ray interaction with matter

Interaction Mechanisms

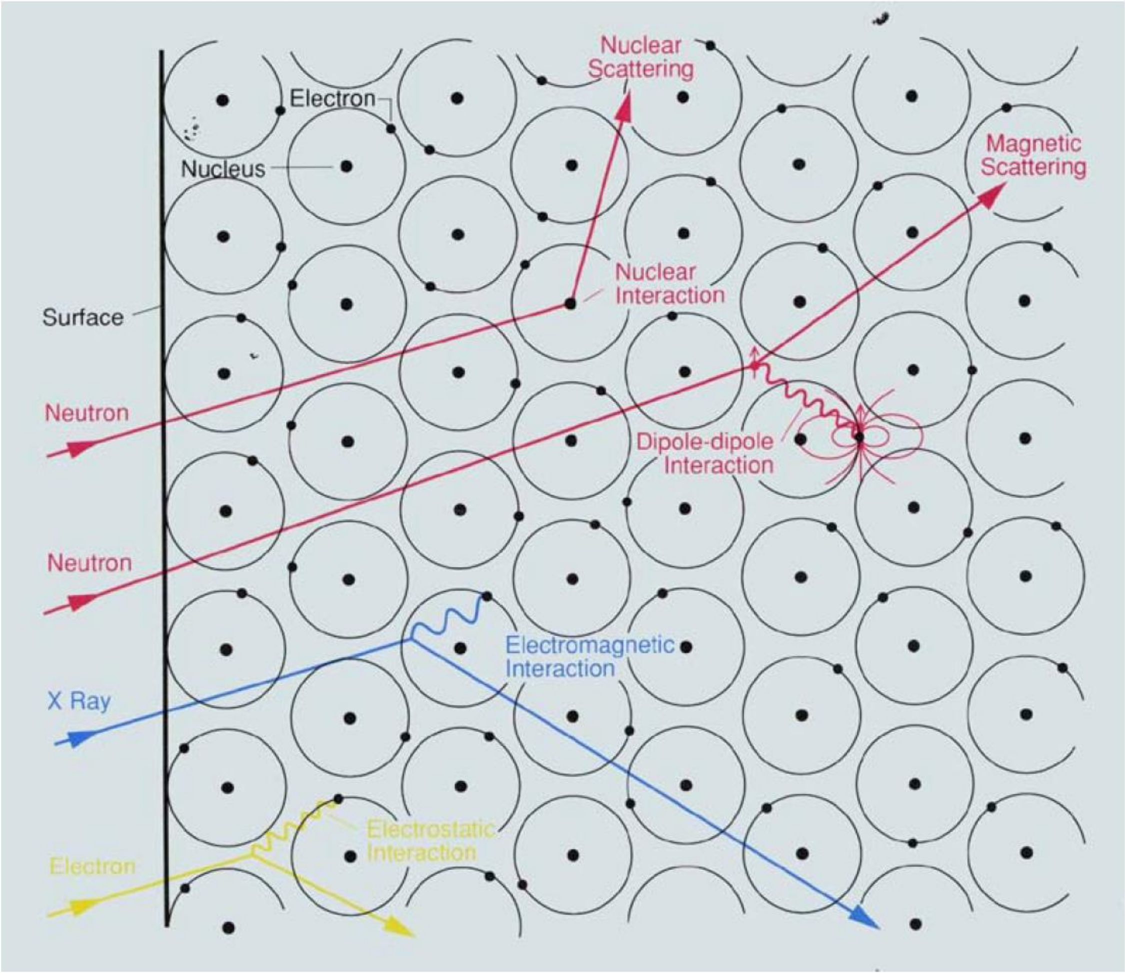

X-rays interact with electrons via an electromagnetic interaction.
(cf. Neutrons interact with atomic nuclei via very short range (~ fm) forces.
Neutrons interact with unpaired electrons via magnetic dipole interaction.)

Penetration in Matter

8 keV X-rays, Thermal Neutrons, & Low Energy Electrons

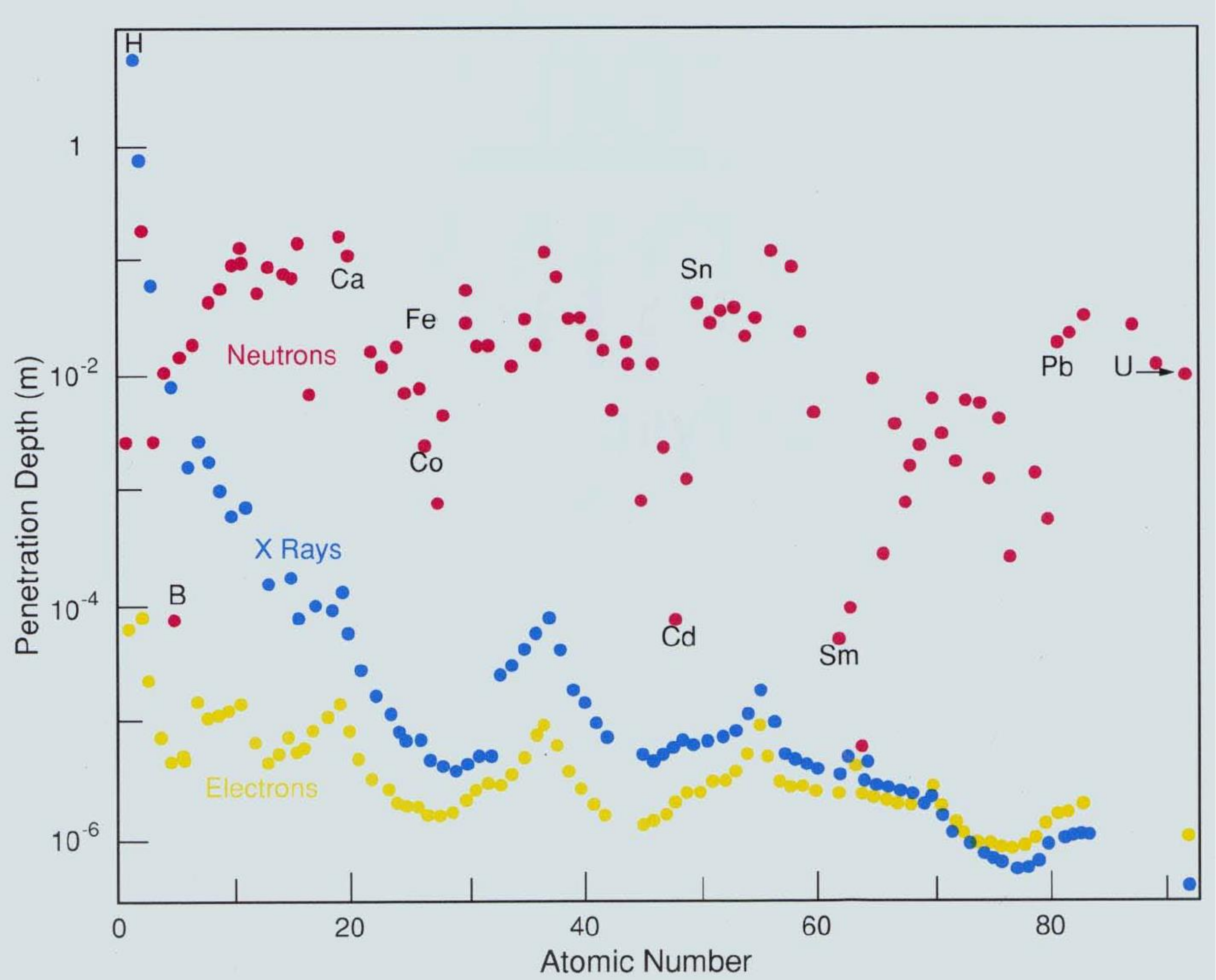

For X-rays
: Decreasing penetration as Z increases

(cf. For Neutrons
: H/D difference
: Cd, B, Sm
: No systematic Z dependence)

X-rays interacting with electrons

(1) **Photoelectric absorption** X-rays kicks electron from shell to continuum

- Leads to fluorescent X-ray emission when hole in shell is filled from outer shell
- Goes as $1/E^3$ but with sharp steps at shell energies when new channel opens

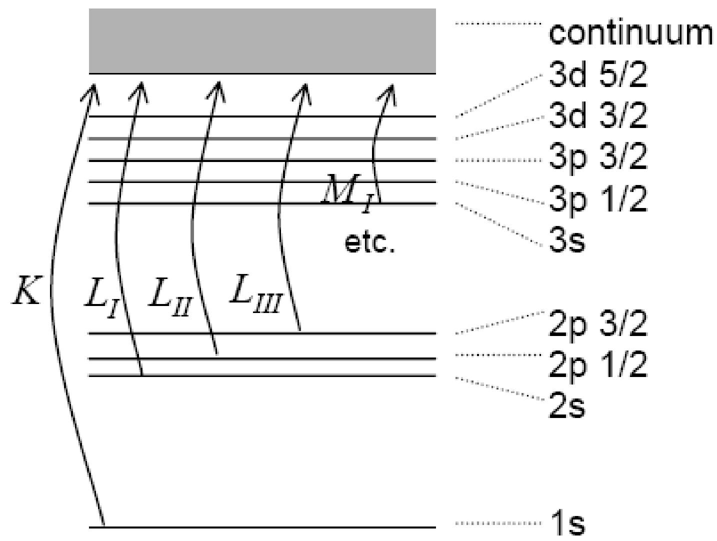

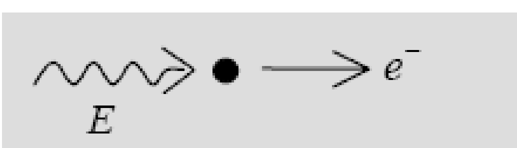

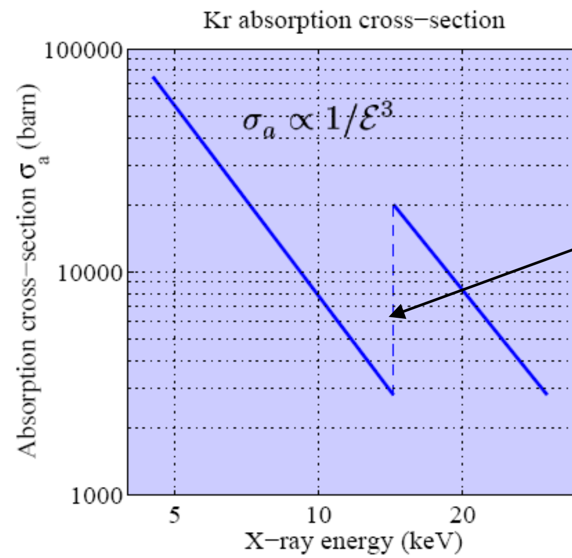

14.32 keV : K-edge energy, the X-ray photon has enough energy to also expel a K-electron, with a concomitant discontinuous rise in the cross section of about one order.

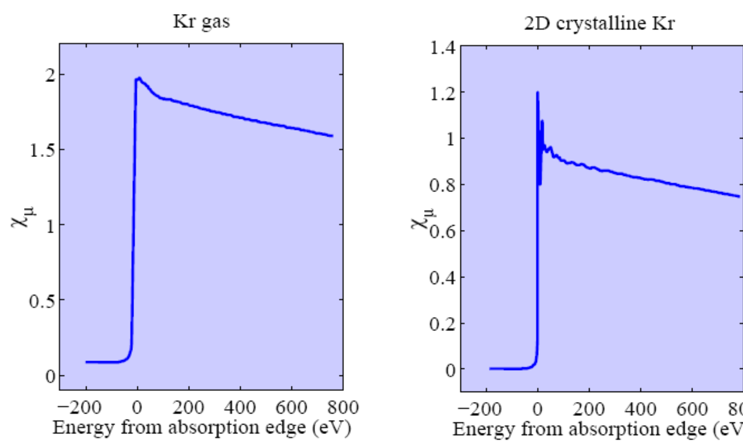

Extended X-ray Absorption Fine Structure

X-rays interacting with electrons

(2) **Thomson scattering** : elastic and coherent

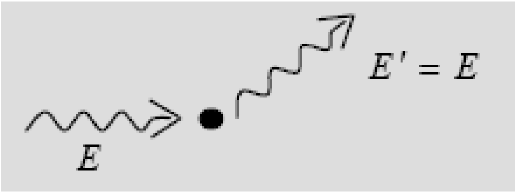

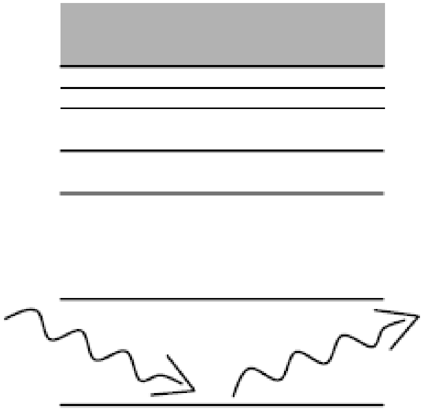

$$\left|\vec{k}\right| = \left|\vec{k}'\right|,\ E = E'$$

(3) **Compton scattering** : inelastic and incoherent

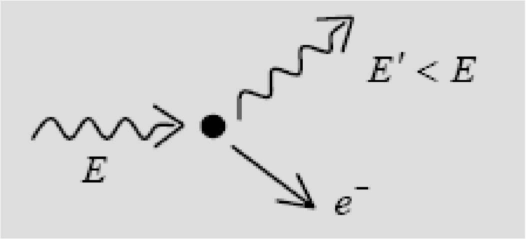

$$\left|\vec{k}\right| \neq \left|\vec{k}'\right|, E \neq E'$$

Refractive Index

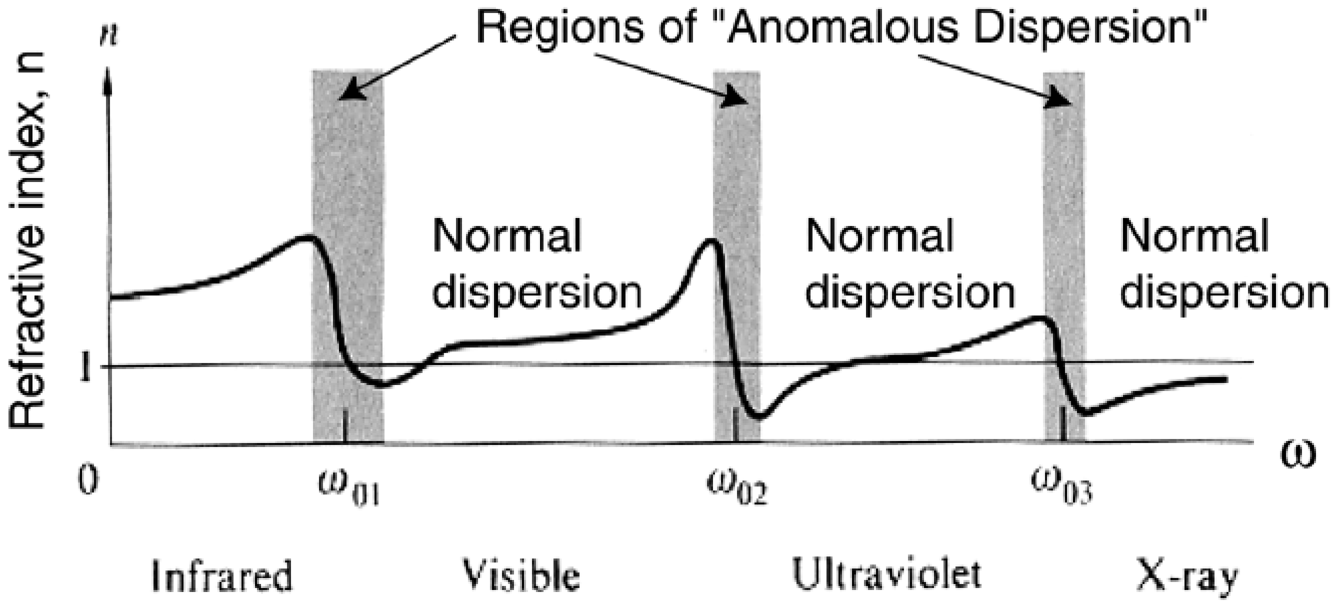

$$n = 1 - \delta + i\beta$$

Visible vs. X-ray

Visible Optical Spectroscopy	*vs.*	X-ray Scattering
n=1: vacuum n>1: 모든 물질, 전반사: 물질→공기		n=1: vacuum n<1: 모든 물질, 전반사: 공기→물질 $n=1-\delta+i\beta$
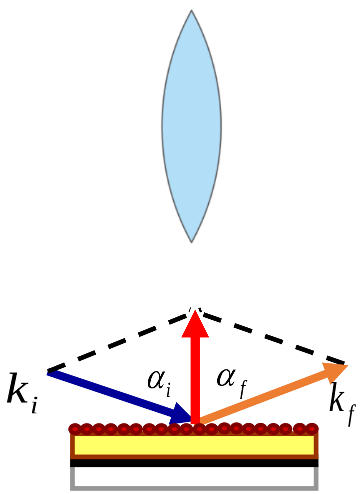		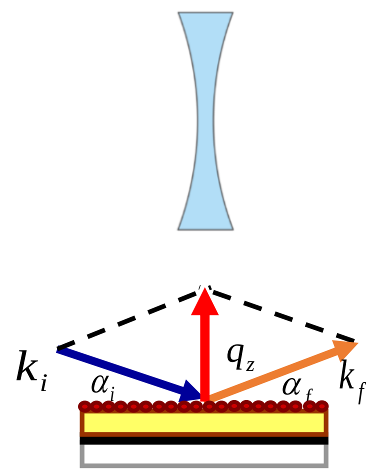
Monochromator: grating Mirror: Metal coated glass		Monochromator: Si single crystal Mirror: Si single crystal
…		…
I(E), I(ω), I(λ)		I(θ), I(q)

Scattering cross-section

Intrinsic cross-section

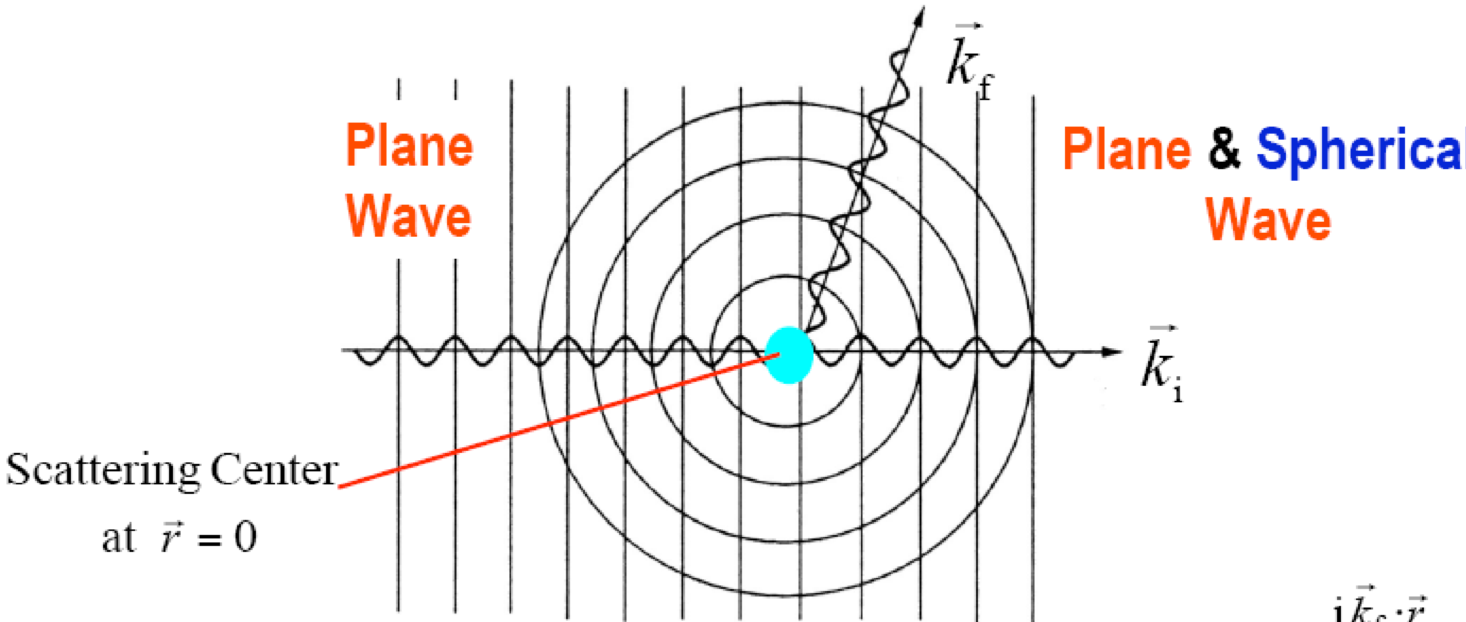

$$e^{i\vec{k}_i\cdot\vec{r}} \rightarrow e^{i\vec{k}_i\cdot\vec{r}} + f(\Omega)\frac{e^{i\vec{k}_f\cdot\vec{r}}}{r}$$

Total Cross Section :

$$\sigma = \iint \left(\frac{d\sigma}{d\Omega}\right)_0 d\Omega$$

$$\left(\frac{d\sigma}{d\Omega}\right)_0 = \left|f(\Omega)\right|^2$$

$$\sigma = \int_0^{2\pi}\int_0^{\pi} \left|f(\vartheta,\phi)\right|^2 \sin\vartheta \, d\vartheta \, d\phi$$

Reciprocal Space Measurement

Schematic layout of a scattering experiment to determine the differential cross-section

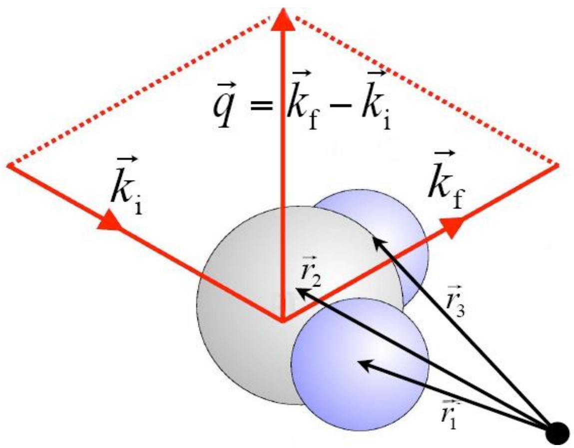

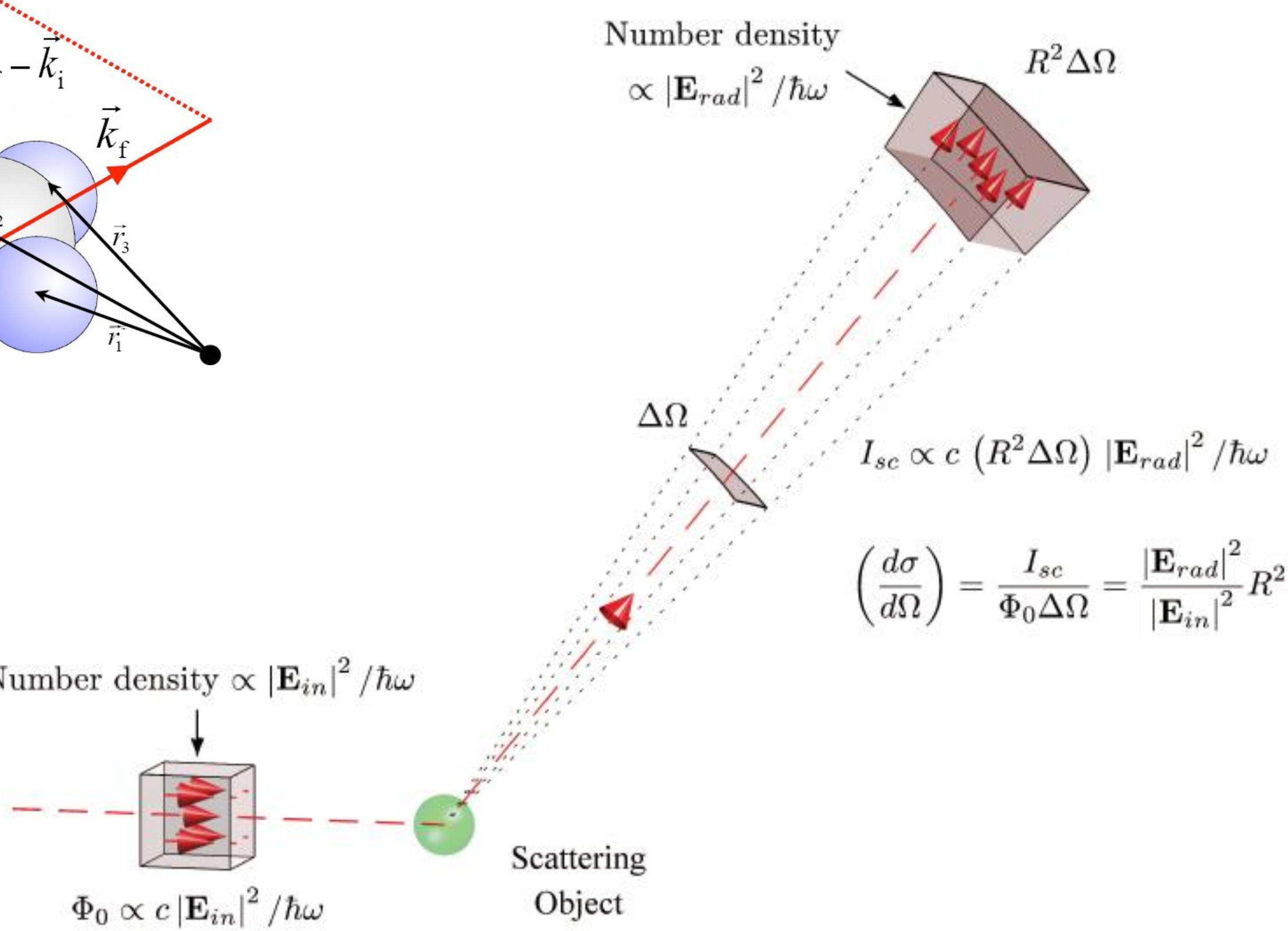

Intrinsic cross-section

One electron

$$\vec{E}_{\text{in}} = \vec{E}_0\, e^{i(\vec{k}\cdot\vec{r}-\omega t)}$$

$$E_{\text{rad}}(R,t) = \frac{e}{4\pi\varepsilon_0 c^2 R}\,\ddot{x}(t-R/c)$$

$$\ddot{x}(t-R/c) = -\frac{e}{m} \quad E_{\text{in}} e^{i\omega R/c}\cos\psi$$

$$\frac{E_{\text{rad}}(R,t)}{E_{\text{in}}} = -r_0 \quad \frac{e^{ikR}}{R}\cos\psi$$

Thomson Scattering Length of the Electron (classical electron radius):

$$r_0 = \frac{e^2}{4\pi\varepsilon_0 mc^2} = 2.82\times10^{-15}\,\text{m}$$

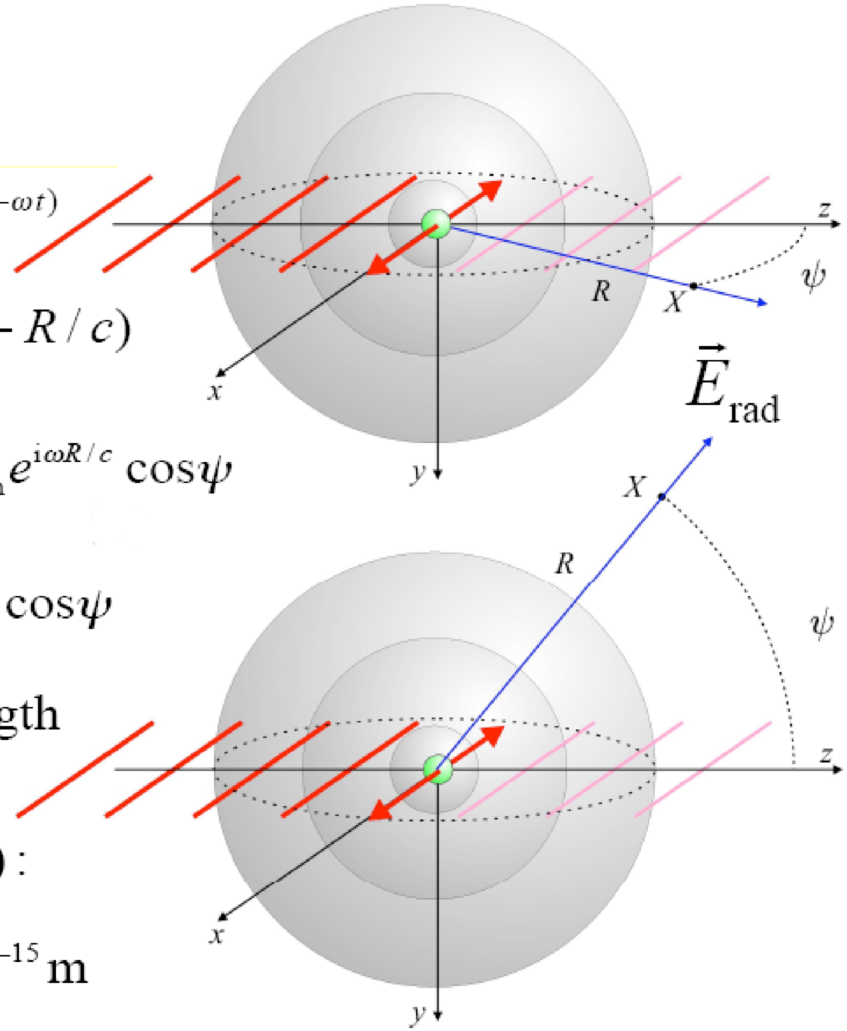

For bound electrons

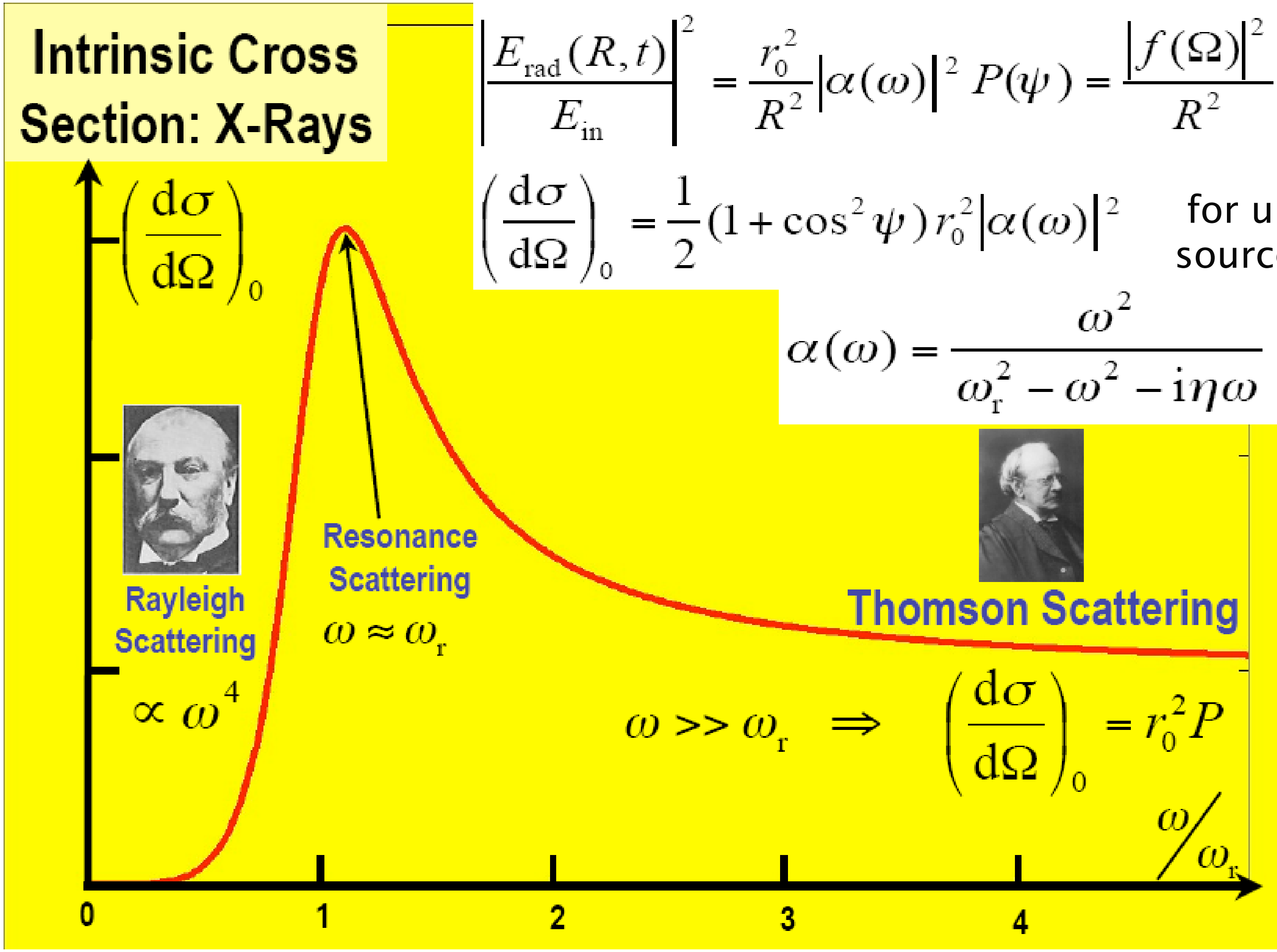

$$\left|\frac{E_{rad}(R,t)}{E_{in}}\right|^2 = \frac{r_0^2}{R^2}\left|\alpha(\omega)\right|^2 P(\psi) = \frac{\left|f(\Omega)\right|^2}{R^2}$$

$$\left(\frac{d\sigma}{d\Omega}\right)_0 = \frac{1}{2}(1+\cos^2\psi)\, r_0^2 \left|\alpha(\omega)\right|^2$$ for unpolarized sources

$$\alpha(\omega) = \frac{\omega^2}{\omega_r^2 - \omega^2 - i\eta\omega}$$ for bound electrons

One atom

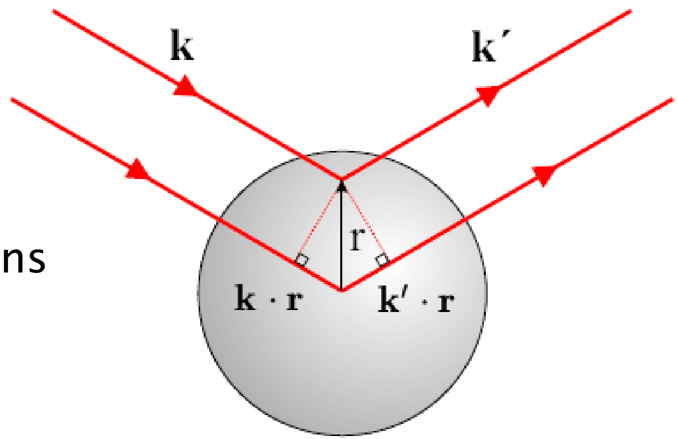

Z electrons

The resultant phase difference: $\Delta\phi(\vec{r}) = (\vec{k} - \vec{k}') \cdot \vec{r} = \vec{Q} \cdot \vec{r}$

$\left|\vec{k}\right| = \left|\vec{k}'\right|$: elastic $\left|\vec{Q}\right| = 2\left|\vec{k}\right| \sin\theta = \frac{4\pi}{\lambda} \sin\theta$

Volume element $d\vec{r}$ at $\vec{r}$: $r_0 \rho(\vec{r}) d\vec{r}$ with phase factor $e^{i\vec{Q}\cdot\vec{r}}$

$$r_0 f(\vec{Q}) = r_0 \boxed{\int \rho(\vec{r}) e^{i\vec{Q}\cdot\vec{r}} d\vec{r}}$$

Atomic Form Factor
: Fourier transform of charge density
(distribution of electrons)

$$f(\vec{Q}) = \int \rho(\vec{r}) e^{i\vec{Q}\cdot\vec{r}} d\vec{r}$$

$Q \rightarrow 0$: all of the different volume elements scatter in phase

$$f^{o}(\vec{Q} = 0) = Z$$

$$f^{o}(\vec{Q} \rightarrow \infty) = 0$$

$$f(Q,\ \hbar\omega) = f^{0}(Q) + \boxed{f'(\hbar\omega) + if''(\hbar\omega)}$$

Anomalous Dispersion Corrections

f' : Real part of scattering length

f'' : Dissipation

Element Specific

One molecule

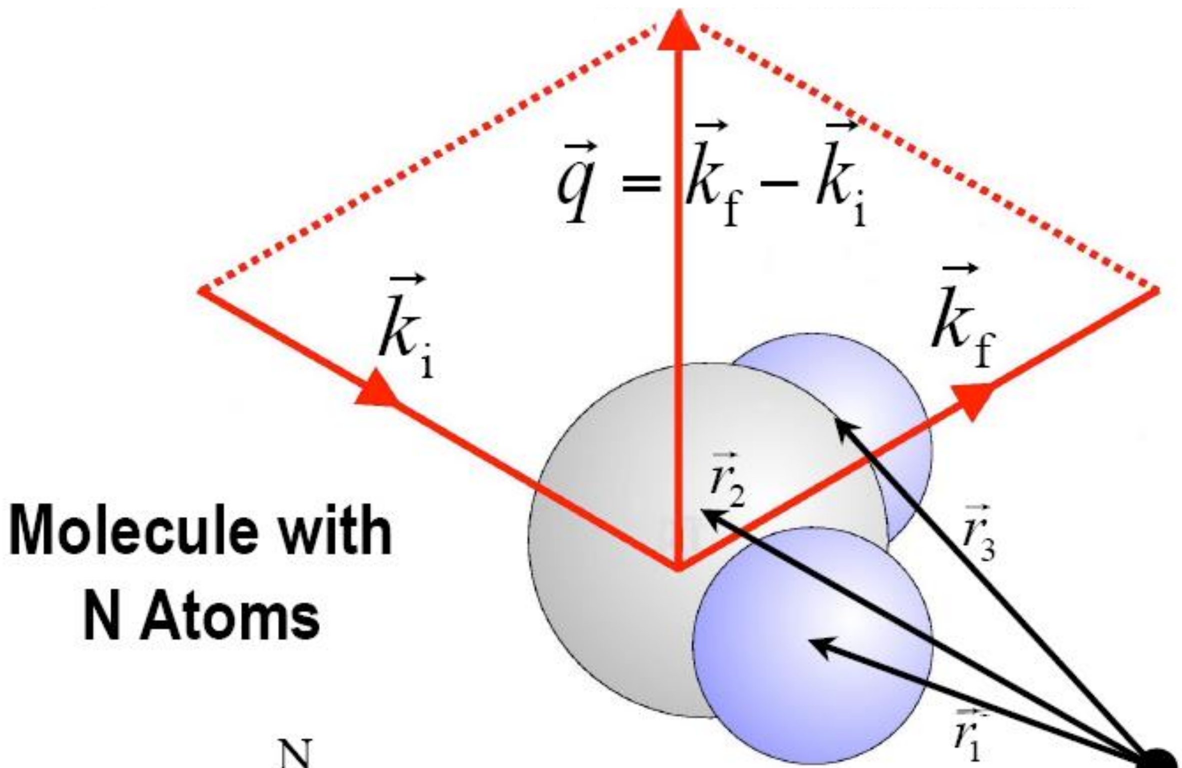

$$F_{mol.}(\vec{q}) = \sum_{j=1}^{N} f_j(\vec{q})\, e^{-i\, \vec{q} \cdot \vec{r}_j}$$

Reciprocal Lattice

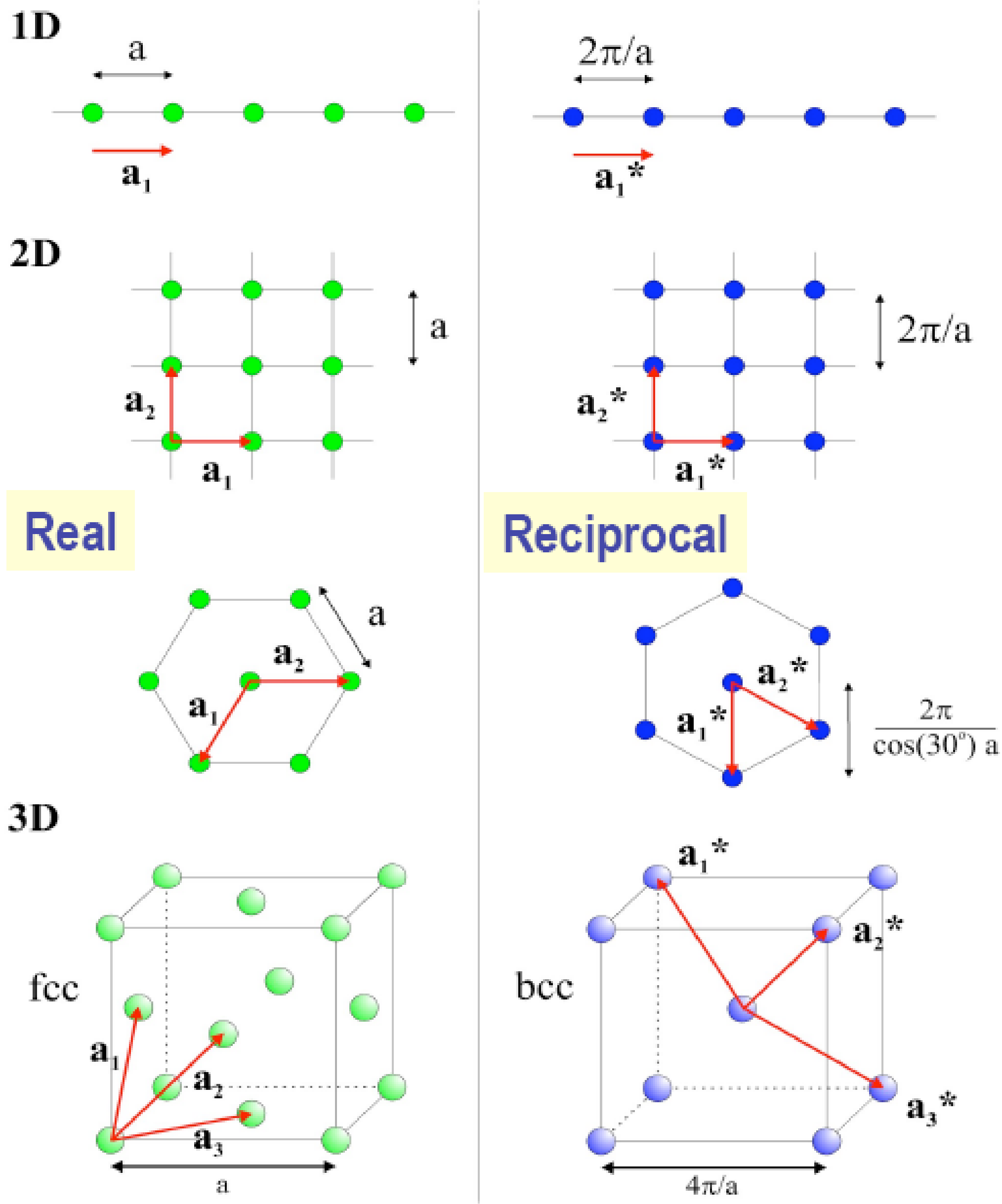

Reciprocal Lattice:

$$V_c = \vec{a}_1 \cdot (\vec{a}_2 \times \vec{a}_3)$$

$$\vec{a}_1^{\,*} = \frac{2\pi}{V_c} \vec{a}_2 \times \vec{a}_3$$

$$\vec{a}_2^{\,*} = \frac{2\pi}{V_c} \vec{a}_3 \times \vec{a}_1$$

$$\vec{a}_3^{\,*} = \frac{2\pi}{V_c} \vec{a}_1 \times \vec{a}_2$$

Reciprocal Space

– An array of points (hkl) that is precisely related to the crystal lattice

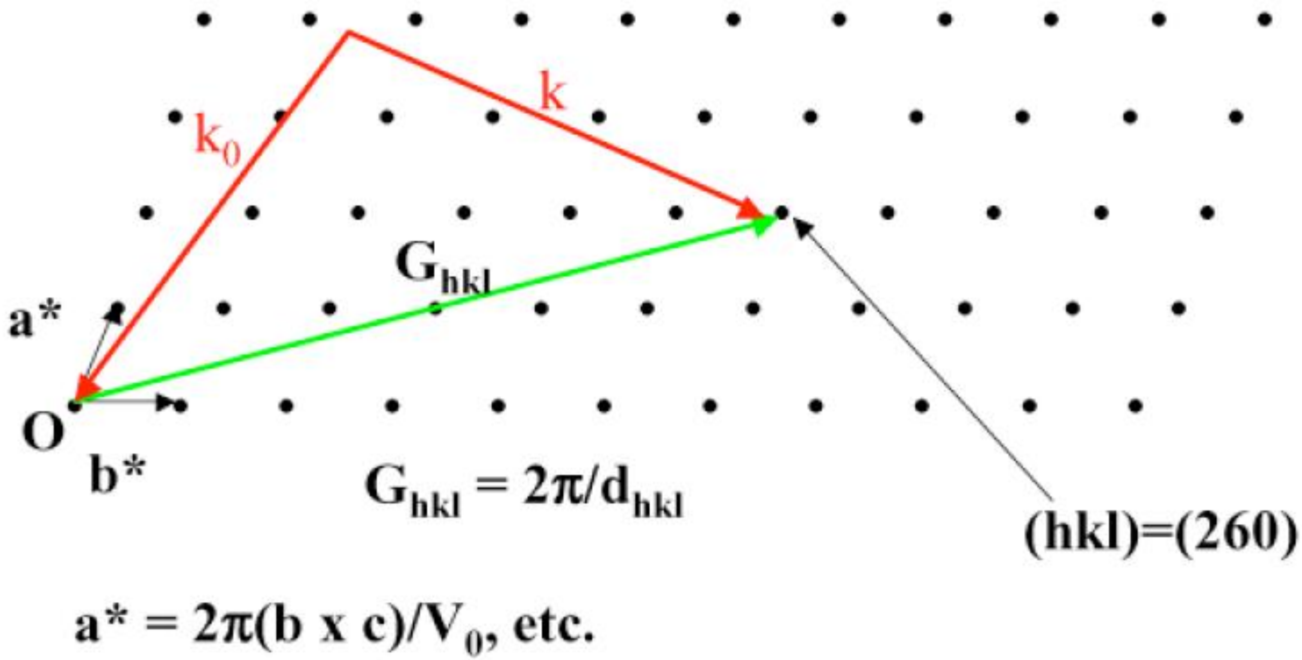

A single crystal has to be aligned precisely to record Bragg scattering

A crystal

$$F_{\text{crystal}}(\vec{q}) = \left(\sum_{j=1}^{N} f_j(\vec{q})\, e^{-i\,\vec{q}\cdot\vec{r}_j}\right) \cdot \left(\sum_{n=1}^{M} e^{-i\,\vec{q}\cdot\vec{R}_n}\right)$$

Unit Cell Structure Factor   Lattice Sum

$$\sum_{n=1}^{M} e^{-i\,\vec{q}\cdot\vec{R}_n} \approx \begin{cases} M >> 1 & \text{for } \vec{q}\cdot\vec{R}_n = 2\pi \times \text{integer} \\ 0 & \text{otherwise} \end{cases}$$

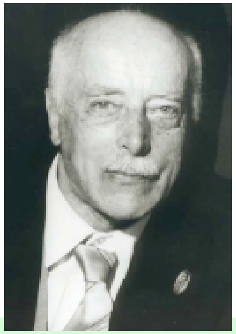

Reciprocal Lattice:

$$\vec{R}_n = n_1\vec{a}_1 + n_2\vec{a}_2 + n_3\vec{a}_3$$

$$\vec{a}_i \cdot \vec{a}_j^* = 2\pi\delta_{ij} \qquad i, j = 1,2,3$$

$$\vec{G}_{hkl} = h\vec{a}_1^* + k\vec{a}_2^* + l\vec{a}_3^*$$

$$\vec{G}_{hkl} \cdot \vec{R}_n = 2\pi(hn_1 + kn_2 + ln_3)$$

Laue Condition

$$\vec{q} = \vec{G}_{hkl}$$

Elastic scattering from a crystal

Differential Scattering Cross Section

$$\frac{d\sigma}{d\Omega} = \left(\frac{d\sigma}{d\Omega}\right)_0 S(\vec{q})$$

Intrinsic Cross Section
Coupling Beam ⇔ Sample

Properties of the Sample without Beam

$$S(\vec{q}) = \left|F_{\text{crystal}}(\vec{q})\right|^2$$

The measured intensity from a crystallite

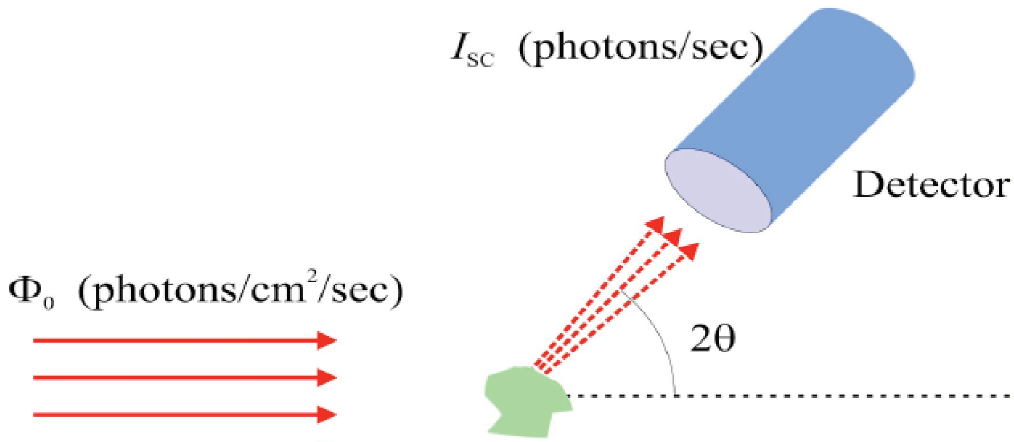

$$\left(\frac{d\sigma}{d\Omega}\right) = \frac{\text{Number of Photons Scattered per Second into } d\Omega}{(\text{Incident Flux})\,(d\Omega)}$$

$$\left(\frac{d\sigma}{d\Omega}\right) = r_0^2 P \left|F_{hkl}(\vec{q})\right|^2 M V_c^* \,\delta(\vec{q} - \vec{G}_{hkl})$$

- r_0^2: Thomson Scattering of an Electron
- F_{hkl}: Structure Factor of the Unit Cell
- M: Number of Unit Cells
- V_c^*: Reciprocal Space Unit Cell Volume

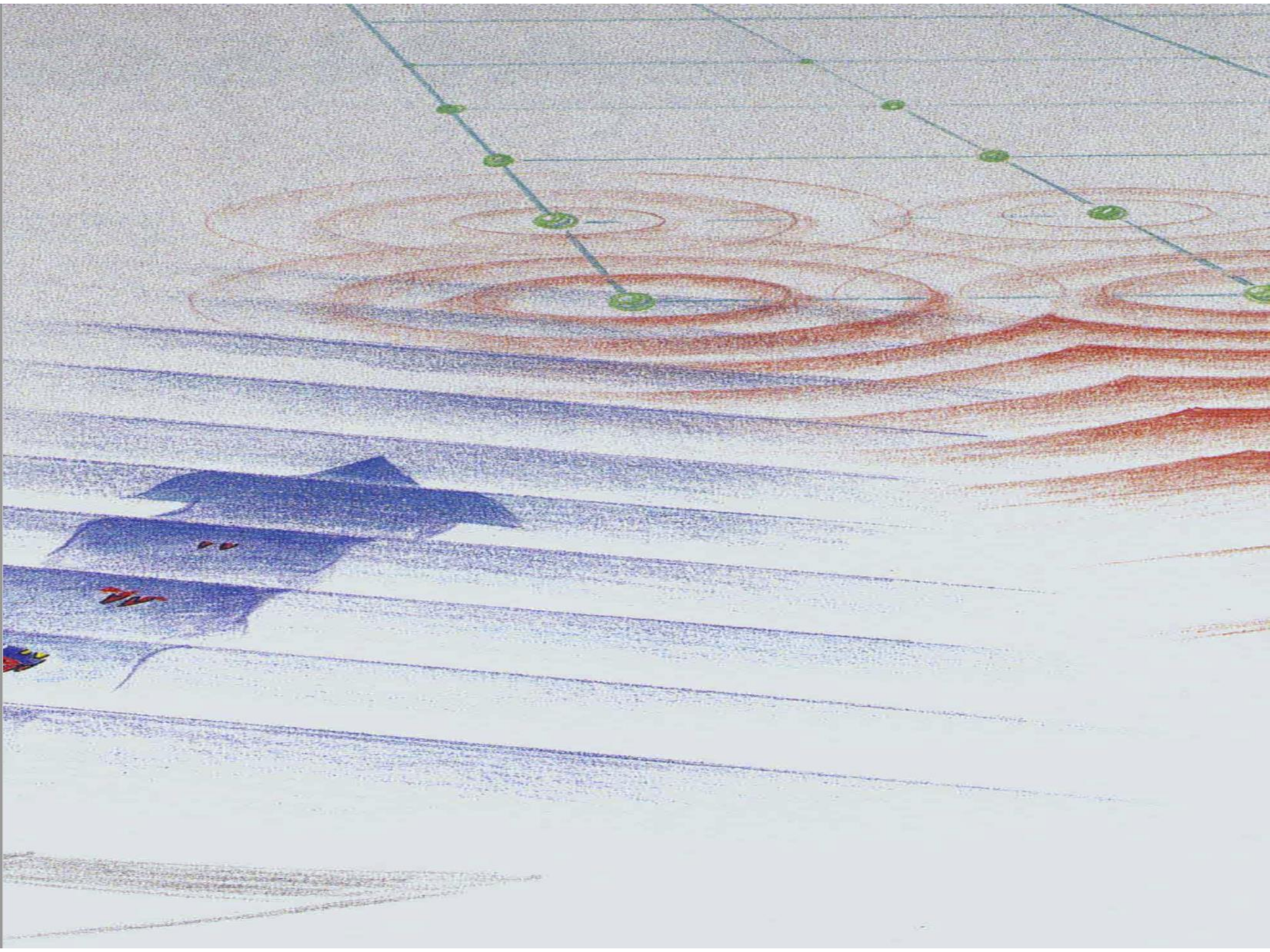

Compton Scattering by a free electron (inelastic scattering)

- Assumption: view the incident x-ray as a beam of photons.
  Electron is at rest and is free.

In a collision, energy will be transferred from the photon to the electron, with the result that the scattered photon has a lower energy than that of the incident one.
: **Compton Effect**

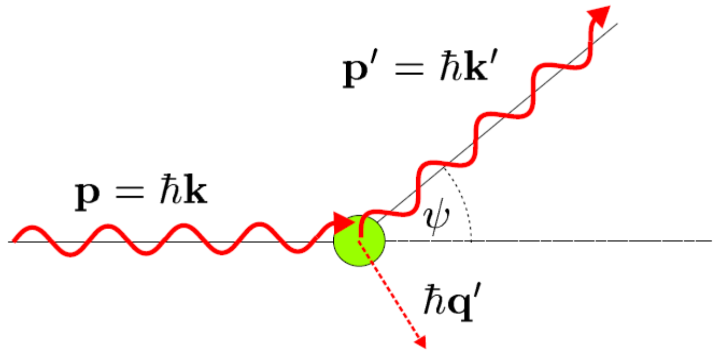

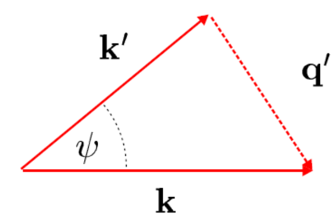

Energy conservation : $E_i + e_i = E_f + e_f$

$$mc^2 + \hbar ck = \sqrt{mc^2 + (\hbar cq')^2} + \hbar ck'$$

divide by mc^2 $\quad \Rightarrow 1 + \dfrac{\hbar c}{mc^2}(k - k') = \sqrt{1 + \left(\dfrac{\hbar c}{mc^2} q'\right)^2}$

compton scattering length $\lambda_C \equiv \dfrac{\hbar c}{mc^2} = 3.86 \times 10^{-3}\ \overset{0}{\mathrm{A}}$

$\alpha = \dfrac{r_0}{\lambda\!\!\!^{-}_C} \approx \dfrac{1}{137}$ Fine structure constant

Momentum conservation

$$\vec{k}' - \vec{k} = \vec{q}'$$

$$\frac{k}{k'} = 1 + \lambda\!\!\!^{-}_C k(1 - \cos\psi) = \frac{E}{E'} = \frac{\lambda'}{\lambda}$$

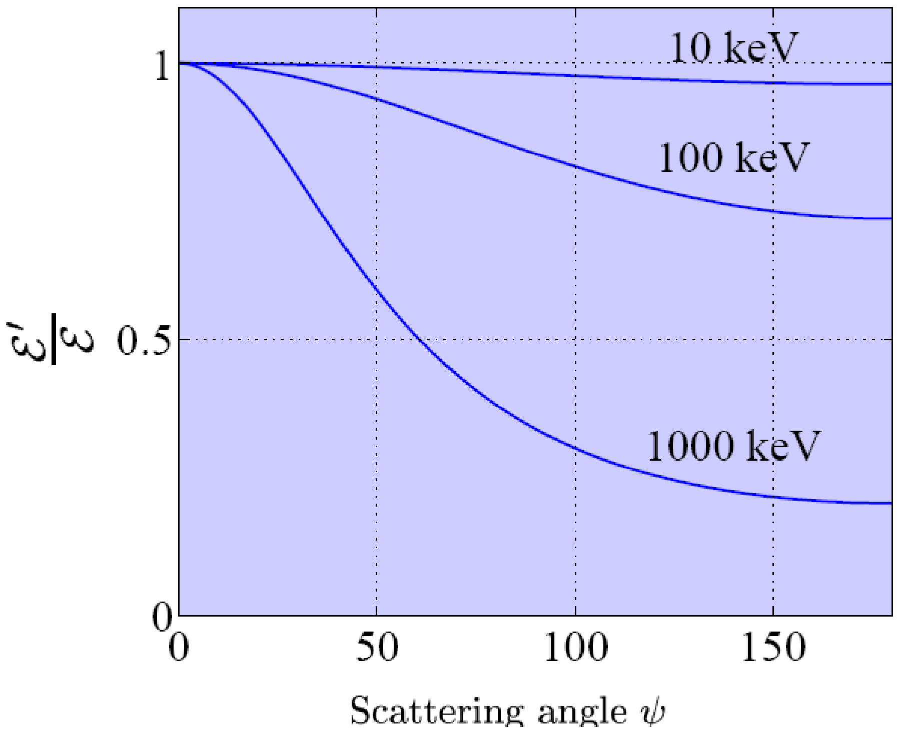

- Vary slowly with scattering angle (more important at higher scattering angle).
- Effective when the x-ray energy approaches the rest mass of electron.
- In a diffraction experiment, it gives rise to a smoothly varying background.

mc^2=511 keV

Diffraction

X-Ray Reflectivity *vs.* Diffraction

reflectivity

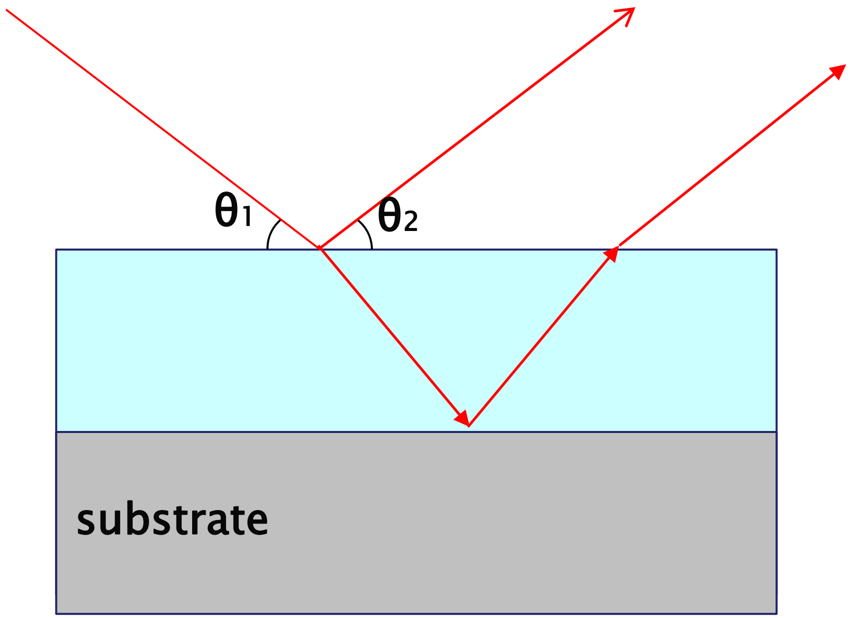

diffraction

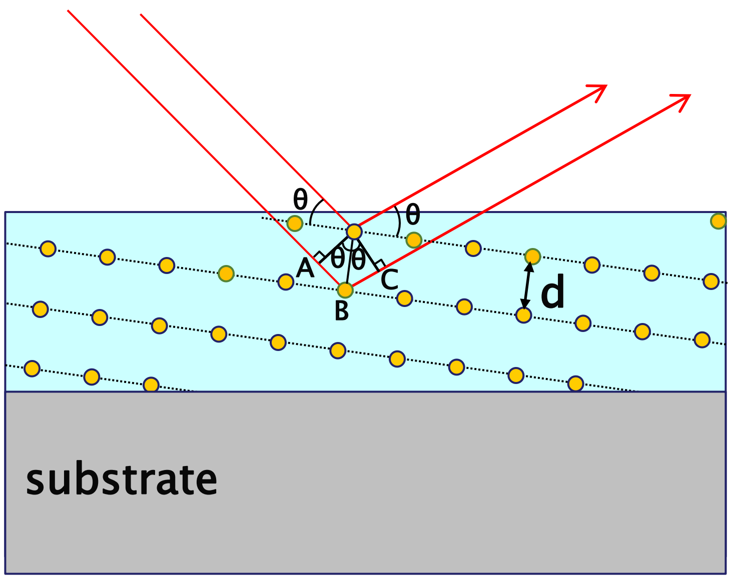

$$2d \sin\theta = m\lambda$$

Bragg's Law

Typical X-ray Diffraction Setup with Lab source

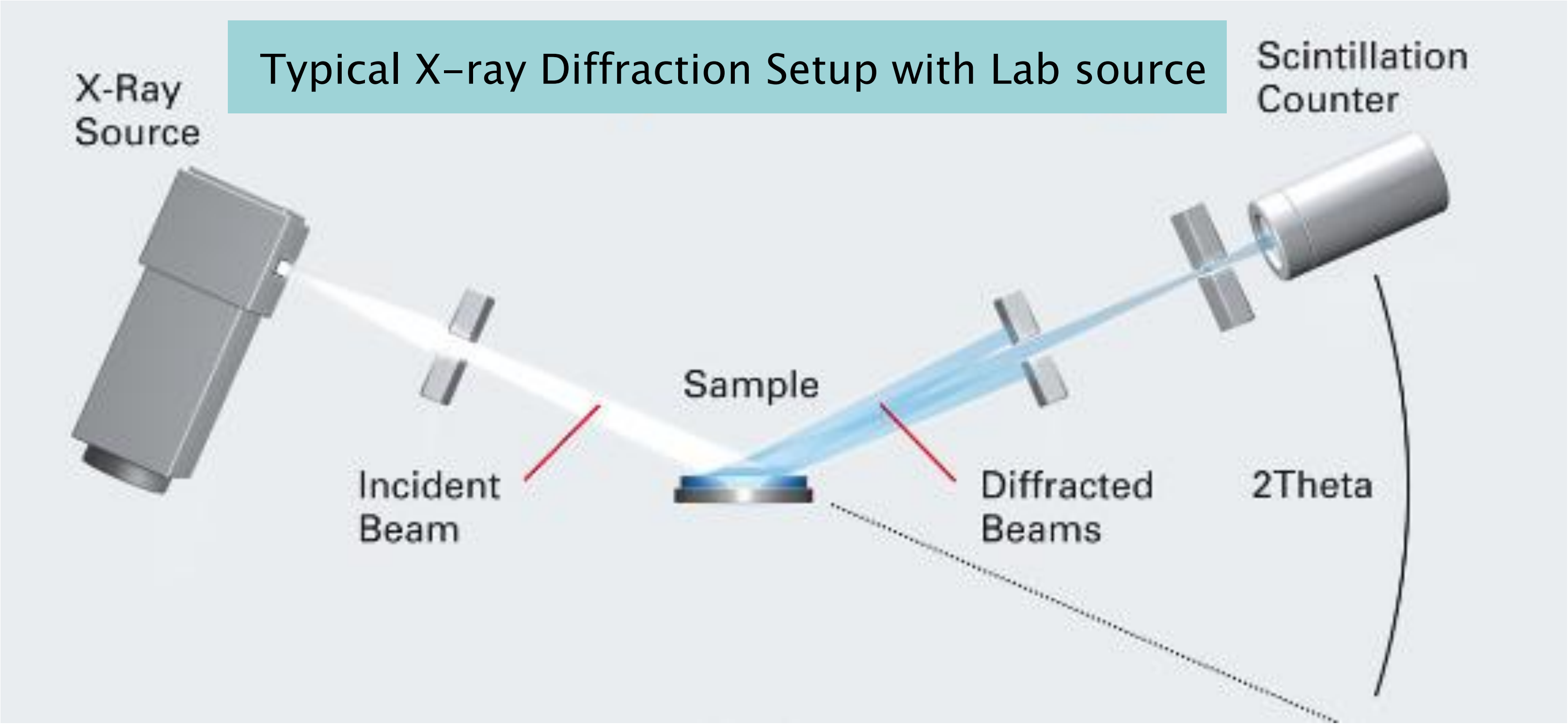

Scattering Geometry

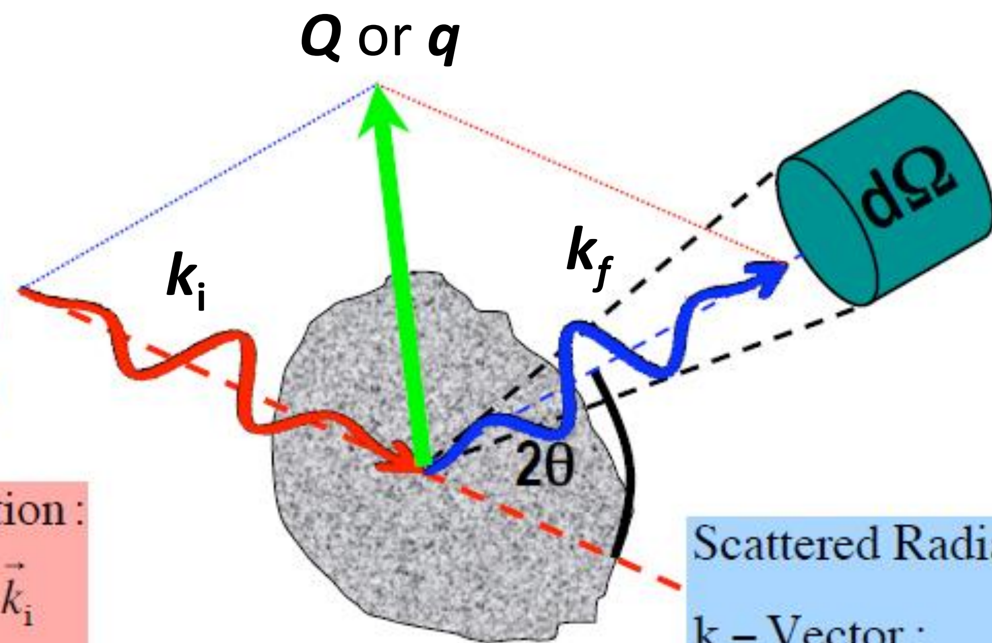

Incident Radiation:

k – Vector: $\vec{k}_i$

$|\vec{k}_i| = 2\pi/\lambda$

Energy: E_i

Polarization: $\vec{p}_i$

Scattered Radiation:

k – Vector: $\vec{k}_f$

Energy: E_f

Polarization: $\vec{p}_f$

Wavevector Transfer:

$\vec{q} = \vec{k}_f - \vec{k}_i$

Energy Transfer:

$\Delta E = E_f - E_i = \hbar\omega$

Polarization:

$\vec{p}_i \rightarrow \vec{p}_f$

For X-Rays:

$\Delta E << E_f, E_i$

$\Rightarrow \quad |\vec{q}| = 2k_i \sin(2\theta/2)$

X-ray Diffractometer (4-circle)

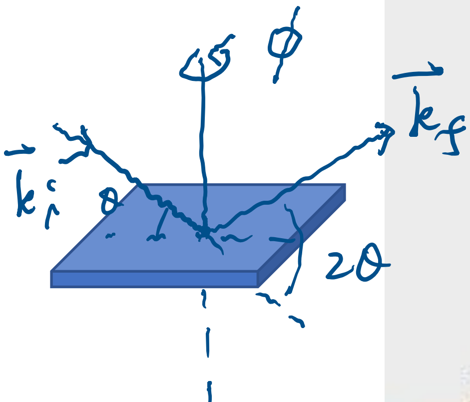

Theta
2-theta
Phi
Chi

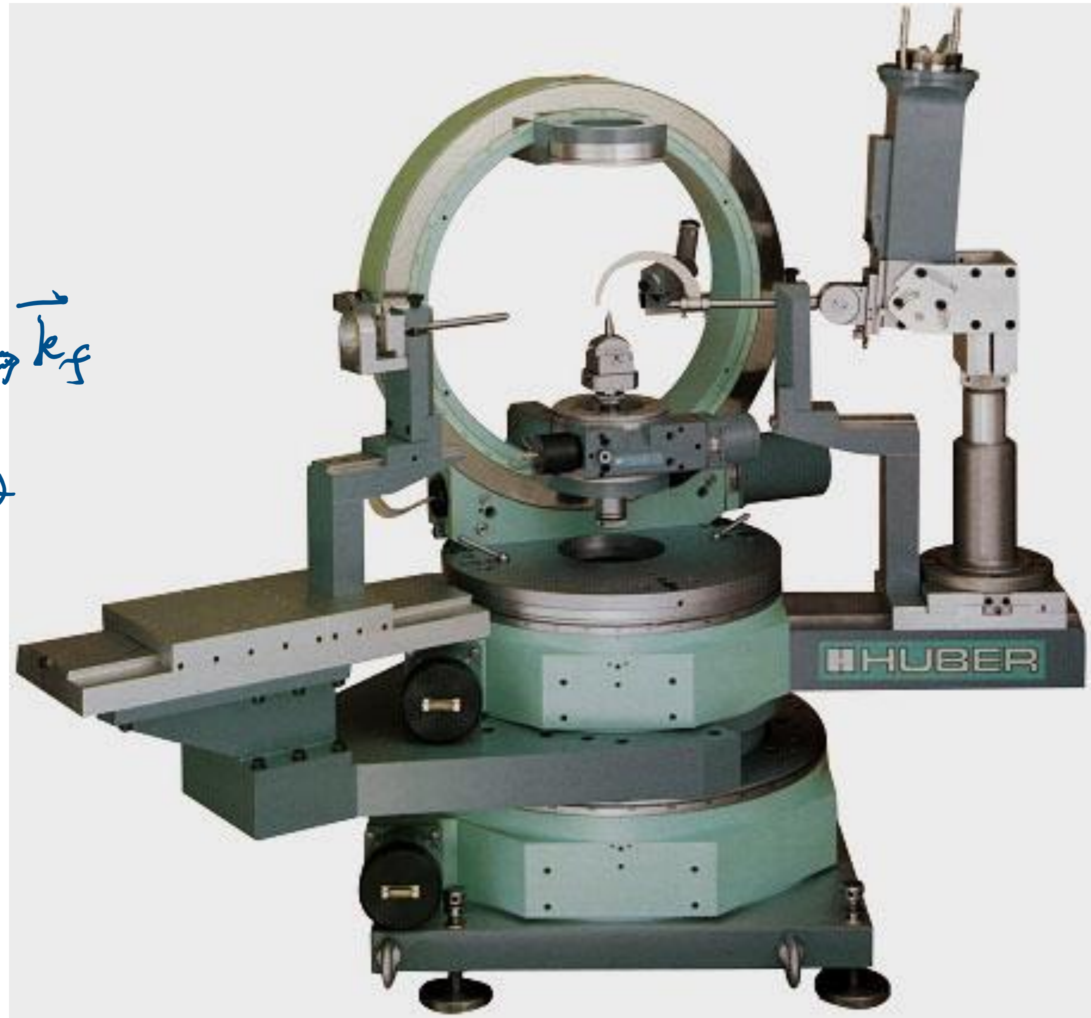

X-ray diffraction from real crystal

Some aspects of real crystals that go beyond these assumptions:

- thermal motion of atoms
- lattice strain
- finite size of crystal
- defects
- disorder

In addition, we had assumed that the photons only scatter once before leaving the sample. In the case of reflectivity, we already know that multiple reflection have to be taken into account when the reflectivity is close to 1.

We have to consider such multiple reflection in Bragg condition.

X-ray Crystallography

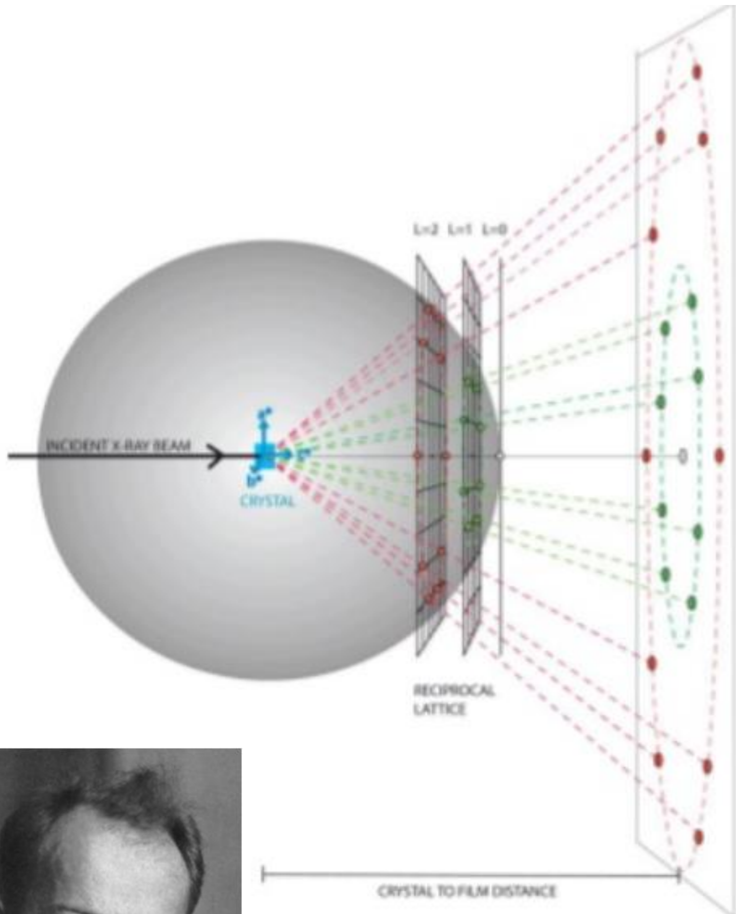

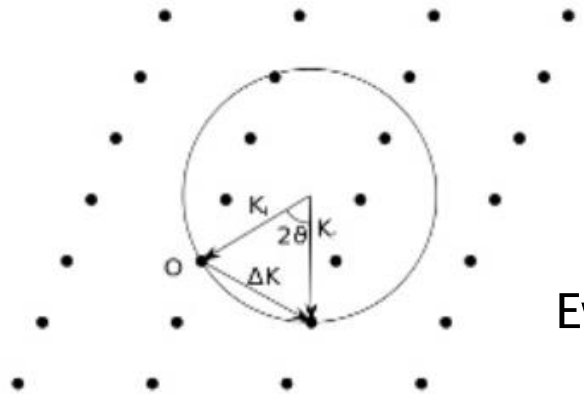

Ewald Sphere

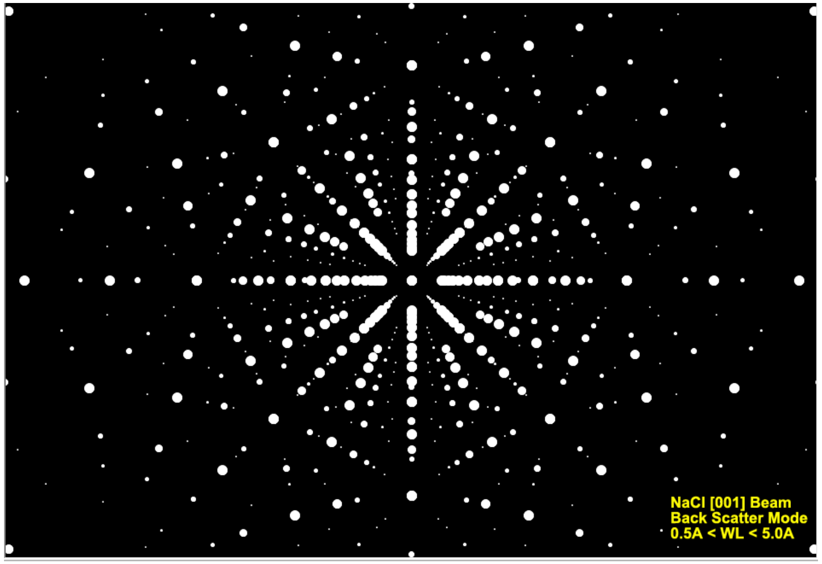

Max von Laue

Nobel Prize Physics 1914

- X-ray crystallography
  : the size of the atoms, the length and types of chemical bonds, the nature and differences of various materials on the atomic scale.
  : knowledge of crystals (the appearance and the symmetry of the crystals)
  : X-rays are just electromagnetic radiation as visible light but of short wavelength

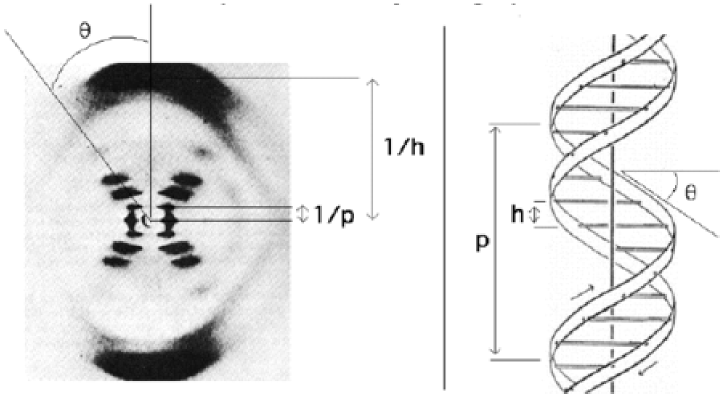

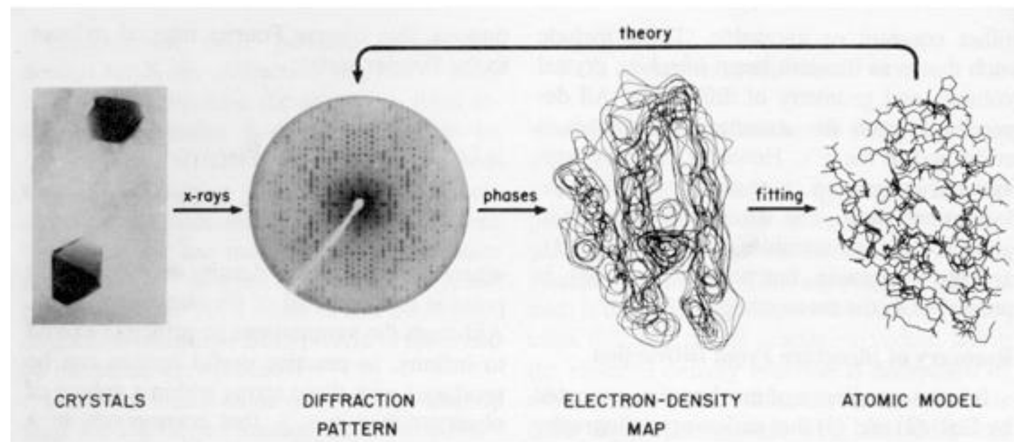

θ - tilt of helix (angle from perpendicular to long axis)

h = 3.4 Å (Distance between bases)

p = 34 Å (Distance for one complete turn of helix; Repeat unit of the helix)

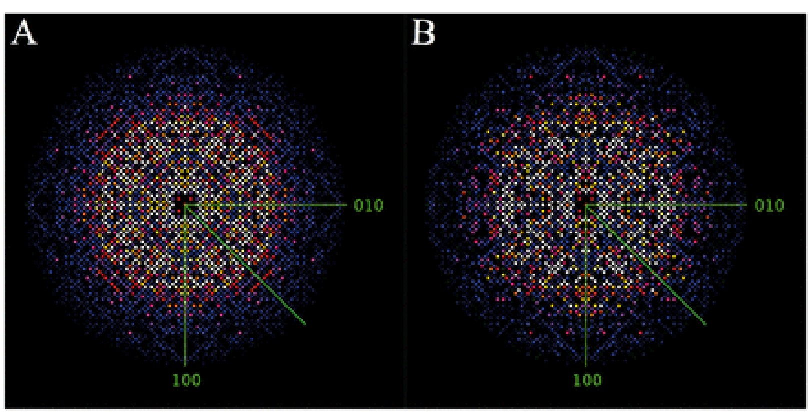

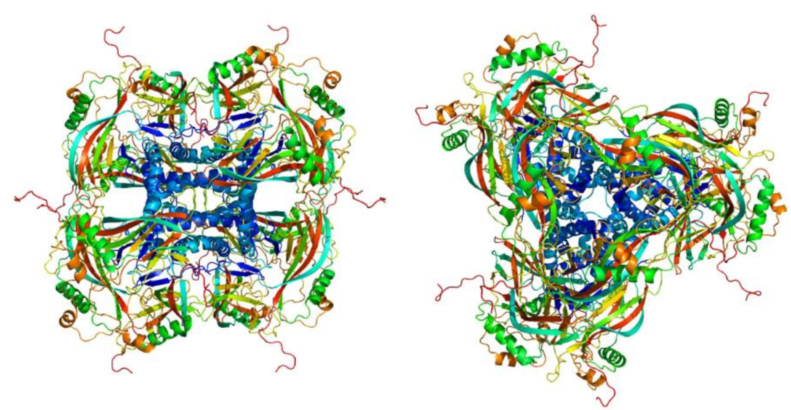

Model of the crystalline protein casing of Cydia pomonella granulovirus, derived from the X-ray diffraction images recorded at LCLS (left, seen from the side; right, seen from above). (Dominik Oberthür, CFEL/DESY)

Powder Diffraction

Powder Diffraction gives Scattering on Debye-Scherrer Cones

Incident beam
x-rays or neutrons

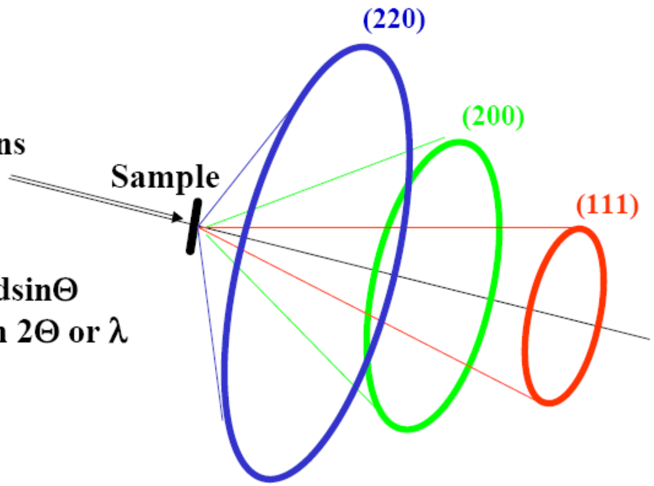

Bragg's Law $\lambda = 2d\sin\Theta$

Powder pattern – scan 2Θ or λ

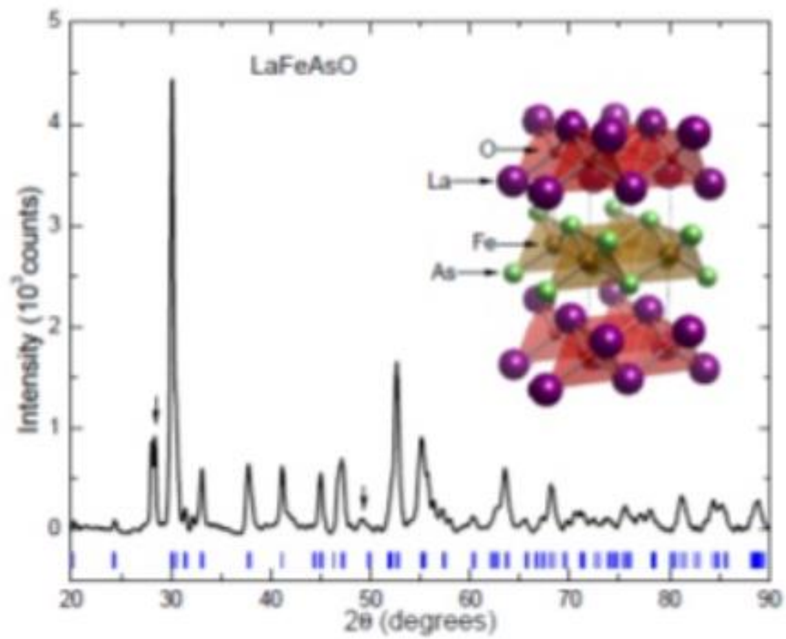

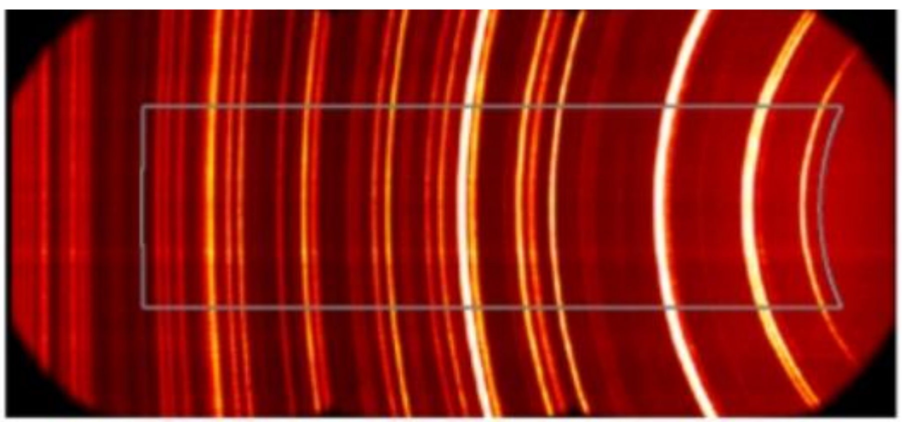

Cubic $$\frac{1}{d^2} = \frac{h^2 + k^2 + l^2}{a^2}$$

Tetragonal $$\frac{1}{d^2} = \frac{h^2 + k^2}{a^2} + \frac{l^2}{c^2}$$

Hexagonal $$\frac{1}{d^2} = \frac{4}{3}\left(\frac{h^2 + hk + k^2}{a^2}\right) + \frac{l^2}{c^2}$$

Why synchrotron radiation?

Synchrotron sources offer

- ✓ Brightnesss (small source, collimated)
- ✓ Tunability (IR to hard x-rays)
- ✓ Polarization (linear, circular)
- ✓ Time structure (short pulses)

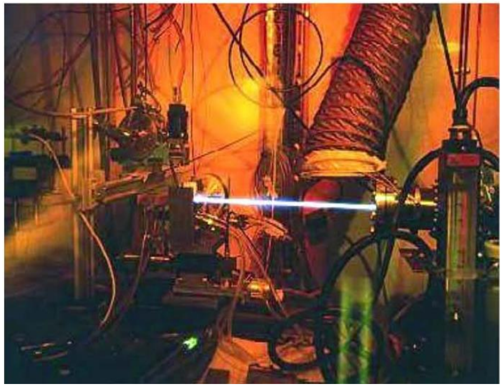

B = photons/source area, divergence, bandwidth

$F_c \sim \lambda^2 B$

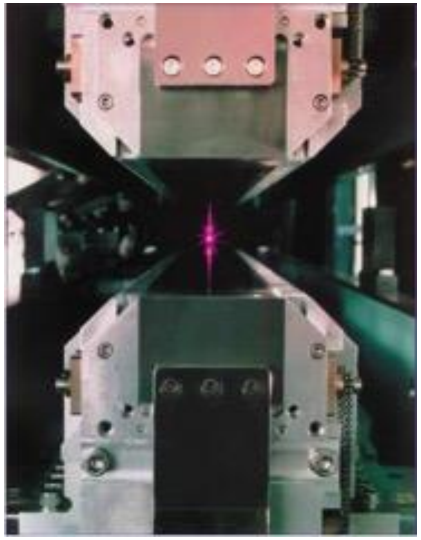

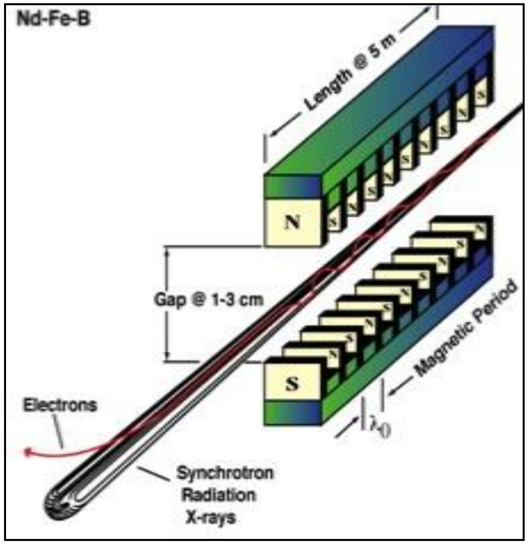

방사광가속기의 진보

Electrons (~GeV)

1st & 2nd Generation

Bending Magnet

3rd Generation

Insertion Device
(Wiggler, Undulator)

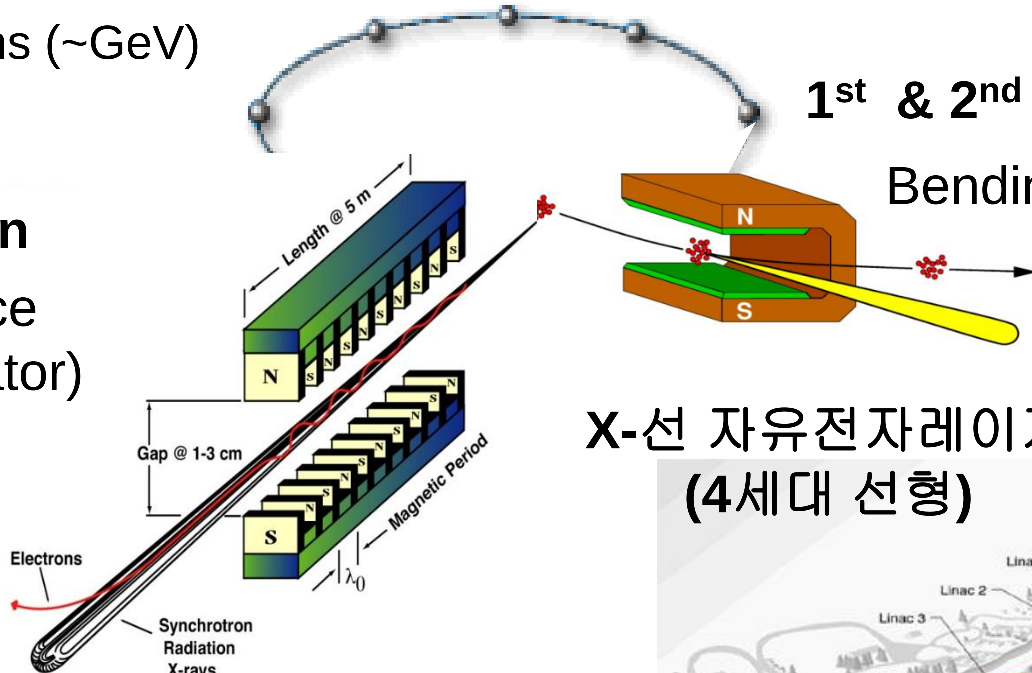

X-선 자유전자레이저 (4세대 선형)

4th Generation (4세대 원형, DLSR)

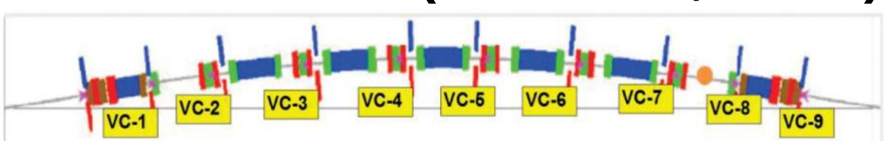

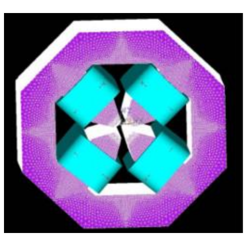

1세대: Parasitic SR mode from existing high-energy machines
2세대: Dedicated SR sources (with IDs later)
3세대: Fully optimized to adopt insertion devices
4세대: Multi-Bend Achromat (MBA)

Intensity and Spectrum

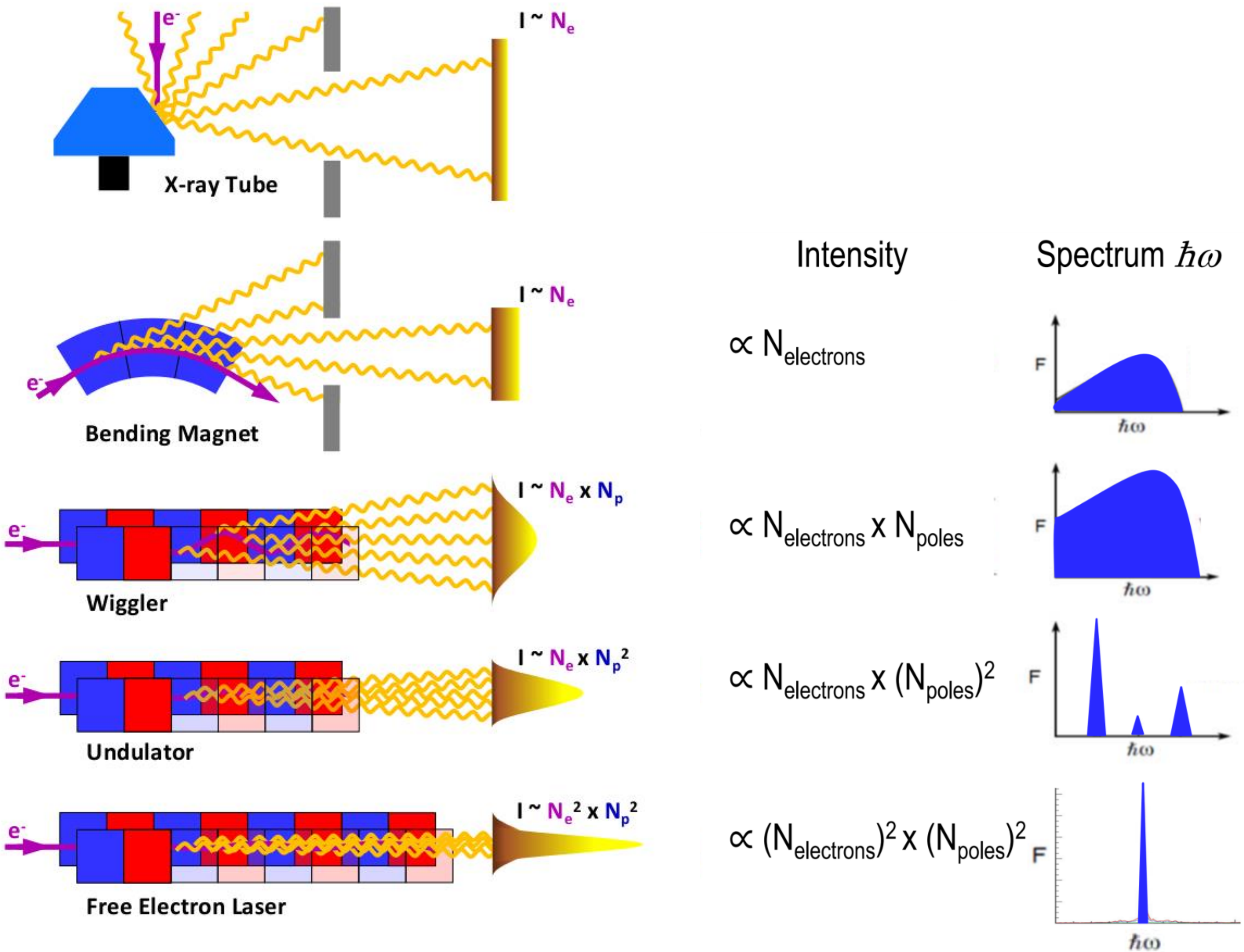

Brilliance & Emittance

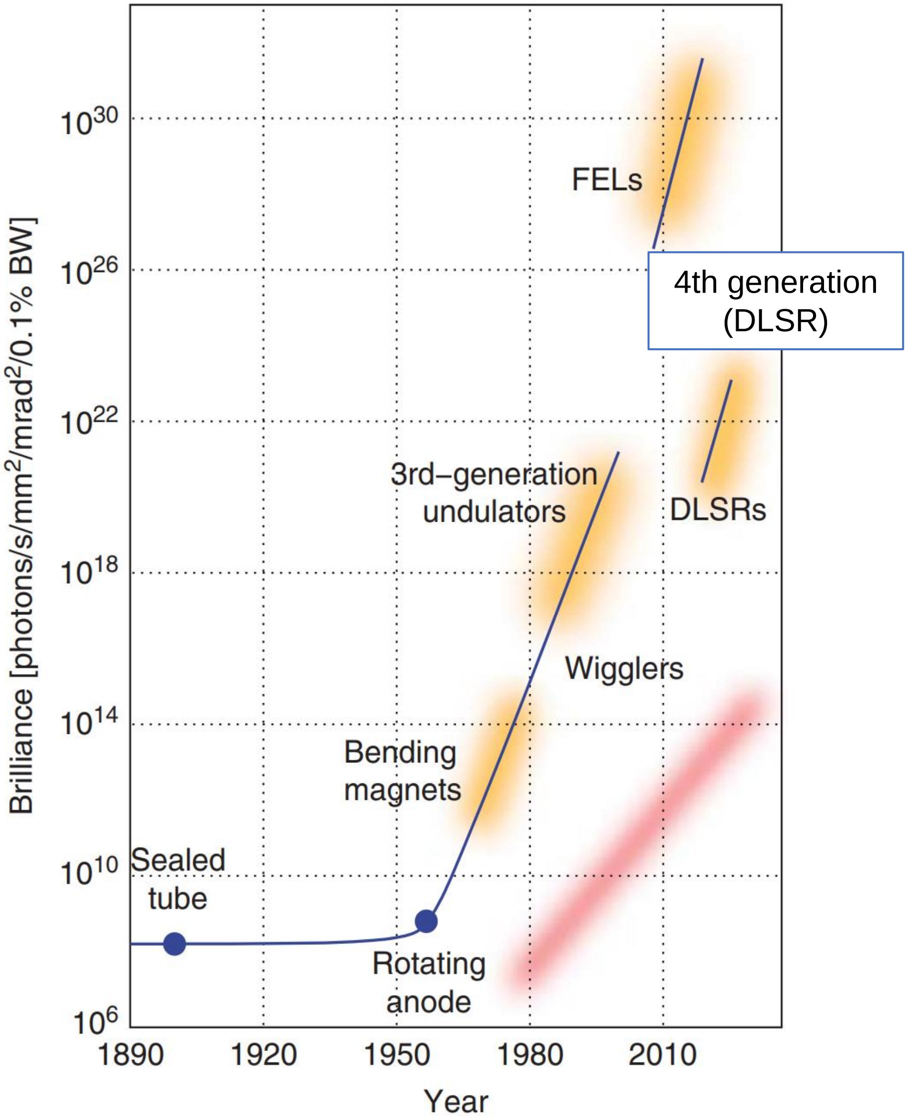

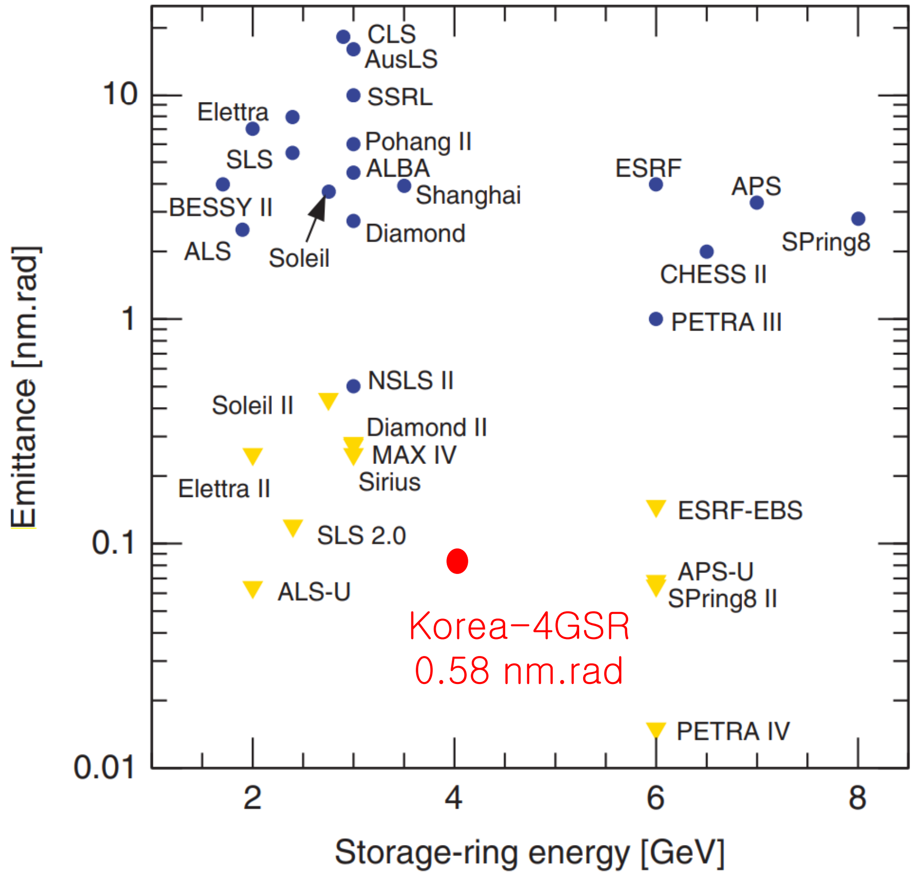

Synchrotron *vs.* XFEL

	Synchrotron 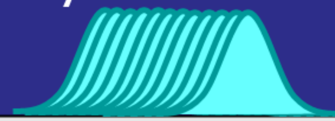	XFEL 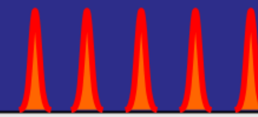
Time Resolution	~ 80 picosec	10–100 femtosec
Rep. Rate	500 MHz	0.1–10 KHz
# Photons/pulse	10^9	10^{12}
Coherent Flux	10^8–10^9 photons/sec	10^{14}–10^{16} photons/sec
Spatial Coherency	0.1%	~100%
Time Coherency	No	0.5%
Bandwidth		0.3×10^{-3}
Photon degeneracy at 9keV	2.2×10^{-4}	3×10^8
Stability	Stable	Not stable

3rd Gen. *vs.* 4th Gen.

	3세대 방사광 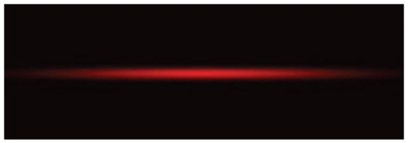	차세대 (4GSR) 
휘도(Brilliance)	10^{20}	$>10^{22}$
빔크기 (Source size)	280μm×11μm (H×V)	8μm×10μm (H×V)
결맞는 X-선 (Transverse coherence lengths (9keV))	12μm×340μm (H×V)	420μm×340μm (H×V)
펄스폭 (Pulse length)	80ps	35-70ps
반복율 (Repetition rate)	~650MHz	10-100 MHz

미국 APS와 APS-U의 사양 비교

- ✓ 높은 에너지의 X-선 빔이 가능
  - : 원자 수준의 구조 분석
  - : 실제 작동 상황에서 측정
- ✓ 작고, 센 X-선 빔 가능
  - : 공간 분해능: 수 나노 미터
  - : 실 상황에서 측정 용이
- ✓ 결맞음성이 좋은 X-선 빔 획득
  - : 나노미터 크기의 프로브
  - : 이미징
  - : 동역학 연구

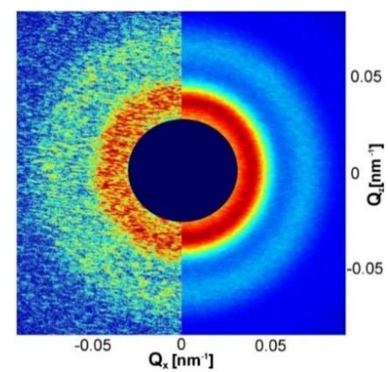

국내 현황

3세대 방사광가속기

- **포항 PLS-II**
- 3 GeV (둘레 280m)
- ~20 keV
- 35 Beamlines
- Emittance: 5800 pm.rad (Hor.)
- 500 MHz
- Pulse duration ~100 ps

4세대 XFEL

- **포항 PAL-XFEL**
- 10 GeV (길이 1.1 km)
- 2-15 keV, 0.25-1.25 keV
- 3 Stations
- ~100% coherence
- Pulse 120Hz
- Pulse duration 10-40 fs

4세대 다목적방사광가속기

- **오창 (2028년 운영 목표)**
- 4 GeV (둘레 800 m)
- ~30 keV (100 keV 까지도 가능)
- ~40 Beamlines
- Emittance: 58 pm.rad (Hor.)
- 500 MHz
- Pulse duration ~100 ps
- 3세대 대비 수 백배 이상의 휘도

Beam 특성

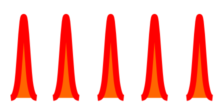

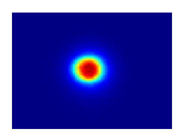

Coherent X-rays

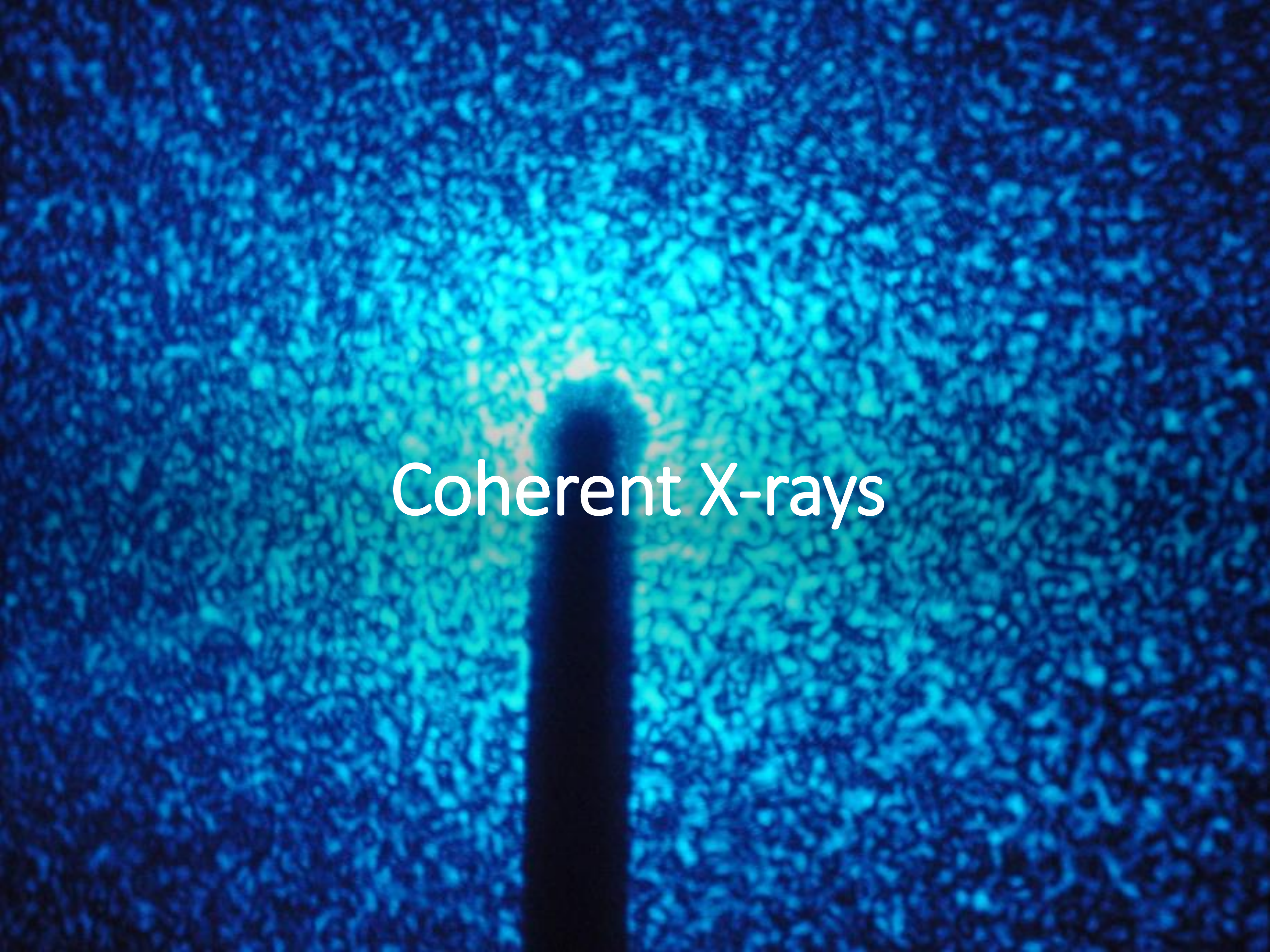

Coherence

$$\Gamma(\mathbf{r}_1, \mathbf{r}_2; \tau) = \langle E^*(\mathbf{r}_1, t) E(\mathbf{r}_2, t+\tau) \rangle$$

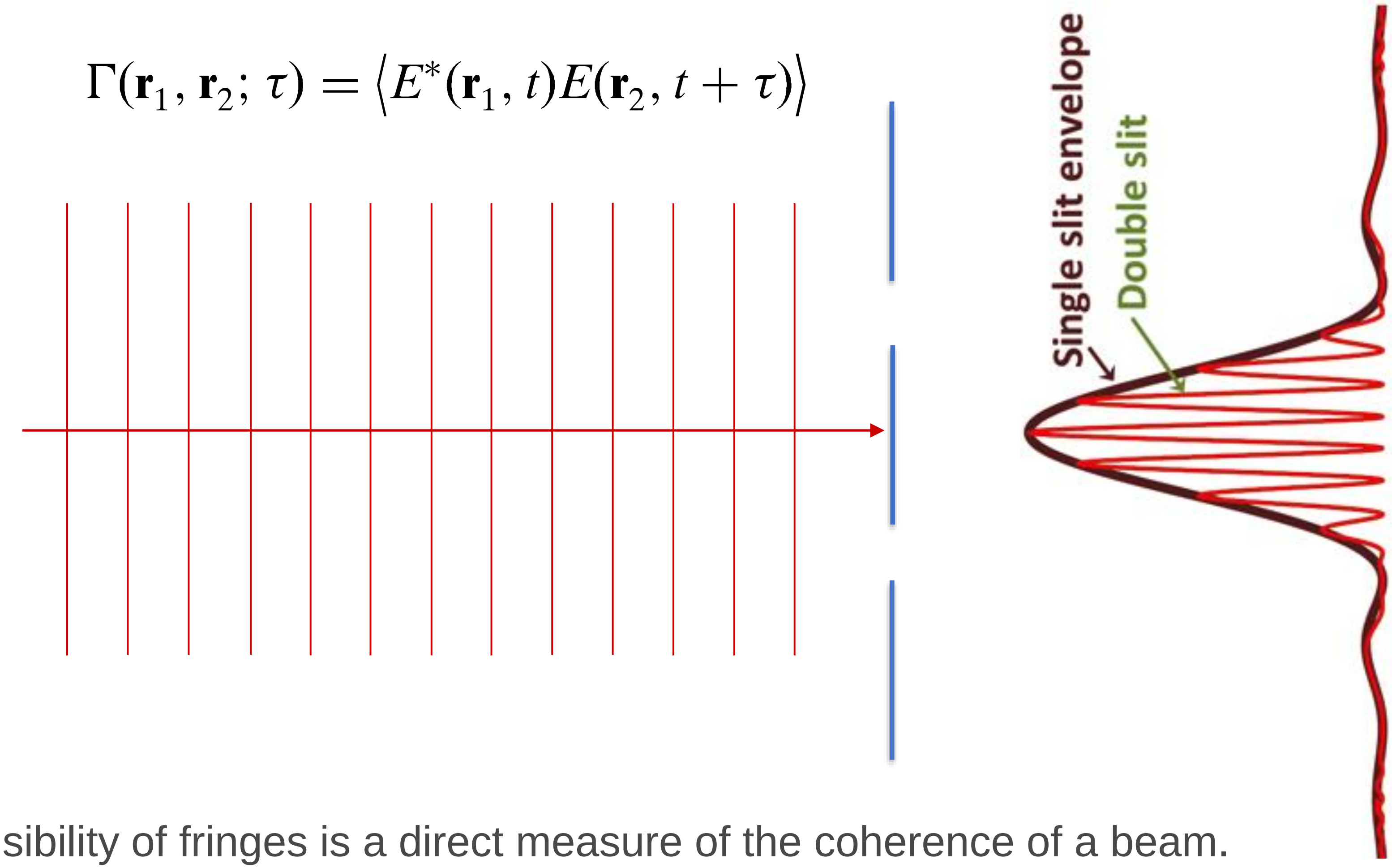

Visibility of fringes is a direct measure of the coherence of a beam.
If beam is coherent across the spacing of the slits a Fourier Transform of the slit structure is observed downstream.

Coherence

longitudinal coherence

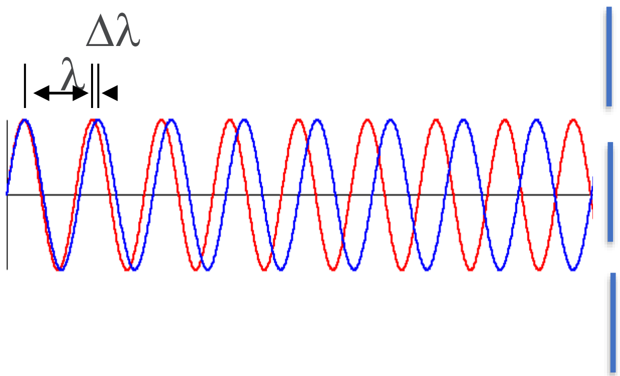

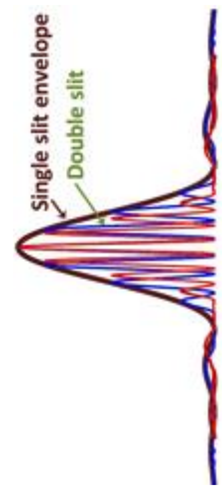

$$l_c \sim \frac{\lambda^2}{\Delta\lambda}$$

$$\tau_c \sim \frac{\lambda^2}{c\Delta\lambda}$$

Si (111)
0.5 um or 1.5 fs

transverse coherence

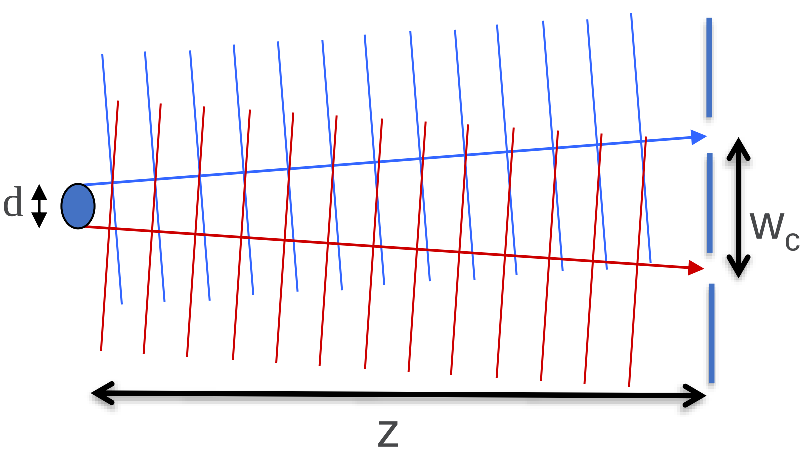

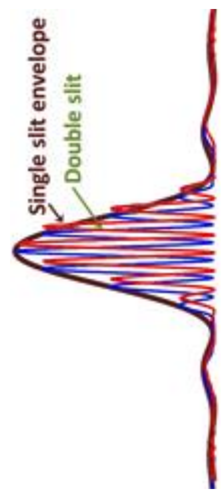

$$w_c \sim \frac{l\,z}{d}$$

d = 50m
25x70 um @ 9 keV
(APS)

Coherence: Laser Speckle

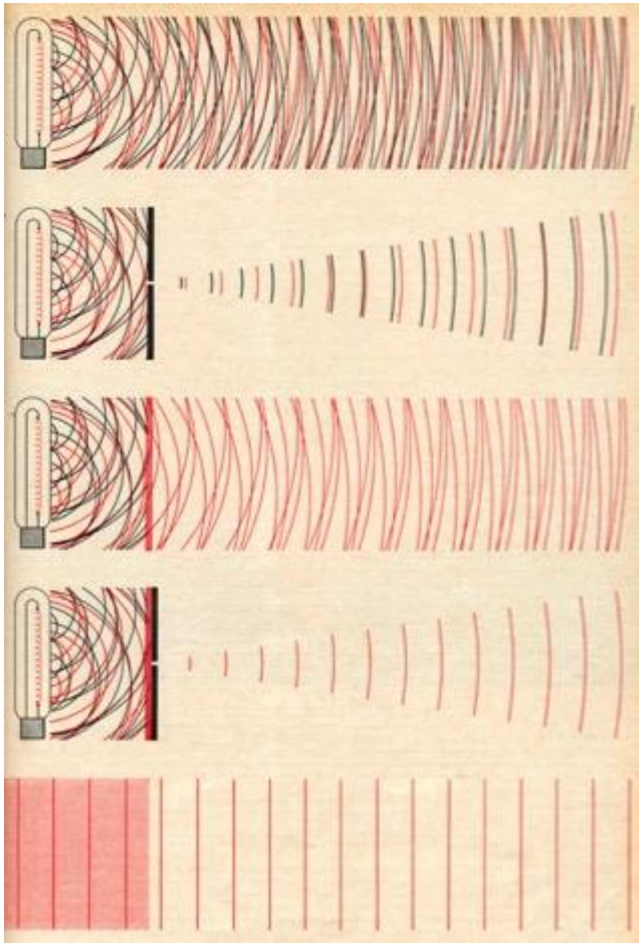

A. L. Schawlow “Laser Light"

Scientific American, 219 (3), p. 120, (1968)

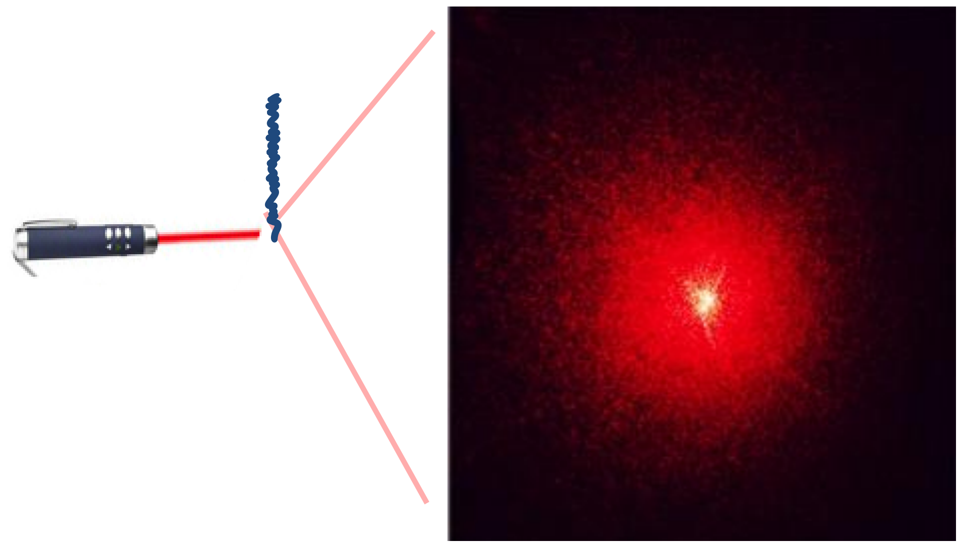

Laser Speckle:
Interference pattern arising from randomly distributed scatterers

Courtesy Prof. Oleg Shpyrko (UCSD)

First Speckle: Exner, 1877

(using candle light)

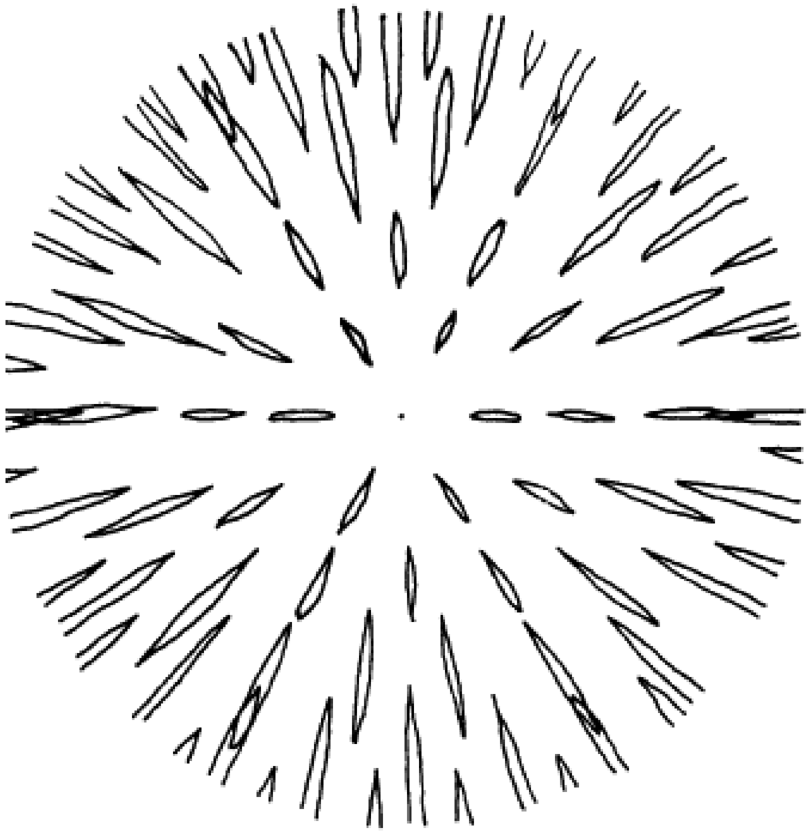

K. Exner: Sitzungsber. Kaiserl. Akad. Wiss. (Wien) 76, 522 (1877)

First Speckle Photo: von Laue, 1914

(using arc discharge lamp)

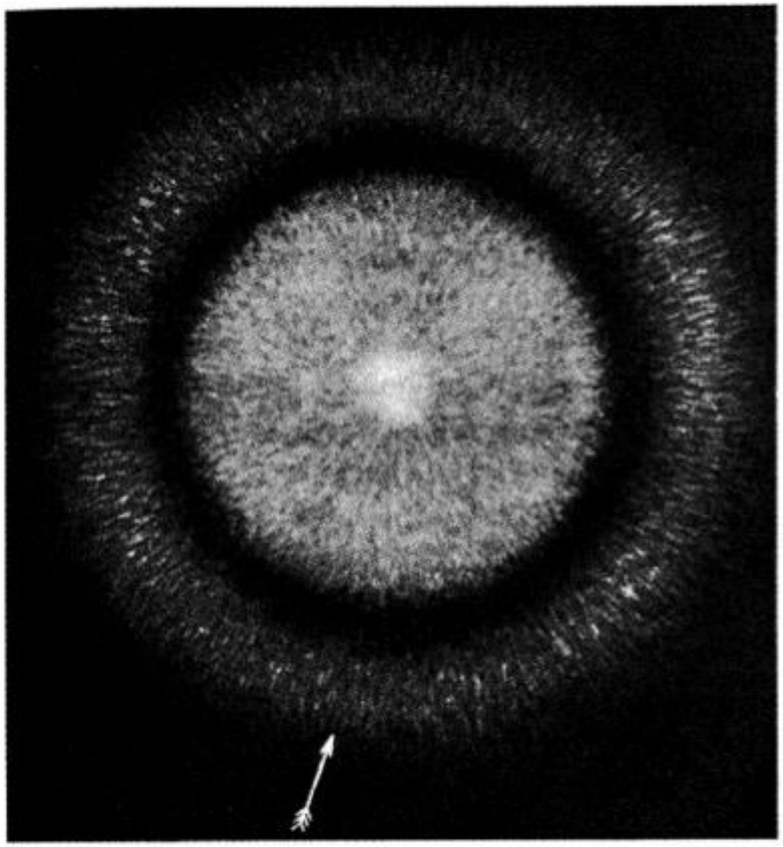

M. von Laue: Sitzungsber. Akad. Wiss. (Berlin) 44, 1144 (1914)

First X-ray Speckle

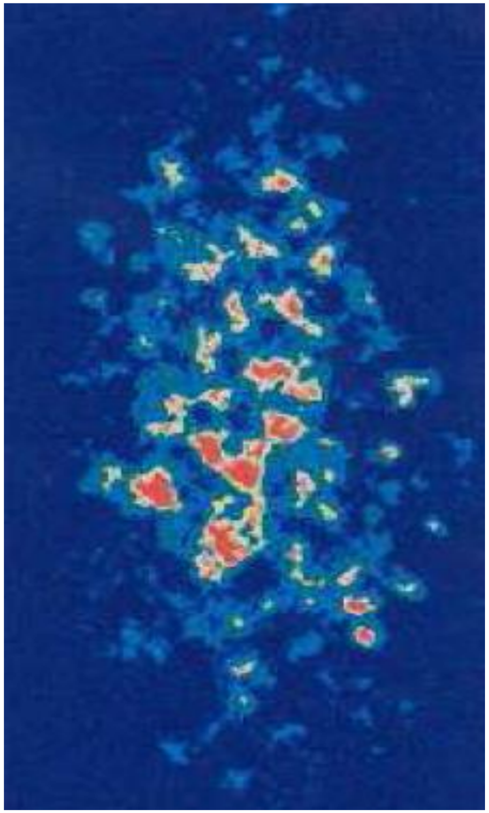

Speckle of (001) Cu_3Au

M. Sutton, et.al., Nature **352**, 608 (1991).

$$I \propto \left|F(q)\right|^2$$

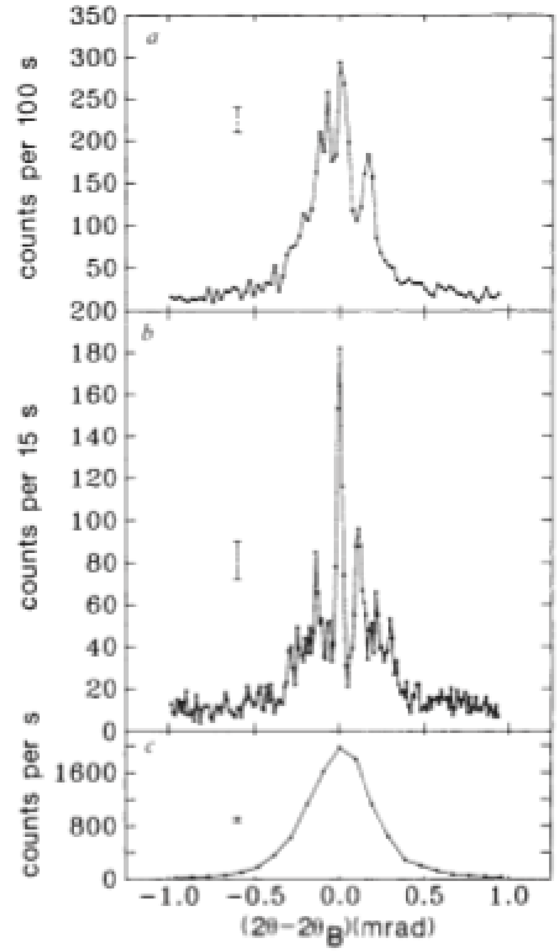

FIG. 4 Speckle patterns measured using a, 2.5-μm, b, 5 μm and c, 50-μm collimating pinholes. The analysing pinholes used were 50, 25 and 100 μm, respectively. Representative error bars are indicated, and the solid lines simply connect the data points. The (001) Bragg angle, $2\theta_B$, is ~23.9°.

Coherent *vs.* Incoherent

Small-angle X-ray scattering pattern of silica nanospheres

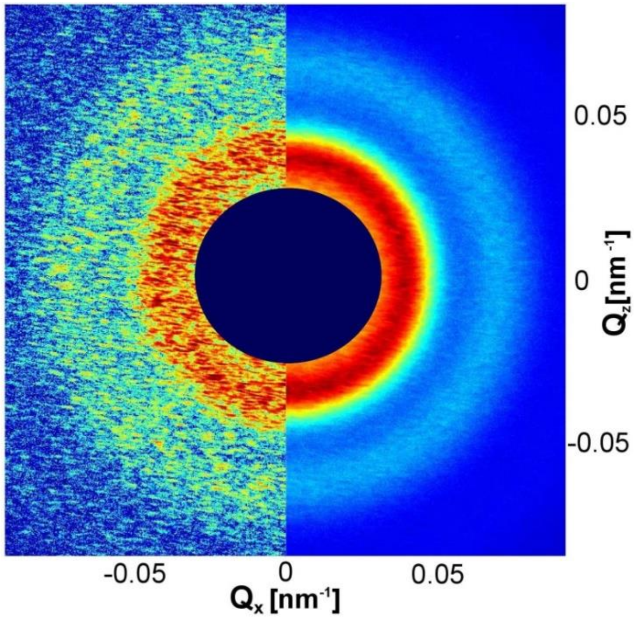

S. Lee, *et al.*,
Optics Express **21**, 24647 (2013).

Coherent scattering
- Speckle pattern directly related to the electron density
- Speckle arising from the path length difference of X-rays in the sample
- Local information

Incoherent scattering
- Statistical average of incoherently scattering regions
- No speckle
- Local information lost

“Speckle” ⇒ Coherence based Techniques

First X-ray Speckle

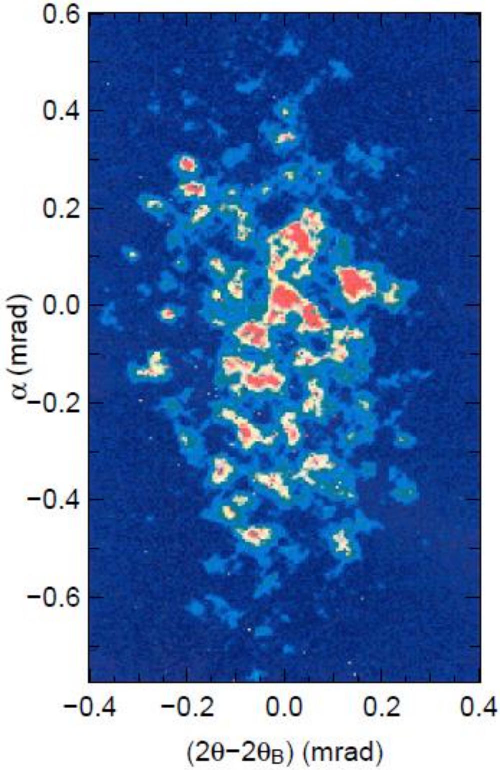

$$I \propto |F(q)|^2$$

Speckle of (001) Cu_3Au

M. Sutton, et.al., Nature **352**, 608 (1991).

Studying Dynamics:
X-ray Photon Correlation Spectroscopy (XPCS)

Imaging:
Coherent X-ray Diffraction (CXD)

Fourier Transform Holography

….

X-ray Photon Correlation Spectroscopy

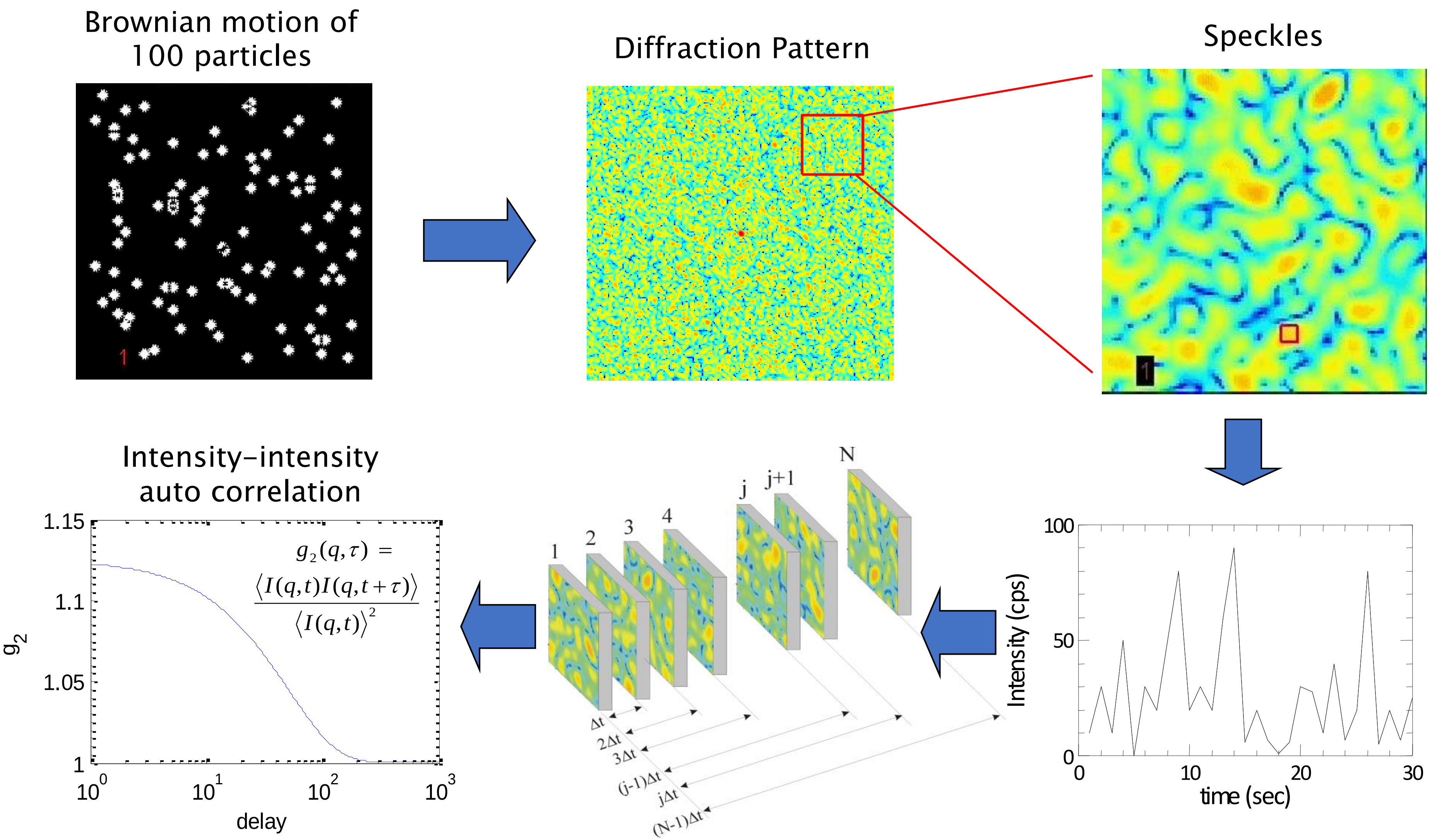

→ S(Q, t) Dynamic Structure Factor

In courtesy of J. Zhang

Application: XPCS

Bulk

Hard

- Equilibrium critical fluctuations
- Decomposition kinetics
- Antiphase-domain dynamics
- Ordering Kinetics
- Domain Fluctuations
- Coarsening

Soft

- Diffusion
- Phase Transition
- Hydrodynamic Fluctuations
- Ordering & relaxation dynamics
- Atomic Diffusion

Surface

- Liquid crystal (Smectic Membranes)
- Liquid (Water, Glycerol, etc)
- Polymer Films: Confinement? Selective detection?
- Organic Semiconductors, etc.

Nano dynamics: Soft materials & Nano system

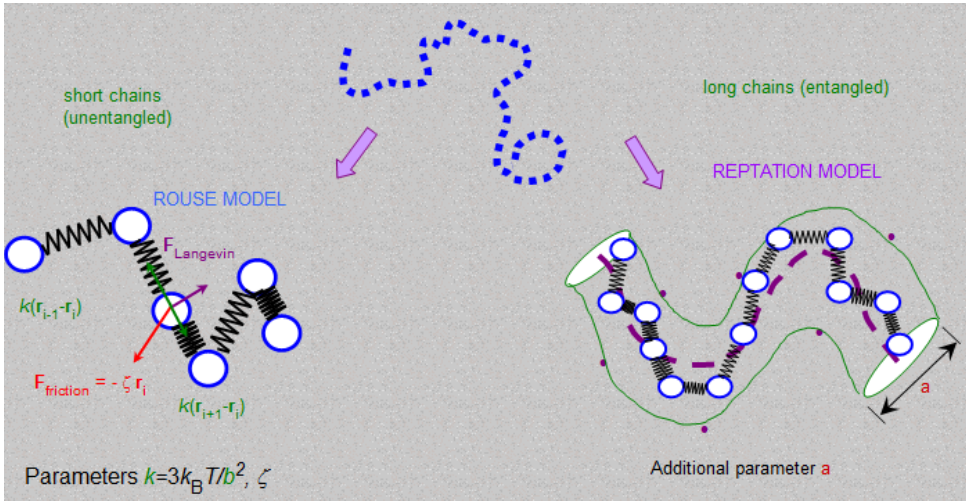

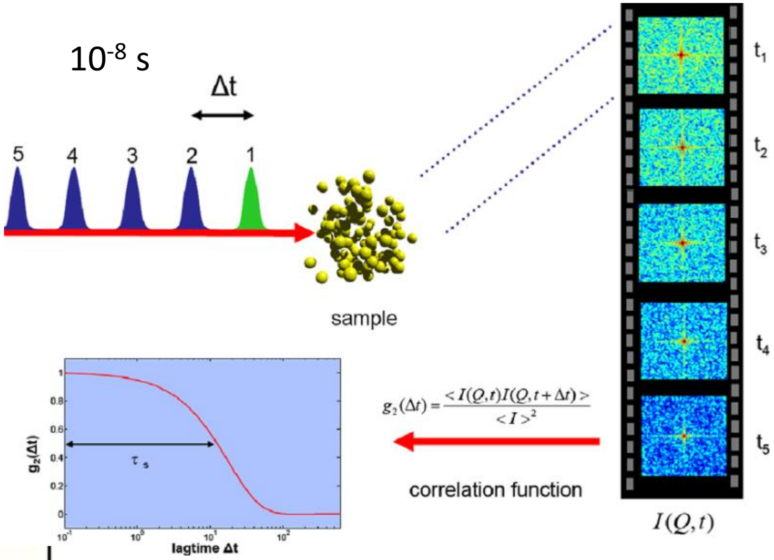

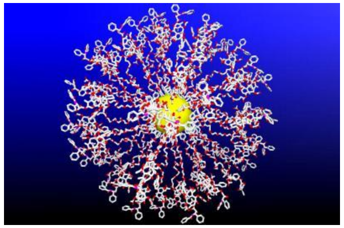

nanoparticles

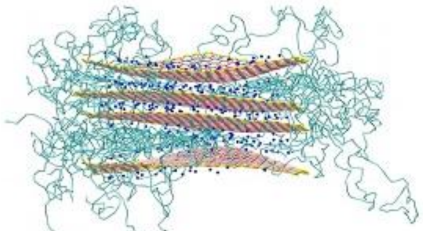

nanocomposites

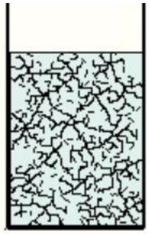

colloids
colloidal jels

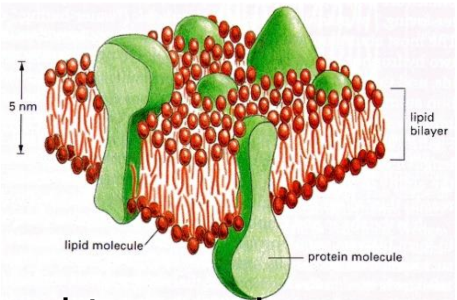

bio-membranes

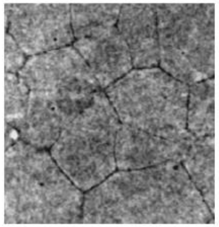

micellar
polycrystal

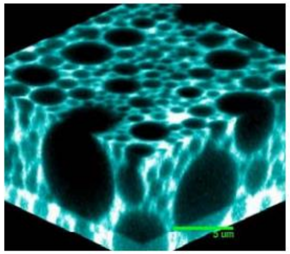

emulsions

나노초-초
Dynamics 가능

Coherent small angle x-ray scattering beamline

Surface Dynamics

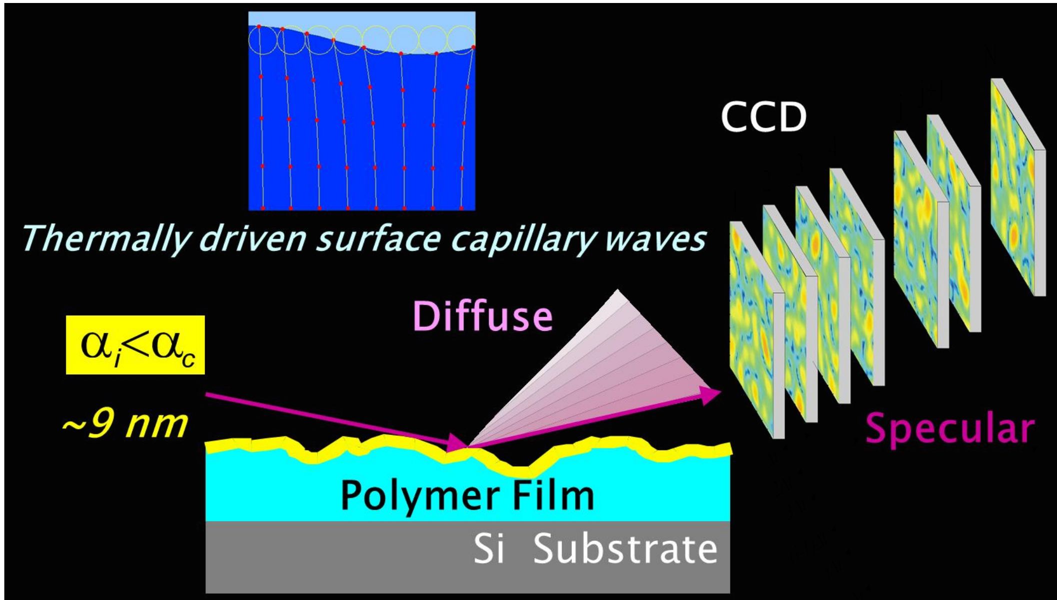

Organic Semiconductors, (OLED, OTFT, OPV)

GISAXS, GID

Surface Dynamics of Polymer Films, PRL 90, 068302 (2003).
Viscoelastic Effects in Ultrathin Films, PRL 98, 227801 (2007).
Surface Dynamics near Tg in High q, PRL 101, 246104 (2008).
Surface Dynamics of “Dry” Homopolymer Brushes, Macromolecules 42, 737 (2009).

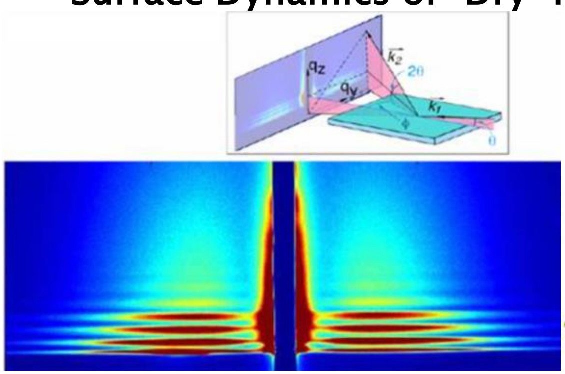

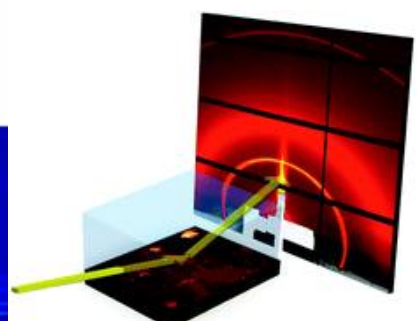

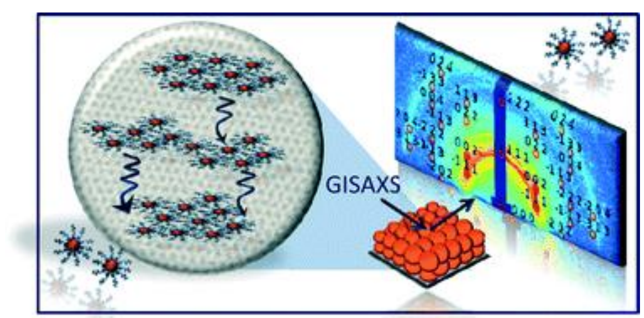

In-situ growth

High Energy E=25.75 keV

MOCVD, GaN growth

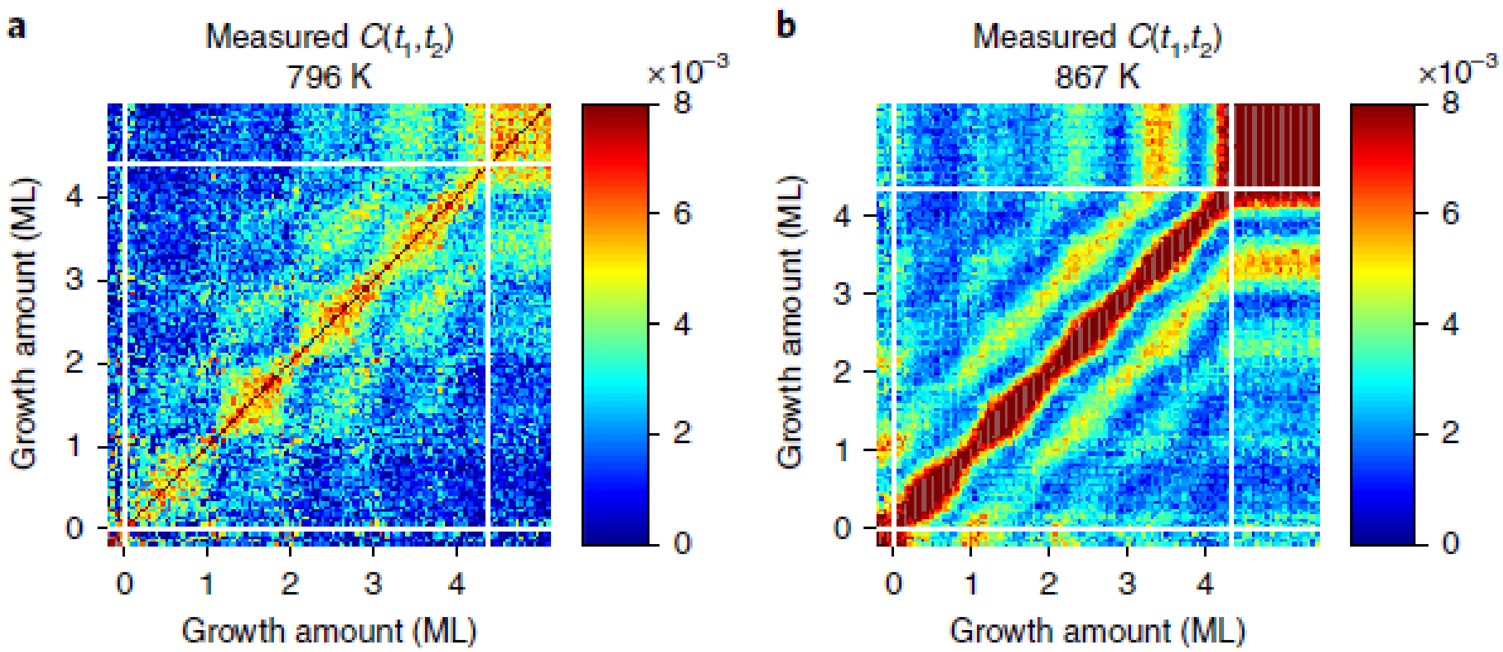

Coherent X-ray spectroscopy reveals the persistence of island arrangements during layer-by-layer growth, **Nature Physics (2019)**

Imaging Regime of Coherent X-rays

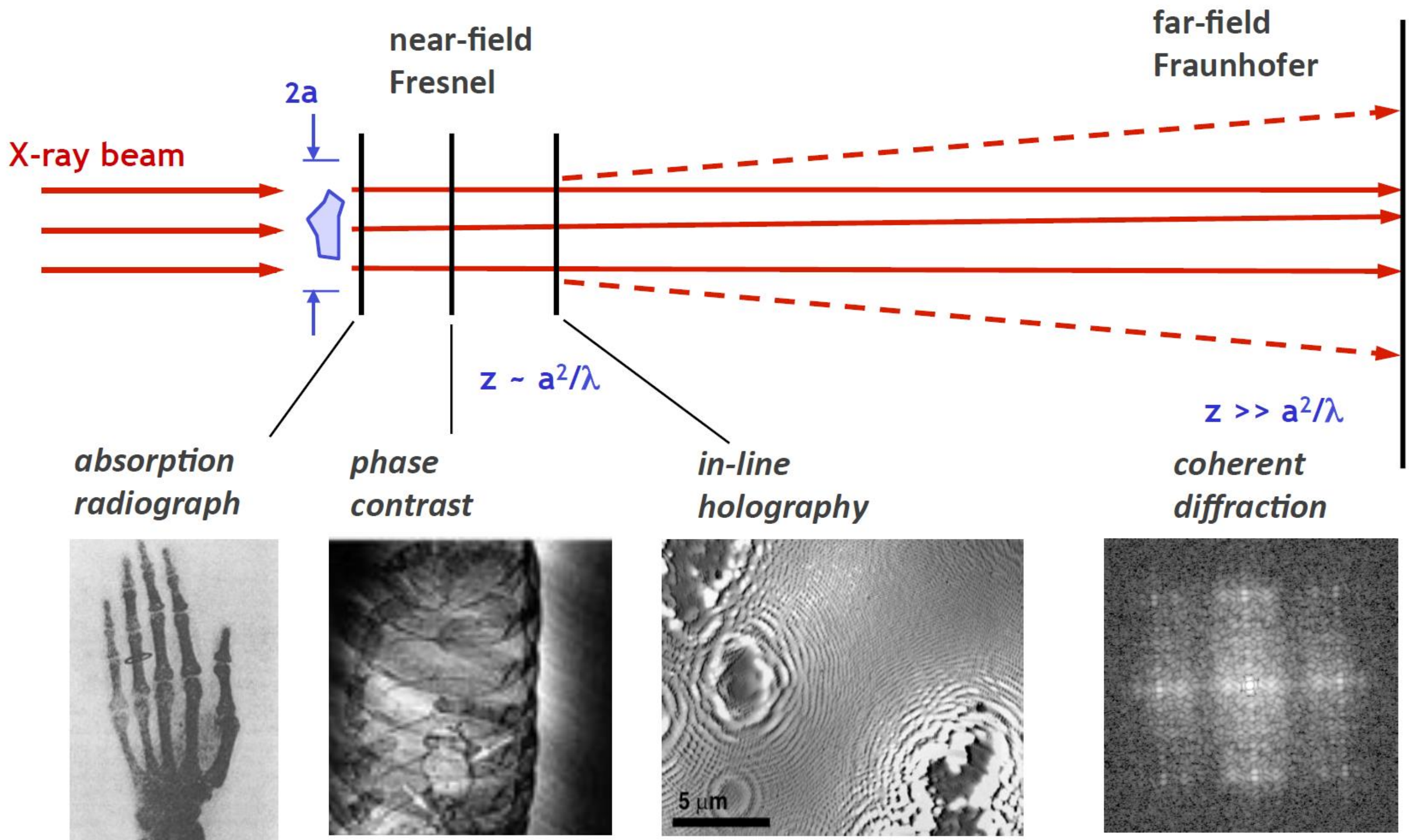

Kagoshima (1999)

Jacobsen (1990)

Miao (1999)

Bragg Coherent Diffraction Imaging

Coherent X-ray Diffraction Pattern

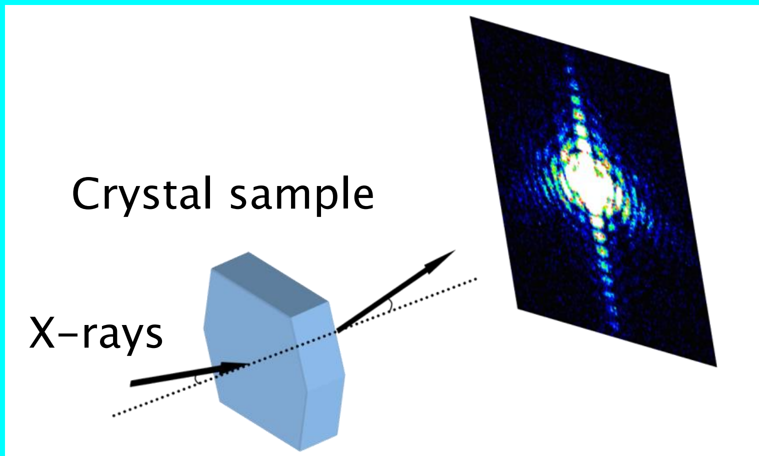

Phase Retrieval Algorithm

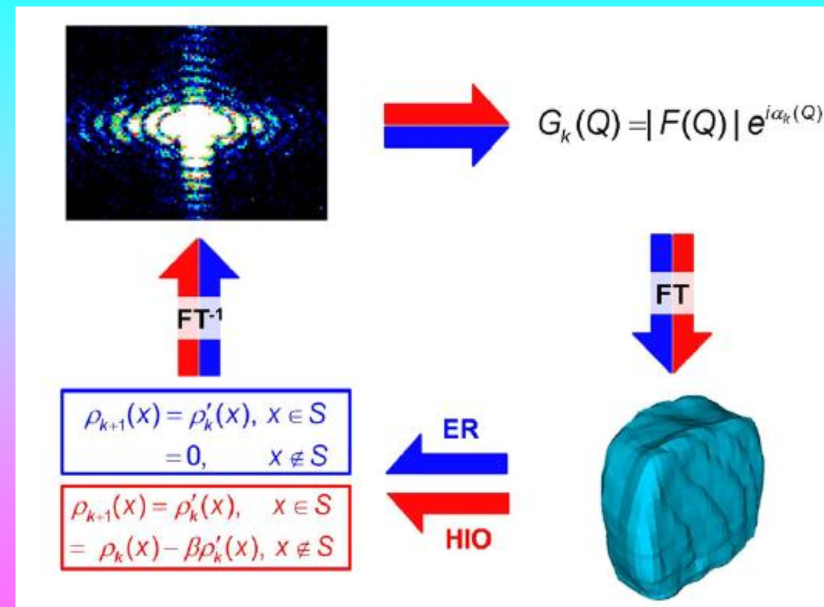

Shape

&

Phase

Atomic Displacement

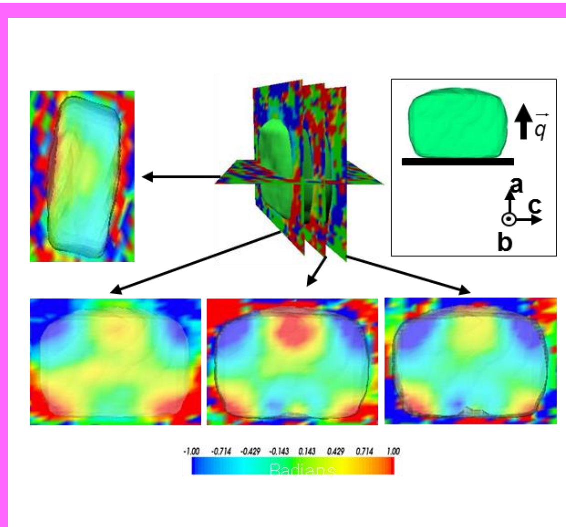

Coherent X-ray Diffraction Studies of Inorganic Crystalline Nanomaterials, Wonsuk Cha, Sungwook Choi, Hyunjung Kim

Reference Module in Chemistry, Molecular Sciences and Chemical Engineering 2022

https://doi.org/10.1016/B978-0-12-823144-9.00082-0

Diffraction vs. Interference

Double Slit

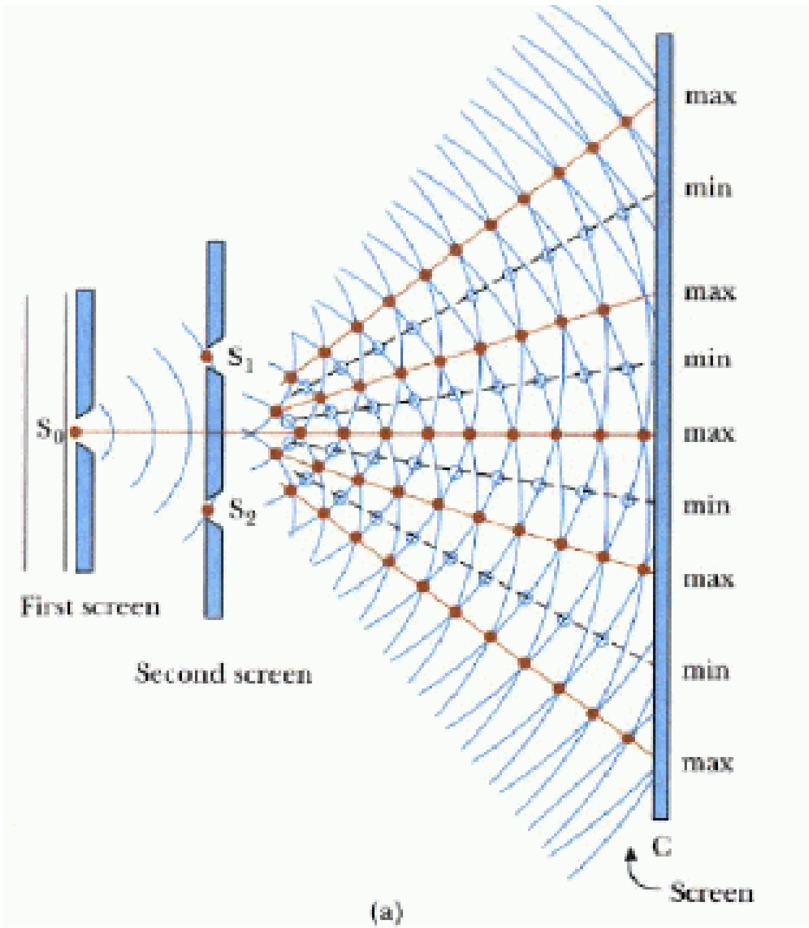

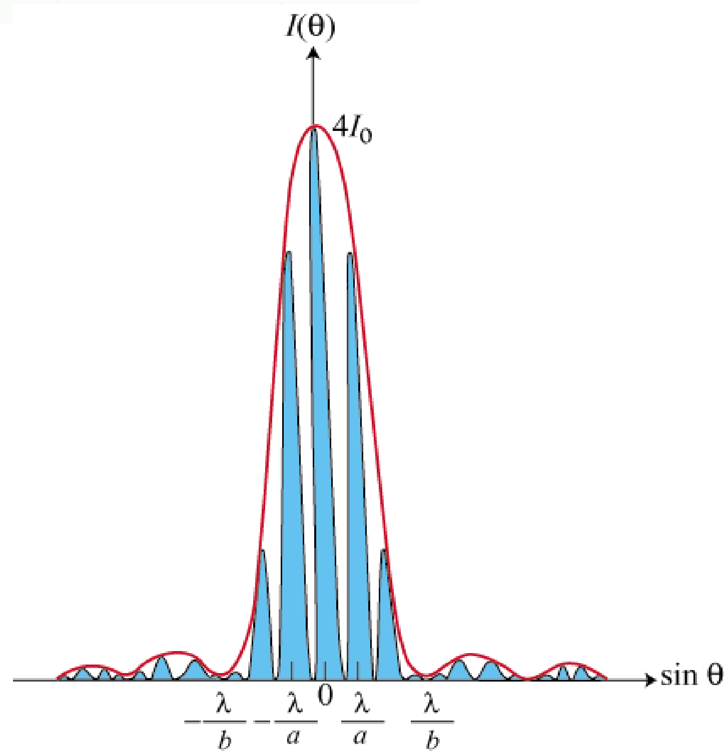

Phase Retrieval Algorithm

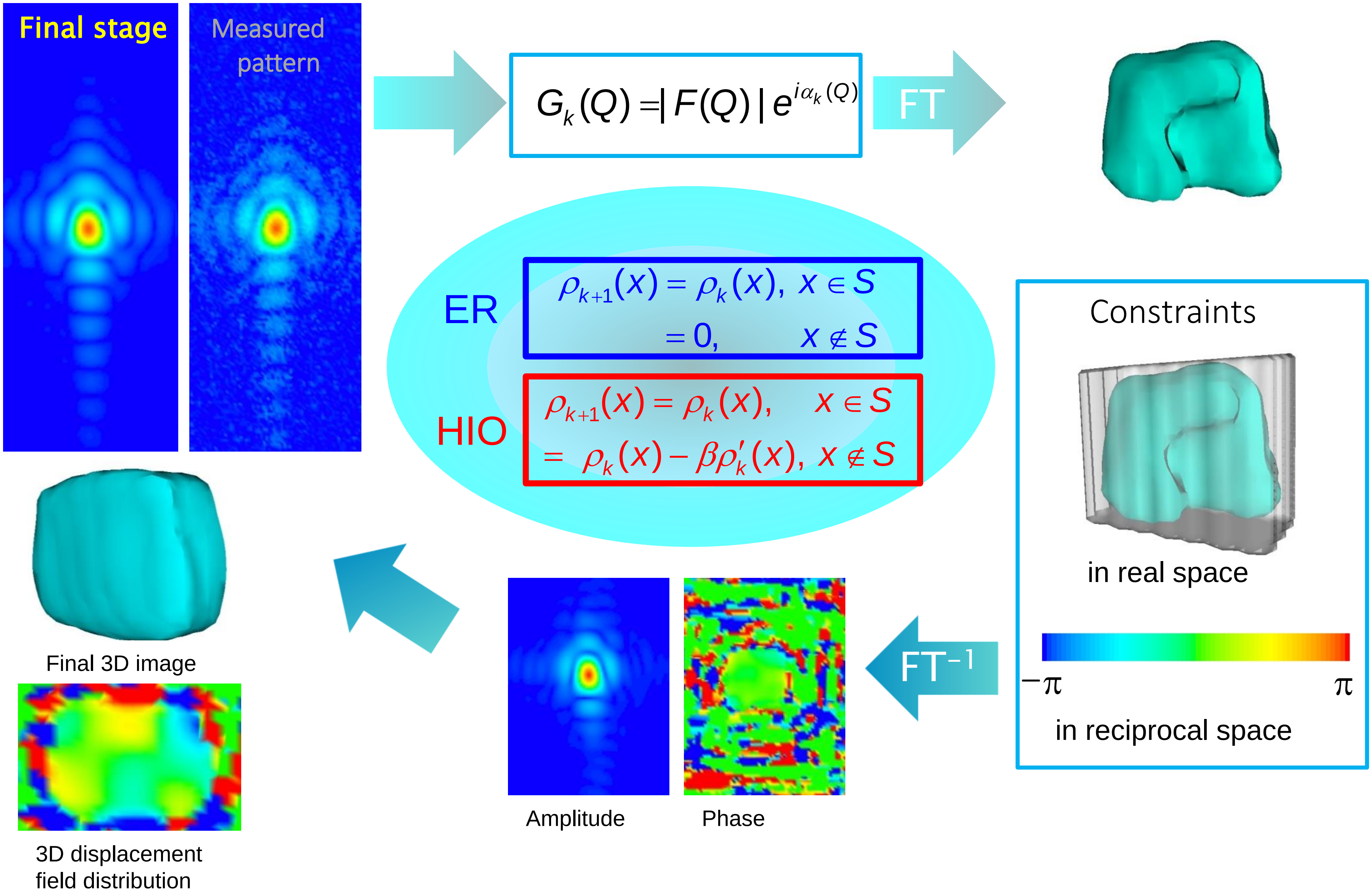

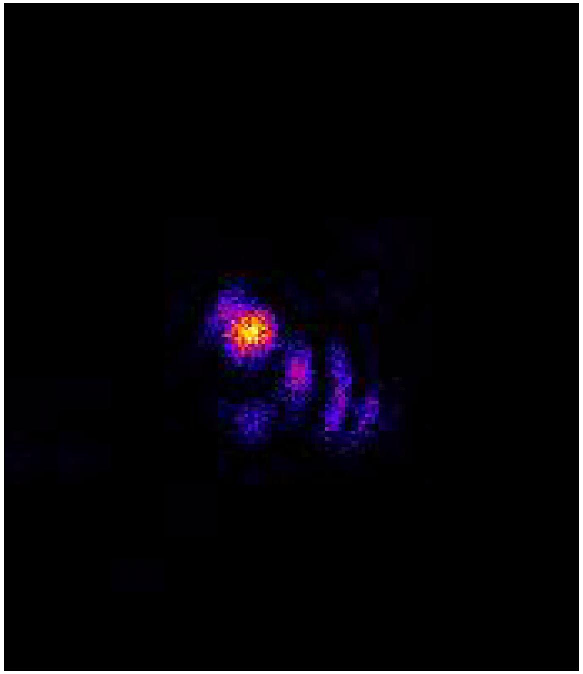

3D scanned
diffraction pattern
at Bragg (1-11) coherent
diffraction peak

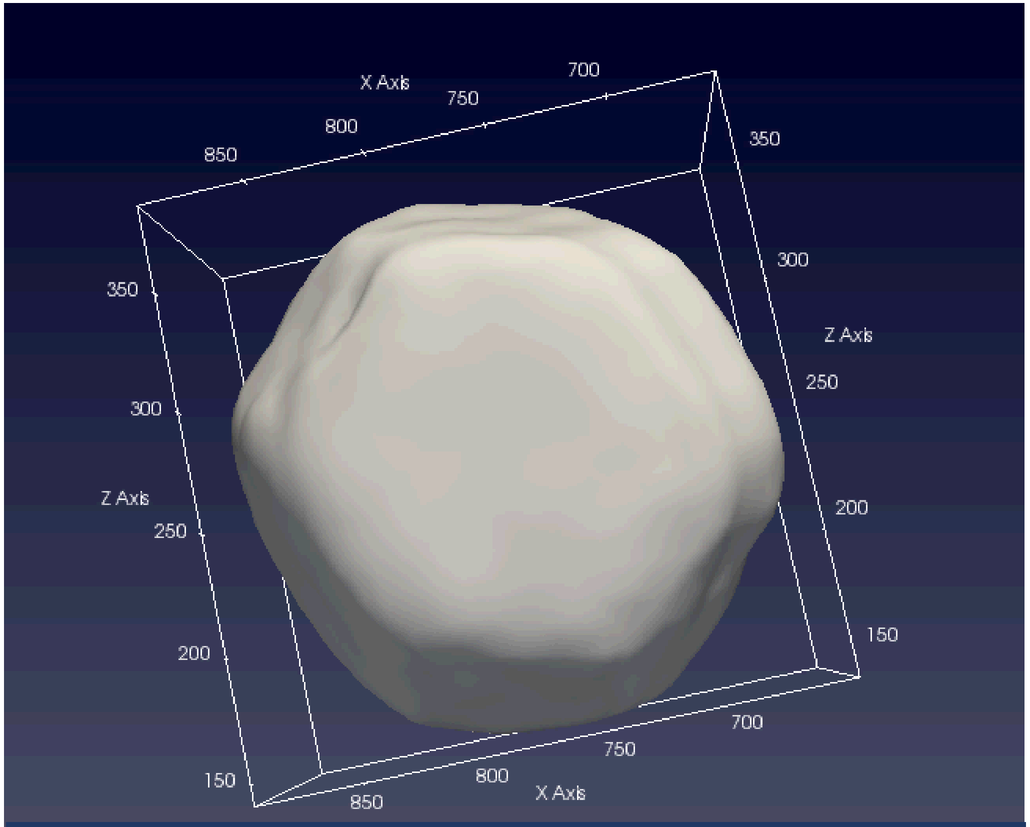

About 180nm size Platinum nanocrystal at 700K in vacuum

34IDC, APS

Structural Sensitivity & In situ Measurement

- ✓ Achievable at the nanoscale with sub-angstrom sensitivity to crystalline lattice distortion.
- ✓ In situ measurements are easily available.

- Gold nanoparticle by adsorption of propane thiols : ~ **pico meter** level distortion

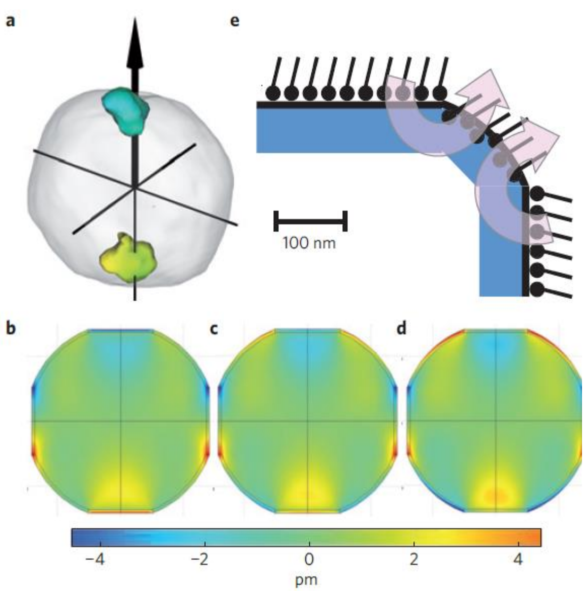

Nat. Mater. **10**, 862 (2011).

- Single zeolite crystal of organic residue effect with "**in situ**" temperature dependence
  : **~ 0.1nm** scale lattice distortion
  - Spatial derivative of the displacement along the entire size of the crystal: 10^{-4}

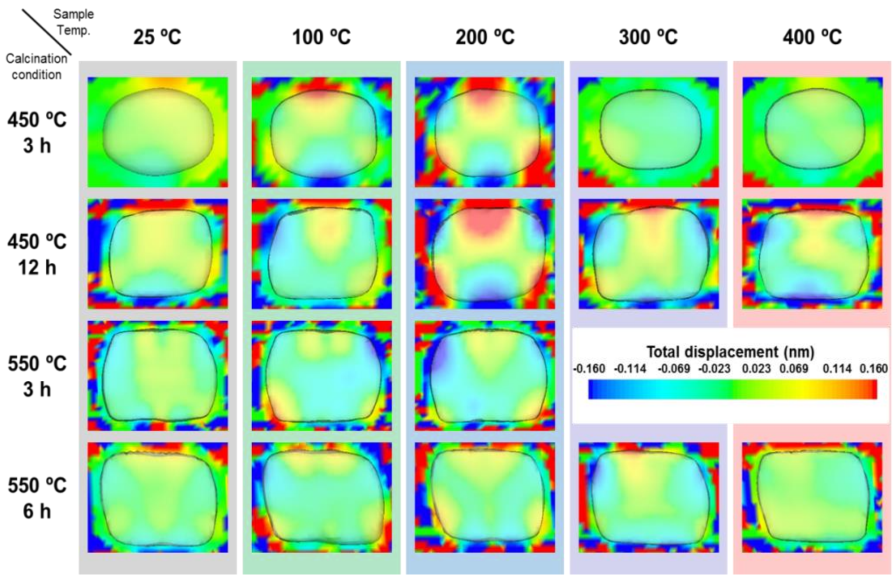

Nat. Mater. **12**, 729 (2013).

Operando techniques

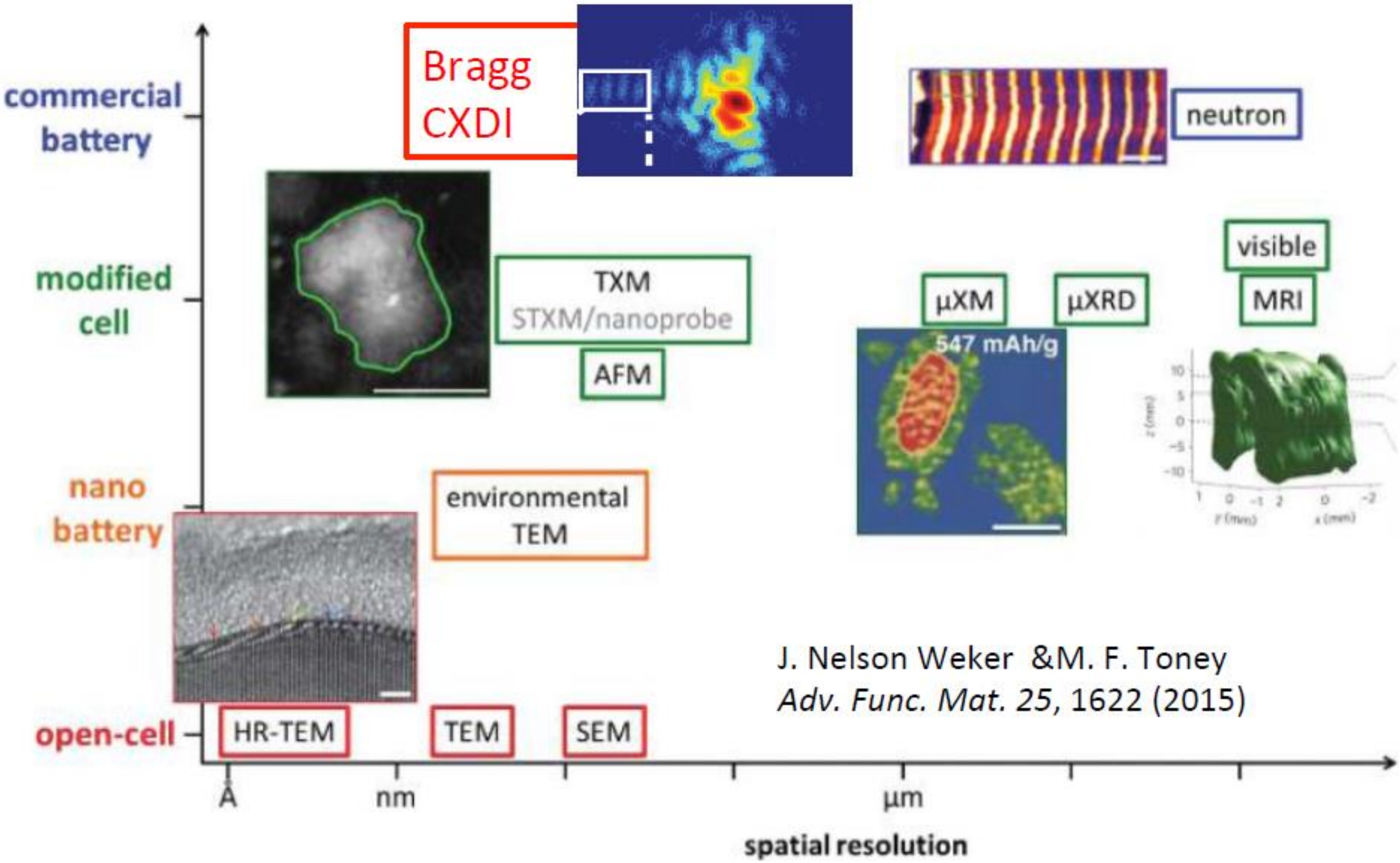

J. Nelson Weker &M. F. Toney
Adv. Func. Mat. 25, 1622 (2015)

Operando Study

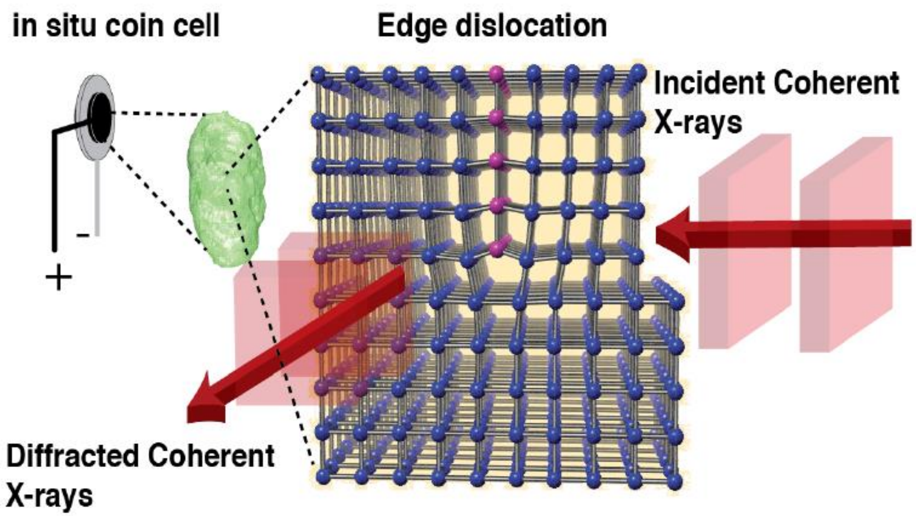

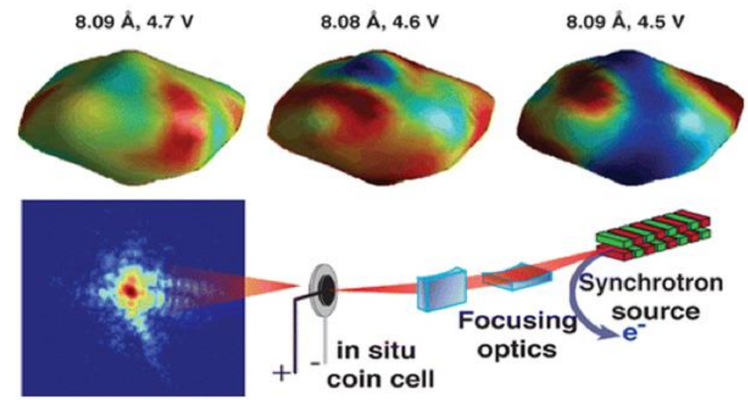

A. Ulvestad, et al., Science 348 (6241), 1344 (2015)

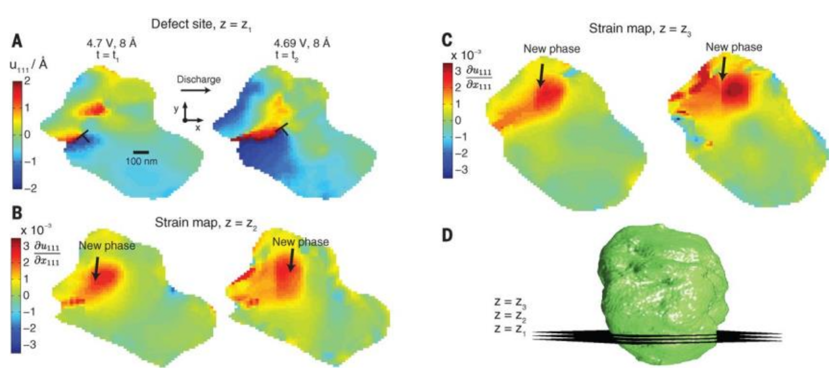

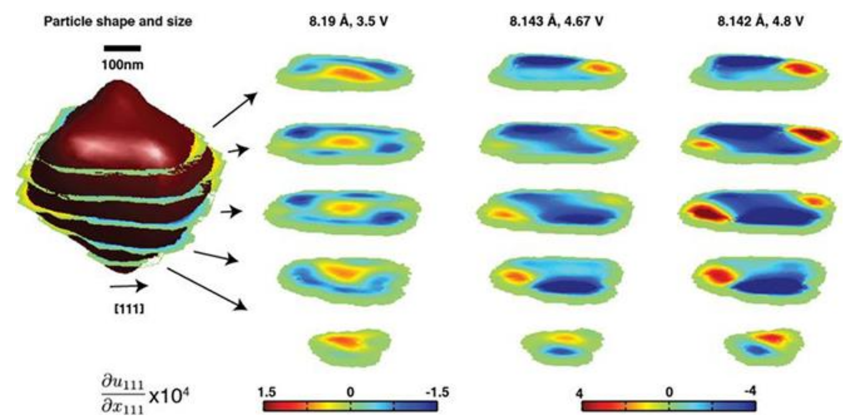

Science 348, 1344 (2015).

Nano Lett. 14, 5123-5127 (2014)

연료전지, Battery, 에너지 소자

In situ Catalysis

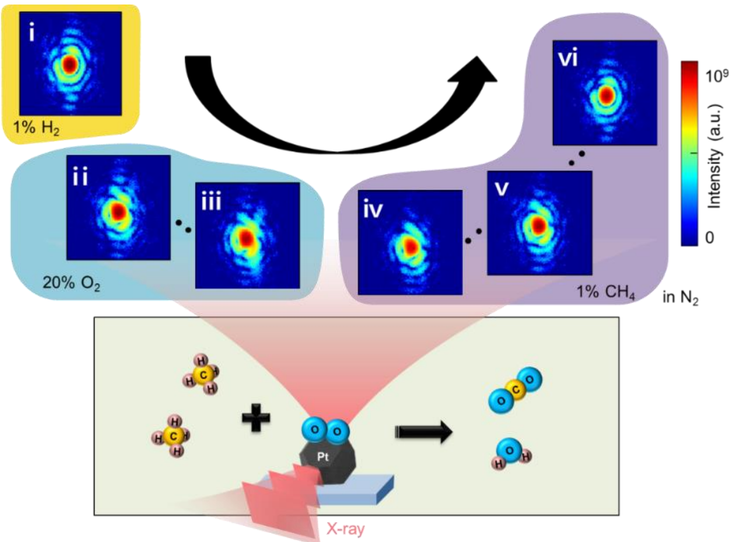

Active site localization

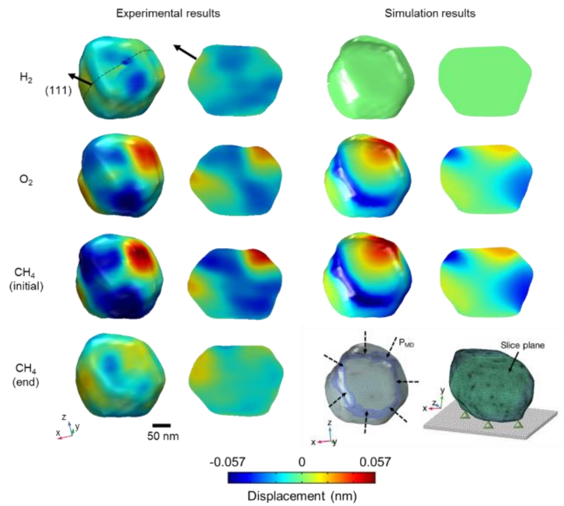

Nat. Commun. **9**, 3422 (2018)

Defect Dynamics

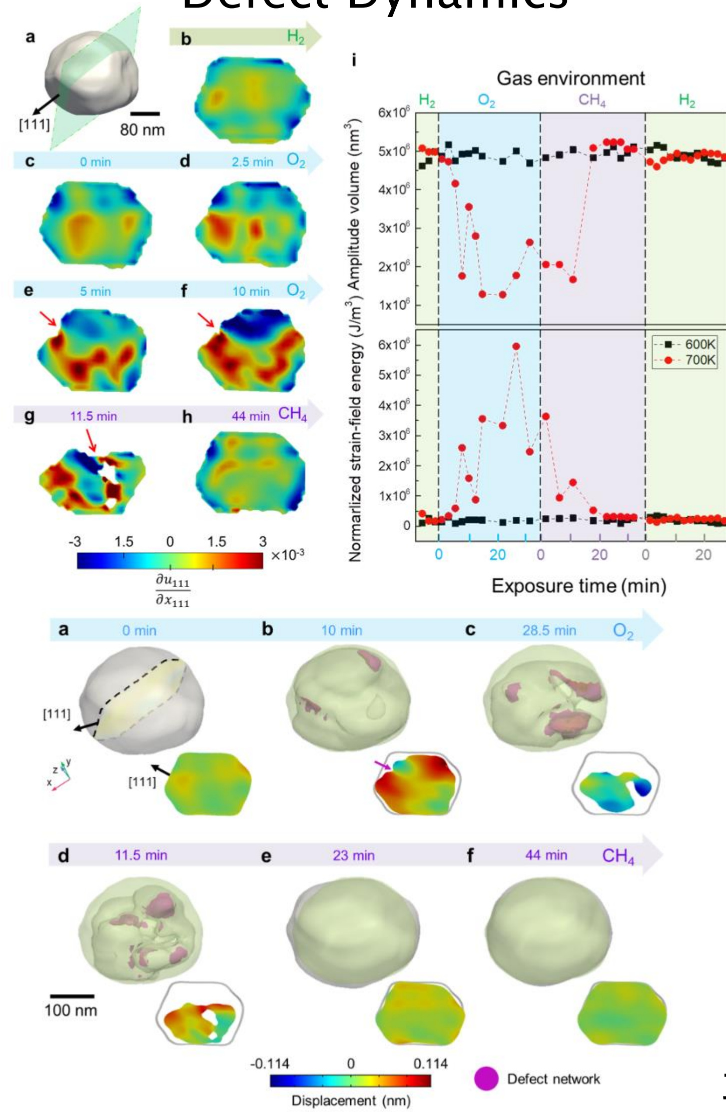

Nano Lett. 19, 5044 (2019)

환경, 촉매

Imaging Lattice Dynamics

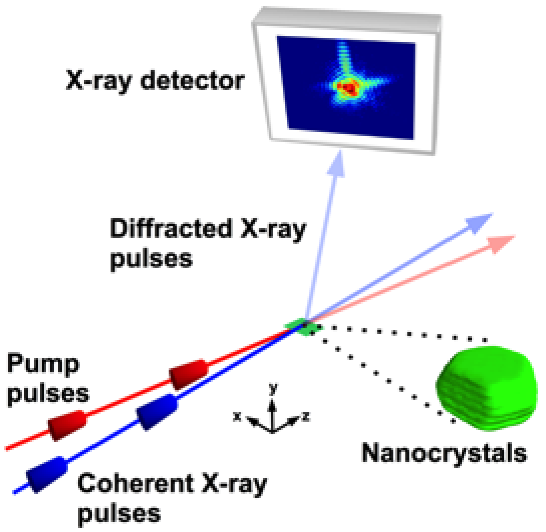

Laser Pump – CXD Probe @ LCLS

$$S(\tau) = \sum_{n=1}^{N} A_n \exp\left[-\frac{\tau}{\tau_{d,n}}\right] \cos\left[\frac{2\pi}{T_n}(\tau + \tau_{0,n})\right] + C_n.$$

600 pm "breathing modes"

Crystal A
101 ps and 241 ps

Crystal B
90 ps and 256 ps

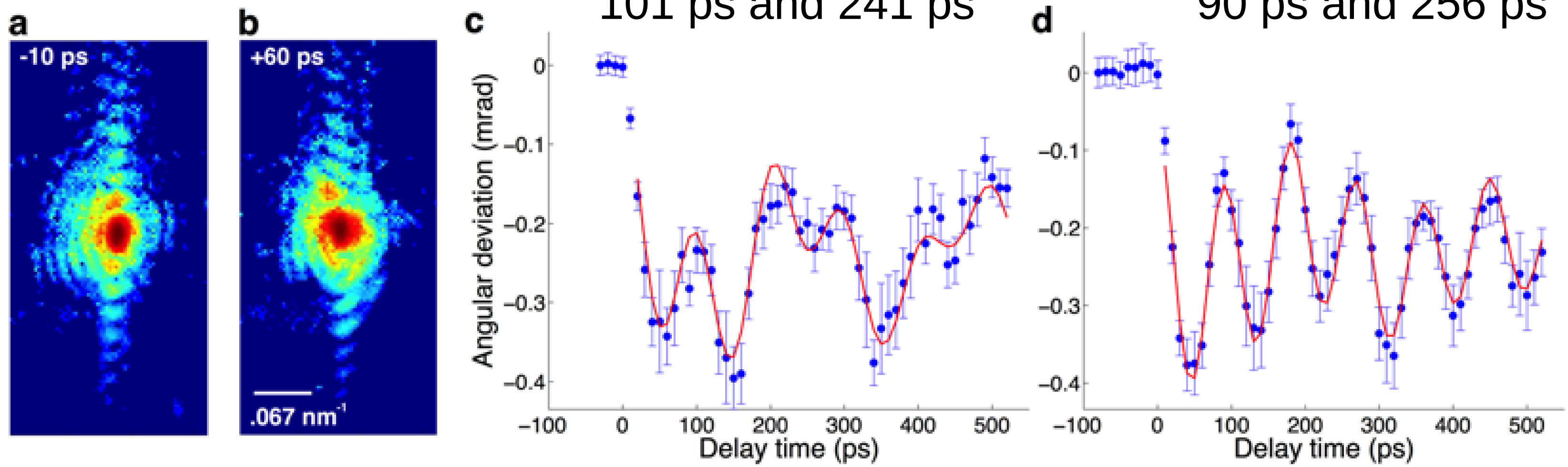

Ultrafast three dimensional imaging of lattice dynamics in individual gold nanocrystals
J. N. Clark, et.al. (2013). *Science*, *341*(6141), 56–59

Imaging Lattice Dynamics

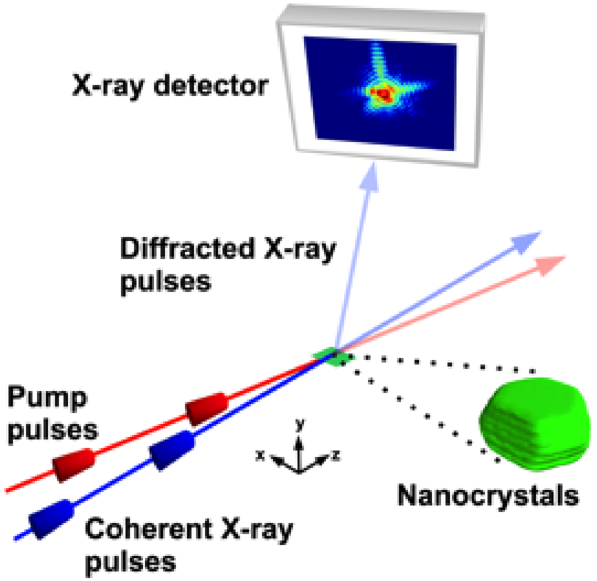

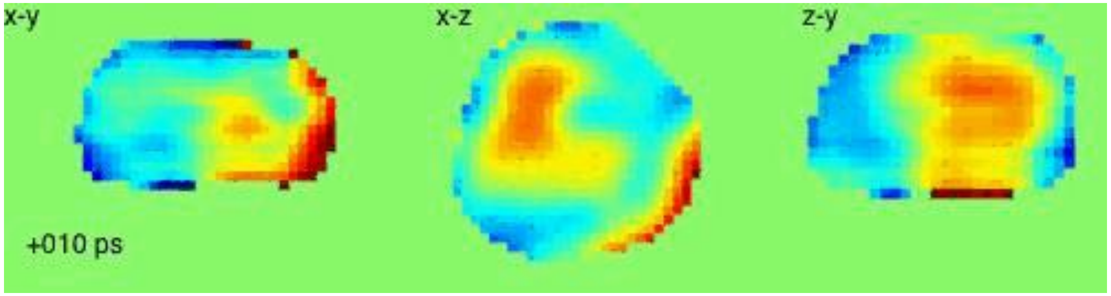

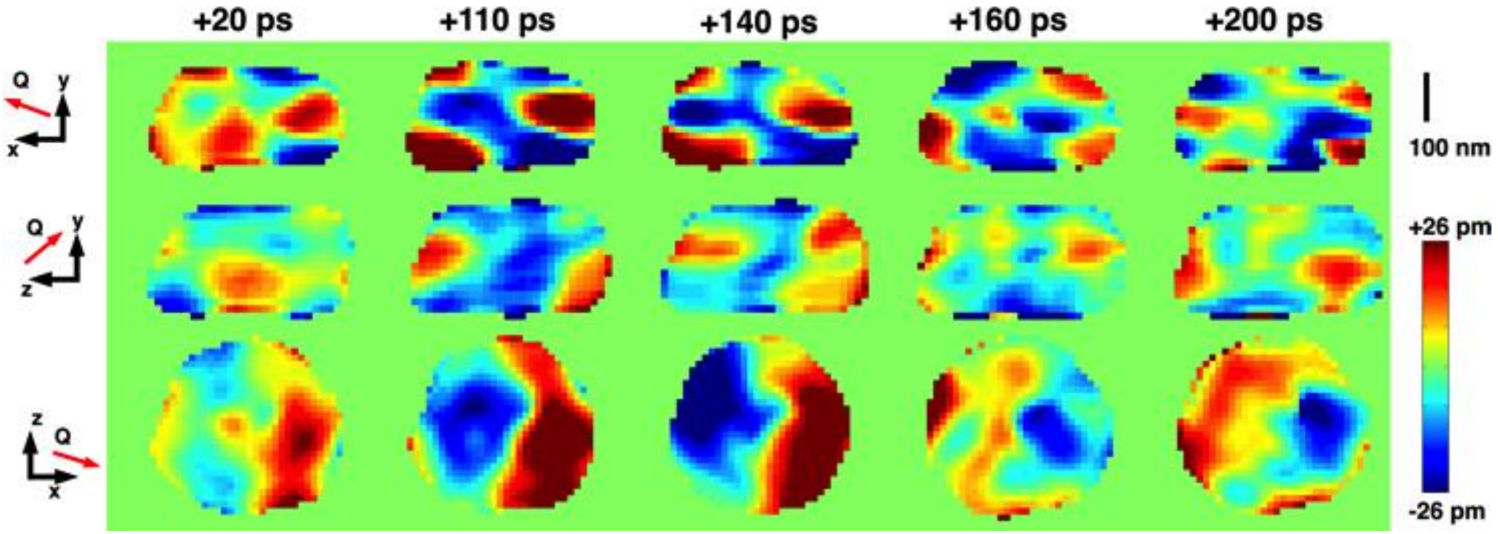

Ptychography

Magnetic materials

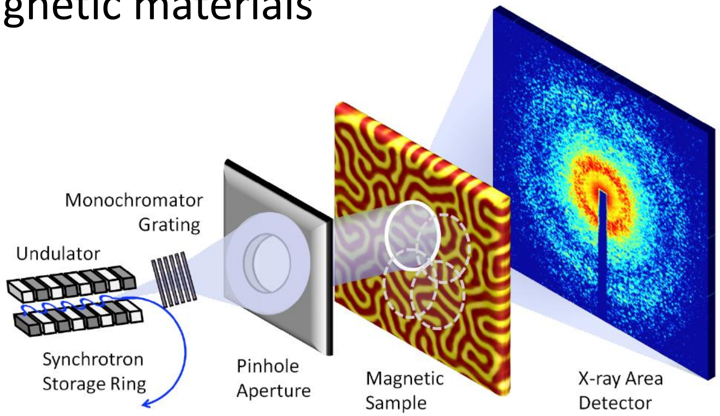

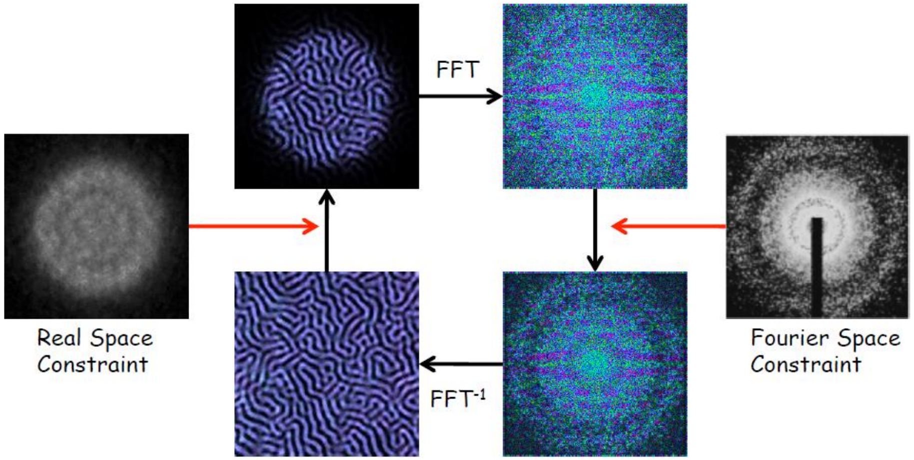

Real space reconstruction

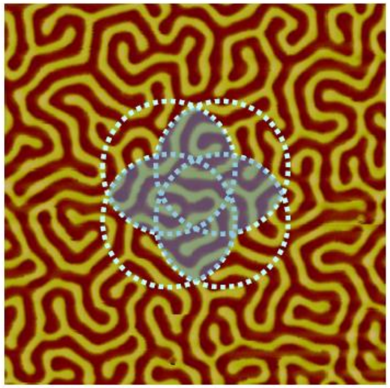

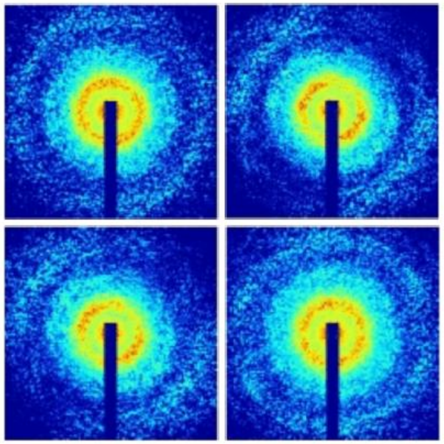

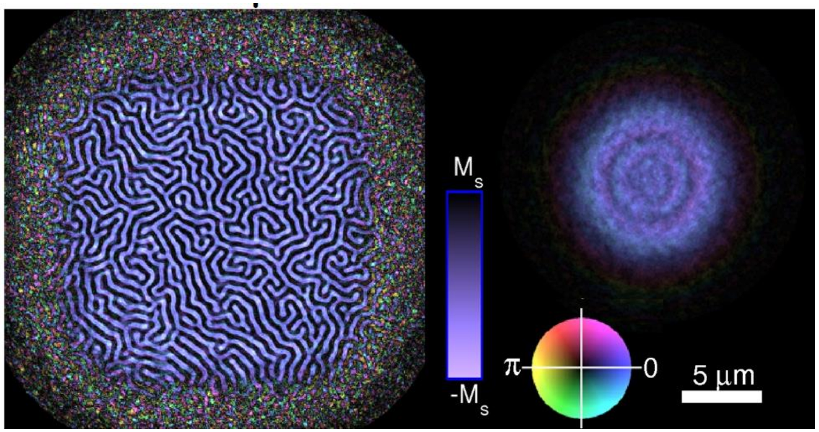

PNAS 108, 13393 (2011)

Advanced coherent/polarized X-ray scattering beamline (ACPXS)

편광, 결맞음

차세대 방사광가속기의 새로운 과학기술

- ✓ Local quantity measurements (nano probes & coherence)
  $\Rightarrow$ Discovery of New Materials?
  Understanding & Control Defects
- ✓ Flux-hungry techniques available! (Inelastic scattering, Resonant magnetic Hard x-ray scattering…)
- ✓ Operando, in situ study

… need more

New Idea
New Instrumentation
New People!

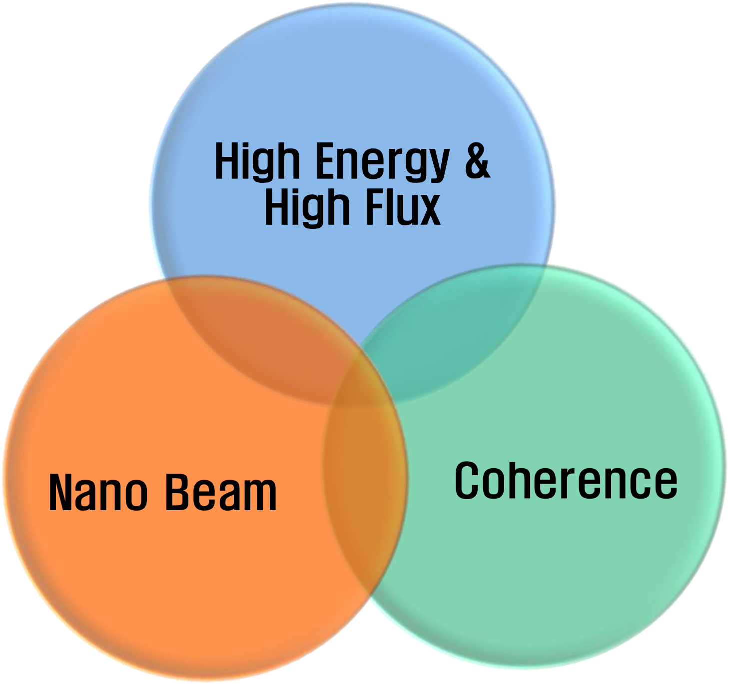

감사합니다.